PEOPLE'S DEMOCRATIC REPUBLIC OF ALGERIA

MINISTRY OF HIGHER EDUCATION AND SCIENTIFIC RESEARCH

UNIVERSITY Larbi Ben M'Hidi –Oum El Bouaghi

FACULTY OF EXACT SCIENCES AND NATURE AND LIFE SCIENCES

MATERIAL SCIENCES DEPARTMENT

Order number: …………

Series: ………

A thesis for *the fulfillment of the requirements for the degree of Doctorate in chemistry*

Option: Materials chemistry

By

Oday Mohammad Ahmad KHAMAYSA

Entitled

Experimental and theoretical studies of some nitrogenous organic compounds as inhibitors of corrosion for carbon steel in acidic medium

Thesis Committee:

President of committee:	Pr. Noureddine Gherraf	Oum El Bouaghi university
Thesis Supervisor:	Pr. Assia Sid	Oum El Bouaghi university
Thesis co-supervisor:	Pr. Merzoug Benahmed	Tebessa university
Examiner :	Pr. Salah Akkal	Constantine university
Examiner :	Dr. Abdelkarim Hazourli	Oum El Bouaghi university

2020-2021

إهـــــــــداء

إلى أولئك الذين علموني الحياة والحب ودعموني طوال الوقت

الى من علمني أن الدنيا كفاح وسلاحها العلم والمعرفة الى الذي لم يبخل علي بأي شي وسعى لأجل راحتي ونجاحي الى أعز انسان **ابي العزيز** .

الى التي رأني قلبها قبل عينيها وحضنتني احشاؤها قبل يديها الى شجرتي التي لا تذبل الى الظل الذي أوي اليه في كل حين **امي الحنونة** .

الى الجوهرة المضيئة والدرة المنيرة والؤلؤة المكنونة **اختي الغالية وزوجها واولادهم**

الى سندي وقوتي وملاذي بعد الله الى من اثروني على انفسهم الى من علموني علم الحياة الى من اظهروا لي ما هو اجمل من الحياة **اخوتي واولادهم وزوجاتهم** .

الى **زوجتي** تؤام روحي و مؤنستي اشكرك على كل السعادة التي قدمتيها لي اتمنى من الله أن لا تزول هذه النعمة و أن تبقي بجانبي حتى أخر يوم بحياتي .

الى فلذة كبدي وقطعة من جسدي ونفس من اعماقي الى انأمل ونعومة يديك التي لم تأتي بعد وقلبك الطاهر ابني الغالي **ابراهيم** .

الى **عائلة زوجتي الكريمة** و الحنونة الذين لم يجعولني اشعر بأني ببلد اخر غير وطني.

الى عائلتي الثانية و من كان لهم بعض الفضل في وصولي وتحقيق هدفي وغايتي و كانو عونا وسندا لي، الى **عمي حاتم و خالتي خيرية و اولادهم**.

لا أعلم ماذا سأكتب عنك بماذا أوصف تلك العلاقة كنت الأب والأخ الكبير والصديق الوفي تعلمت منك الصبر والمعرفة بفترة قليلة شكرا لك من أعماق قلبي **المستشار الدكتور رائد عدنان (ابو عدنان)**.

الى رفيق دربي ومن رافقني منذ حملنا حقائب صغيرة نحو غربتنا وسرنا معا الدرب خطوة بخطوة الى من اعتمد عليه في كل صغيرة وكبيرة الى اخي الذي لم تنجبه امي **الدكتور صهيب شاهين** .

إلى من دعمني وعزز لي ثقتي بنفسي ، ولم يبخل على بالنصيحةَ **سيادة اللواء عارف صالح أبو يزن.**

الى من تمنوا لي النجاح والتوفيق وكان لهم بالغ الاثر في كثير من العقبات والصعاب ووقفوا بجواري وساعدوني بكل ما يملكون **حمزة الطيراوي** و **اسحق ابو علاء, نظير حداد , عمر ابو غسان وعائلته الكريمة, معاذ عبد العال, أحمد الاقطش, فريد سليم.**

الى الصغيرات المدللات اخواتي في غربتي **الدكتورة هيا الشرعة و المهندسة مروة جرار و المحامية ازاد ابو سعود.**

Acknowledgements

Without the support and advice of many people, I would not have made it to this point, and it is here that I intend to express my gratitude.

First, I should give my thanks to ***Pr. Assia SID***, Professor at Oum El Bouaghi University, who not only gave me the opportunity to pursue this PhD project, but also consistently provided mentorship throughout the last few years. This was invaluable while navigating the tumultuous and initially perplexing results documented in these pages. I could not have asked for a more supportive and experienced supervisor.

I also would like to thank to my co-supervisor ***Pr. Merzoug BENAHMED,*** Professor at Tebessa University for his constant support, availability and constructive suggestions, which were determinate for the accomplishment of the work presented in this thesis.

Also need to thank:

Pr. Noureddine GHERRAF, professor at Oum El Bouaghi university, who honored me by accepting to be president of the committee. I would like to express to him here my respectful gratitude and my deep consideration.

I express my gratitude to ***Pr. Salah AKKAL***, professor at Constantine University, and ***Dr. Abdelkrim HAZOURLI***, doctor at Oum El Bouaghi university for having accepted to examine my thesis.

I would also thank ***Dr. Nacer HEBIR*** and ***Dr. Aissaoui ZIAR***, dean and vice dean, of the faculty of exact sciences and nature and life sciences, respectively, and ***Dr. Fayçal GOUMEIDANE*** head of the Department of Chemistry, for their invaluable support and useful suggestions, encouragement, and keeping me on track whenever I ran into problems throughout years.

I would also like to express my gratitude to all the people whose help and enthusiasm allowed the progress of this work, and in particular ***Professor Paul MOSSET*** who carried out numerous NMR spectra at the school of chemistry in Rennes without forget the engineers: ***Mrs. Nadia GHERRAF***, ***Mrs Safia***, ***Mrs, Hadjam Mariem*** and ***Mrs Oualida*** who helped me to do the IR and UV / Visible analyzes.

I would also acknowledge the Centre de Recherche en Technologie des Semi conducteurs pour l'énergétique ***'CRTSE"*** specially ***Mr. Hocine CHERAGA*** and Centre de Recherche Scientifique et Technique en Analyses Physico-Chimiques ***CRAPC.*** Algeria.

To my little friend ***Dr. Hadjer ZEGHACHE***, I express my gratitude for their unconditional friendship, support and patience throughout these years.

Last, but not least, I extend my heartfelt thanks to my wife, ***Dr. Ilhem Selatnia***, for all her support during my Ph.D. in chemistry journey. She bore me and had my shoulder to lean on her throughout the whole process, and never stopped wanting the best for me, even in the hardest of times.

Abbreviations & Symbols used

A
API: American Petroleum Institute
ASTM : American Society for Testing and Materials
B
β_a : Tafel anodic slop
β_c : Tafel cathodic slop
C
C_{dl} : Double layer capacitance
Conc. : Concentration.
CPE : Consant phase element
C_R : Corrosion rate
CS : carbon steel
D
DCM: Dichloromethane
DFT: Density functional theory
DNPH : 2,4-dinitrophenylhydrazine
E
E_a : Activation energy
E_{corr} : Corrosion potential
EEC: Equivalent circuit electric
EIS: Electrochemical impedance spectroscopy
E_{OCP} : Open circuit potential
F
Fe: Iron
FTIR: Fourier transform infrared spectroscopy
fs: Femto second (10^{-15}s)
G
GDP: Gross national product
GGA: Generalized Gradient Approximation
Gr: Grade
H
HCl: Hydrochloric acid
HOMO : Highest Occupied Molecular Orbital
Hz : Hertz.
I
i_{corr}: Corrosion current density
ISO: International Standard Organization
IUPAC: International Union of Pure and Applied Chemistry
K
K_{ads}: Equilibrium adsorption constant
L
LUMO: Lowest Unoccupied Molecular Orbital
M
Me : Methyle.
MEP : Molecular electrostatic potential
MD: Molecular dynamics simulation
Mp : Melting point
N
NMR: Nuclear magnetic resonance

P
PDP: potentiodynamic polarization
ppm: parts per million
ps : Pico second (10^{-12} s)
R
R_{dt} : yeild
R_p : Polarization resistance
R_s : Solution resistance
RDF: Radial distribution function
S
SEM : Scanning electron microscope
T
THF : Tetrahydrofurane.
U
UV : Ultra violet
V
VCI: Volatil corrosion inhibitors
W
WL: Weight loss
X
XPS: X-ray photoelectron spectroscopy
θ: Surface coverage
η: Inhibition efficiency

Table of Contents

Section C: *Literature review*

Part II: *Experimental methodology*

List of Figures

Part I- Section A

Part I- Section B

Part II- Section A

Part II- Section B

Part III

Appendix

List of schemes

Part II- Section B

Part III

List of Tables

Part I- Section A

Part II- Section B

Part III

General Introduction

"Nothing happens quite by chance.
It's a question of accretion of information and experience"

Jonas Salk

1. Thesis purpose and context

The API-grade low carbon steels are the most dominant materials used by different industries, especially in oil wells and gas transportation fields due to their low cost, durability and mechanical efficiency **[1, 2]**. However, it is very prone to undergo corrosion when exposed to aggressive environments, especially those containing SO_4^{2-} and Cl^- anions during various industrial processes such as acid pickling, rust removal, boiler cleanings, acidizing of oil wells, descaling processes in petroleum processing, and pipeline cleaning, etc. **[3]**, leading to considerable economic and health hazards. In order to mitigate corrosion problems, several methods were adopted, such as highly corrosion-resistant materials selection, coating and anodic protection **[4]**, but the employment of inhibitors was still the most cost-effective and widely adopted approach **[5]**. Different kinds of inhibitors have been used throughout the years involving inorganic and organic compounds. Despite excellent inhibitive performance of inorganic inhibitors (Chromates, phosphates, nitrite, etc.), their use is restrictive due to their environmental unfriendliness and bio-toxicity **[6, 7]**. Thus, the development of less toxic, more effective and environmentally friendly corrosion inhibitors has become highly recommended **[8]**. Recently, the researchers focused on the use of organic compounds as a promising alternative solution to traditional toxic corrosion inhibitors **[9-12]**. The employment of such compounds in acidic solutions significantly reduces the corrosion rate, thereby maintaining the lifecycle of the metal. These compounds act by adsorption on the steel surface by forming a protective barrier that protects the metal from the destructive medium through their active centers such as polar functional groups, heteroatoms (N, S, O, P, etc.), aromatic rings as well as π-electrons **[13-15]**. Up until today, researchers tested many kinds of organic compounds for mitigating the corrosion of various steel grades, especially those including nitrogen **[16-22].** Recently, hydrazone and its derivatives have gained much attention in the research community and have proven usefulness in several research fields, especially in biological and medicinal applications **[23-26]**. As reported in literature, these organic class of compounds has recently attracted considerable attention as promising corrosion inhibitor candidates **[27-30]**. Two main reasons can be highlighted for using this class of compounds: (a) they are classified as nontoxic organic compounds, (b) their molecular structure involves an azomethine group –NHN=CH– that has both nucleophilic and electrophilic characters along with π-electrons as active sites

[31]. These features facilitate a strong adsorption of hydrazones on the surface of metal, which results in a higher protection efficiency, which encouraged our research team to carry on in this research path and synthetize some hydrazone derivatives for corrosion mitigation.

2. Objectives

The following specific objectives are defined to be achieved through our work:

- Synthesize and characterize four newly hydrazones derivatives that would be effective as corrosion inhibitors of carbon steel, based on a literature review.
- Investigate the dissolution of carbon steel in 1.0 M HC1 solution and evaluate the inhibiting effect of the four synthesized hydrazones on carbon steel by weight loss, potentiodynamic polarization (PDP) and electrochemical impedance spectroscopy (EIS) measurements.
- Study various factors that affect the inhibition efficiency (effect of inhibitor concentration and effect of temperature).
- Assess the kinetic and thermodynamic parameters by using the weight loss method.
- Study the nature of adsorption of hydrazones on carbon steel surfaces in an acidic medium.
- Study the mode of inhibition (anodic or cathodic or mixed) of the tested hydrazones.
- Characterize the adsorbed film formed at the carbon steel/solution interface using scanning electron microscopy (SEM), contact angle, and X- ray photoelectron spectroscopy (XPS).
- Determination of molecular electronic properties and their correlation with experimental efficiency.
- Evaluate the adsorption of the inhibitor's molecules on metal surfaces.
- Elucidate the possible mechanism of the corrosion inhibition.

With these objectives, an exploration of new potential and eco-friendly corrosion inhibitors was effectively achieved and developed to be used for carbon steel in acidic medium.

3. Thesis structure

This thesis involves 3 parts. The content of each part is presented below:

Part I is a bibliographical reminder on the corrosion and corrosion inhibitors which presented in three sections:

- **Section A:** Deals with the general aspects of corrosion. Meaning and importance of corrosion, consequences of corrosion and types of corrosion are presented. Classification of corrosion, factors which influence corrosion and corrosion prevention methods are discussed.
- **Section B:** Definition of inhibitors, global demand of corrosion inhibitors, types of inhibitors, factors which affect inhibition action and mechanism of inhibition in acidic, alkaline and neutral media have been elaborated.
- **Section C:** presents the literature survey on nitrogenous compounds and hydrazone derivatives and their role in corrosion inhibition
- **Part II:** This part deals with chemical and electrochemical methods for the measurement of corrosion rate as well as the experimental details which includes the materials and methods used during the experimental work. This part also includes the procedure of synthesis of hydrazones. The details of corrosion tests that have been undertaken to investigate the inhibition behavior of hydrazone derivatives have also been described in this part.

Part III: presents the basic results establishing corrosion inhibition effect of hydrazone derivatives using chemical and electrochemical techniques as well as characterization of the inhibiting film formed on the carbon steel surface using SEM, contact angle and XPS methods. Additionally, theoretical studies using Density Functional Theory (DFT) and molecular dynamics simulation (MD) were performed to explore the most reactive sites of the hydrazone molecule and its adsorption mechanism.

Finally, a conclusion of the undertaken research and the recommended future work.

4. References

[1] N.A. Odewunmi, M.M. Solomon, S.A. Umoren, S.A. Ali, Comparative Studies of the Corrosion Inhibition Efficacy of a Dicationic Monomer and Its Polymer against API X60 Steel Corrosion in Simulated Acidizing Fluid under Static and Hydrodynamic Conditions, ACS Omega (2020).

[2] H.M. Abd El-Lateef, W. Albokheet, M. Gouda, Carboxymethyl cellulose/metal (Fe, Cu and Ni) nanocomposites as non-precious inhibitors of C-steel corrosion in HCl solutions: synthesis, characterization, electrochemical and surface morphology studies, Cellulose 27(14) (2020) 8039-8057.

[3] D.I. Njoku, P.C. Okafor, H. Lgaz, K.J. Uwakwe, E.E. Oguzie, Y. Li, Outstanding anticorrosion and adsorption properties of 2-amino-6-methoxybenzothiazole on Q235 and X70 carbon steels: Effect of time, XPS, electrochemical and theoretical considerations, Journal of Molecular Liquids (2020) 114663.

[4] M. Benahmed, I. Selatnia, N. Djeddi, S. Akkal, H. Laouer, Adsorption and Corrosion Inhibition Properties of Butanolic Extract of Elaeoselinum thapsioides and Its Synergistic Effect with Reutera lutea (Desf.) Maires (Apiaceae) on A283 carbon Steel in Hydrochloric Acid Solution, Chemistry Africa 3(1) (2020) 251-261.

[5] P. Kannan, T.S. Rao, N. Rajendran, Improvement in the corrosion resistance of carbon steel in acidic condition using naphthalen-2-ylnaphthalene-2-carboxammide inhibitor, Journal of colloid and interface science 512 (2018) 618-628.

[6] G. Gece, Drugs: A review of promising novel corrosion inhibitors, Corrosion Science 53(12) (2011) 3873-3898.

[7] S.E. Manahan, Fundamentals of environmental chemistry, CRC press2011.

[8] L.O. Olasunkanmi, A.O. Idris, A.H. Adewole, O.O. Wahab, E.E. Ebenso, Adsorption and Corrosion Inhibition Potentials of Salicylaldehyde-based Schiff Bases of Semicarbazide and p-Toluidine on Mild Steel in Acidic Medium: Experimental and Computational Studies, Surfaces and Interfaces (2020) 100782.

[9] S. Pareek, D. Jain, S. Hussain, A. Biswas, R. Shrivastava, S.K. Parida, H.K. Kisan, H. Lgaz, I.M. Chung, D. Behera, A new insight into corrosion inhibition mechanism of copper in aerated 3.5 wt.% NaCl solution by eco-friendly Imidazopyrimidine Dye: experimental and theoretical approach, Chemical Engineering Journal 358 (2019) 725-742.

[10] M. Ramezanzadeh, G. Bahlakeh, Z. Sanaei, B. Ramezanzadeh, Corrosion inhibition of mild steel in 1 M HCl solution by ethanolic extract of eco-friendly Mangifera indica (mango)

leaves: Electrochemical, molecular dynamics, Monte Carlo and ab initio study, Applied Surface Science 463 (2019) 1058-1077.

[11] W.Y. Wang, Z.J. Song, M.Z. Guo, L.H. Jiang, B.B. Xiao, Q.G. Jiang, H.Q. Chu, Y.Q. Liu, Y.J. Zhang, N. Xu, Employing ginger extract as an eco-friendly corrosion inhibitor in cementitious materials, Construction and Building Materials 228 (2019).

[12] A. Dehghani, G. Bahlakeh, B. Ramezanzadeh, M. Ramezanzadeh, Potential role of a novel green eco-friendly inhibitor in corrosion inhibition of mild steel in HCl solution: Detailed macro/micro-scale experimental and computational explorations, Construction and Building Materials 245 (2020).

[13] L. Zhu, X. Zheng, X. Zeng, M. Gong, L. Guo, Experimental and theoretical investigation on the effect of N-substituent position on the inhibition performance of l-lysine derivatives for carbon steel in H 2 SO 4 solution, Research on Chemical Intermediates (2020) 1-20.

[14] F. Benhiba, H. Serrar, R. Hsissou, A. Guenbour, A. Bellaouchou, M. Tabyaoui, S. Boukhris, H. Oudda, I. Warad, A. Zarrouk, Tetrahydropyrimido-Triazepine derivatives as anti-corrosion additives for acid corrosion: Chemical, electrochemical, surface and theoretical studies, Chemical Physics Letters 743 (2020) 137181.

[15] B. Chugh, A.K. Singh, A. Chaouiki, R. Salghi, S. Thakur, B. Pani, A comprehensive study about anti-corrosion behaviour of pyrazine carbohydrazide: Gravimetric, electrochemical, surface and theoretical study, Journal of Molecular Liquids 299 (2020) 112160.

[16] K. Abderrahim, I. Selatnia, A. Sid, P. Mosset, 1, 2-bis (4-chlorobenzylidene) Azine as new and effective corrosion inhibitor for copper in 0.1 N HCl: A combined experimental and theoretical approach, Chemical Physics Letters 707 (2018) 117-128.

[17] K. Khaled, Corrosion control of copper in nitric acid solutions using some amino acids–a combined experimental and theoretical study, Corrosion Science 52(10) (2010) 3225-3234.

[18] H.M.A. El-Lateef, Experimental and computational investigation on the corrosion inhibition characteristics of mild steel by some novel synthesized imines in hydrochloric acid solutions, Corrosion Science 92 (2015) 104-117.

[19] H.M.A. El-Lateef, A.M. Abu-Dief, L.H. Abdel-Rahman, E.C. Sañudo, N. Aliaga-Alcalde, Electrochemical and theoretical quantum approaches on the inhibition of C1018 carbon steel corrosion in acidic medium containing chloride using some newly synthesized phenolic Schiff bases compounds, Journal of Electroanalytical Chemistry 743 (2015) 120-133.

[20] G. Sığırcık, T. Tüken, M. Erbil, Inhibition efficiency of aminobenzonitrile compounds on steel surface, Applied Surface Science 324 (2015) 232-239.

[21] I. Selatnia, A. Sid, M. Benahmed, T. Ozturk, N. Gherraf, Synthesis and Characterization of a Bis-Pyrazoline Derivative as Corrosion Inhibitor for A283 Carbon Steel in 1M HCl: Electrochemical, Surface, DFT and MD Simulation Studies, Protection of Metals and Physical Chemistry of Surfaces 54(6) (2018) 1182-1193.

[22] A. Fouda, A.E.-M. SA, A. El-Hossiany, A. Ibrahim, Evolution of the corrosion-inhibiting efficiency of novel hydrazine derivatives against corrosion of stainless steel 201 in acidic medium, Int J Electrochem Sci 14 (2019) 2187-2207.

[23] M. Krátký, Š. Štěpánková, M. Brablíková, K. Svrčková, M. Švarcová, J. Vinšová, Novel Iodinated Hydrazide-hydrazones and their Analogues as Acetyl-and Butyrylcholinesterase Inhibitors, Current Topics in Medicinal Chemistry (2020).

[24] J. de Oliveira Carneiro Brum, T.C. França, S.R. LaPlante, J.D.F. Villar, Synthesis and Biological Activity of Hydrazones and Derivatives: A Review, Mini Reviews in Medicinal Chemistry 20(5) (2020) 342-368.

[25] P. Sharma, D. Sharma, A. Sharma, N. Saini, R. Goyal, M. Ola, R. Chawla, V. Thakur, Hydrazone comprising compounds as promising anti-infective agents: chemistry and structure-property relationship, Materials Today Chemistry 18 (2020) 100349.

[26] S. Saouli, I. Selatnia, B. Zouchoune, A. Sid, S.M. Zendaoui, C. Bensouici, E.-E. Bendeif, Synthesis, spectroscopic characterization, crystal structure, DFT studies and biological activities of new hydrazone derivative: 1-(2, 5-bis ((E)-4-isopropylbenzylidene) cyclopentylidene)-2-(2, 4-dinitrophenyl) hydrazine, Journal of Molecular Structure (2020) 128203.

[27] H. Lgaz, A. Chaouiki, M.R. Albayati, R. Salghi, Y. El Aoufir, I.H. Ali, M.I. Khan, S.K. Mohamed, I.-M. Chung, Synthesis and evaluation of some new hydrazones as corrosion inhibitors for mild steel in acidic media, Research on Chemical Intermediates 45(4) (2019) 2269-2286.

[28] N. Chafai, S. Chafaa, K. Benbouguerra, A. Hellal, M. Mehri, Synthesis, spectral analysis, anti-corrosive activity and theoretical study of an aromatic hydrazone derivative, Journal of Molecular Structure 1181 (2019) 83-92.

[29] H. Lgaz, I.-M. Chung, M.R. Albayati, A. Chaouiki, R. Salghi, S.K. Mohamed, Improved corrosion resistance of mild steel in acidic solution by hydrazone derivatives: an experimental and computational study, Arabian Journal of Chemistry 13(1) (2020) 2934-2954.

[30] T.K. Chaitra, K.N. Mohana, D.M. Gurudatt, H.C. Tandon, Inhibition activity of new thiazole hydrazones towards mild steel corrosion in acid media by thermodynamic,

electrochemical and quantum chemical methods, Journal of the Taiwan Institute of Chemical Engineers 67 (2016) 521-531.

[31] O.M.A. Khamaysa, I. Selatnia, H. Zeghache, H. Lgaz, A. Sid, I.-M. Chung, M. Benahmed, N. Gherraf, P. Mosset, Enhanced corrosion inhibition of carbon steel in HCl solution by a newly synthesized hydrazone derivative: Mechanism exploration from electrochemical, XPS, and computational studies, Journal of Molecular Liquids 315 (2020) 113805.

Part I

Introduction to corrosion and corrosion inhibitors

Section A

General aspects of Corrosion

"Lay not up for yourselves treasures upon earth where moth and rust doth corrupt and where thieves break through and steal"
Matthew

I. A. 1. Definition

The term corrosion is a derivative from the Latin word '*Corrodere*' which means "to attack or gnaw away", and it first appeared in the 'Philosophical Transactions' in 1667 **[1]**. Generally, corrosion is a spontaneous process and is referred to as the disintegration of material or its properties, through chemical ,electrochemical or biochemical reaction with the surrounding environment, which converts a pure metal to a chemically- stable form, such as its oxide or hydroxide **[2]** . the technical definition of corrosion given by International Standard Organization (ISO) denotes that it is the "*Physicochemical interaction between a metal and its surrounding conditions which result in changes in the properties of the metal and which may often lead to mutilation of the function of the technical system of which these form a part*" **[3]**. But as per the International Union of Pure and Applied Chemistry IUPAC , "*Corrosion is an irreversible interfacial reaction of a material (metal, ceramic, and polymer) with its environment which results in its consumption or dissolution into the environment*" **[4]** . In the other side , the ASTM terminology (G15), corrosion is defined as, "*the chemical or electrochemical reaction between a material, usually a metal, and its environment that produces a deterioration of the material and its properties*" **[5].**

I. A. 2. History of corrosion

The ancient Greek Historian Heyrodotus (Fifth century BC) and the ancient Roman naturalist, Piny the Elder (First century BC) mentioned the adsorption of tin for the protection of iron from corrosion. Alchemists through centuries made fertile attempts to transform base metals into noble ones. Early attempts to mitigate corrosion of metals were empirical and centered largely on the use of organic and metallic coatings. Inhibitors for acid corrosion of metals were known from the middle ages. These were obvious measures to protect metal structures constructed by early artisans, often at the expense of much time and very hard work.

- **Lomonosov (1743 – 1750)** was the first to make broad systematic experiments on the study of the action of acids on metals.
- **Faraday (1820–1882)**, established a very important relationship between chemical action and the generation of electric current.

- **Davy (1826)** proposed an electrochemical method using sacrificial anode for the protection of copper sheathed ocean going ships.
- **De La Rive (1830)** attributed the pronounced corrosion of impure zinc metal to the operation of short-circuited microcells on the metal surface.
- **Marangoni and Stephanelli (1872)** used extracts of glue and gelatin and bran to inhibit the corrosion of iron in acids. This and subsequent discoveries of effective corrosion inhibitors were to a large extent: the result of empirical studies.
- **Wagner (1938)** proposed a mixed potential theory. The theory proclaimed that (i) any electrochemical reaction comprised of two or more partial oxidation and reduction reactions, (ii) there can be no net accumulation of electrical charges during an electrochemical reaction and the potential at the entire surface of an isolated electrode should be the same.
- The first patent in corrosion inhibition was awarded to **Baldwin (1960),** British patent, which involved the use of molasses and vegetable oils for pickling steel sheet in acid. Later, increased research activities in corrosion inhibition studies were started.

I. A. 3. Basic Processes of metallic corrosion

The corrosion is a complicated process but the basic process of metallic corrosion in aqueous solution involving the following steps [6] (**Fig I. A. 1**):

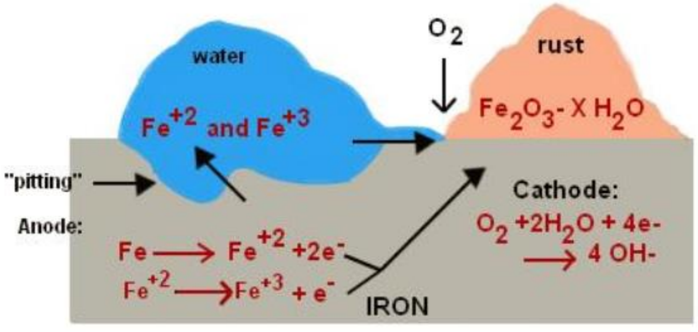

Figure. I. A. 1. Reaction occurring during the corrosion of steel [7].

- ✓ When a metal is placed in aggressive environment, it loses electrons and forms positively charged ions.
- ✓ As a result of the formation of positively charged ions, electrons are released to flow through the steel to the cathodic area.

- ✓ Oxygen in aqueous solution moves to the cathode and completes the electric circuit by using the electrons that flow to the cathode to form OH^- at the surface of the metal.

- Anodic reaction: $Fe \rightarrow Fe^{2+} + 2e^-$ **(I. A. 1)**
- Cathodic reaction: $O_2 + 2H_2O + 4e^- \rightarrow 4OH^-$ **(I. A. 2)**

In the absence of oxygen, hydrogen ion participates in the reaction at the cathode instead of oxygen and completes the electrical circuit as follows:

$$2H^+ + 2e^- \rightarrow H_2 \uparrow \quad \textbf{(I. A. 3)}$$

Ferrous ions produced by dissolution of the metal combine with hydroxyl ions as follow:

$$Fe^{2+} + 2OH^- \rightarrow Fe(OH)_2 \downarrow \quad \textbf{(I. A. 4)}$$

The ferrous hydroxide produced has a very low solubility and quickly precipitates

$$4Fe(OH)_2 + O_2 + 2H_2O \rightarrow 4Fe(OH)_3 \quad \textbf{(I. A. 5)}$$

Dehydrolysis of this product leads to the formation of the corrosion products normally seen on the metal surface **(Eq. I. A. 6 and I. A. 7).**

$$2Fe(OH)_3 \rightarrow Fe_2O_3 \downarrow + 3H_2O \quad \textbf{(I. A. 6)}$$

$$Fe(OH)_3 \rightarrow FeO(OH) \downarrow + H_2O \quad \textbf{(I. A. 7)}$$

I. A. 4. Different forms of Corrosion

Corrosion can affect the metal in a variety of ways, depending on its nature and the precise prevailing environmental conditions, resulting, for example, in failure by cracking or in loss of strength or ductility **[8]**.

I. A. 4. 1. Uniform corrosion

The uniform attack is the most common type of corrosion, which is also called general corrosion. it is usually the result of a chemical or electrochemical reaction **[9]** over the entire exposed area to the aggressive medium, resulting in the uniform decrease of metal thickness . Usually, this form of corrosion does not cause major technical problem because the service life of the equipment can be estimated using relatively simple tests.

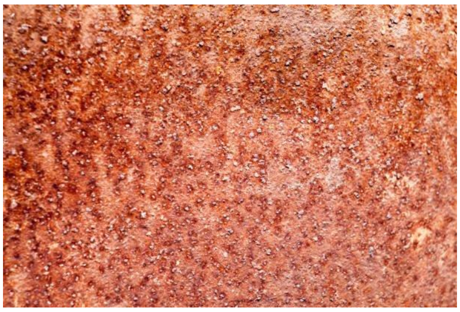

Figure. I. A. 2. Schematic representation of uniform corrosion **[9]**.

I. A. 4. 2. Pitting corrosion

Pitting corrosion is a form of corrosion classified as localized attack often results in localized penetration in the metal at concentrated places forming pits or holes. Nevertheless, this form is one of the most insidious forms of corrosion. Equipment failed because of perforation with only a small percent weight loss of the entire surface. The detection of the pits is a difficult task because of their small size and the pits are often covered by corrosion products.

Figure. I. A. 3. Schematic representation of pitting corrosion **[10]**.

I. A. 4. 3. Crevice corrosion

It refers to corrosion that occurs if a crevice between different metallic objects, e.g. bolts, nuts and rivets, is in contact with liquids. This is usually attributed to changes in acidity in the crevice, absence of O_2 in the species and concentration of a detrimental ionic species. A typical example of crevice corrosion is the crevice formed at the junction of two metal surfaces in close contact with a gasket or another metal surface.

Figure. I. A. 4. Schematic representation of crevice corrosion **[11]**.

I. A. 4. 4. Galvanic corrosion

Galvanic corrosion is a type of electrochemical corrosion in which two different types of metals in contact are jointly exposed to corrosive media. The corrosion of the less noble metal is thus accelerated (the metal with more negative electrode potential will become the anode and corrode). e.g. * zinc and copper metals,* steel pipe connected to copper plumbing.

Figure. I. A. 5. Schematic representation of galvanic corrosion **[11]**.

I. A. 4. 5. Intergranular corrosion

Intergranular corrosion is a localized form of corrosion and is observed mainly in case of alloys; which is often a preferential attack on the grain boundary phases or the zones immediately adjacent to them. Little or no attack is observed on the main body of the grain. This results in the loss of strength and ductility. The attack is often rapid, penetrating deeply into the metal and causing failure. When it occurs, the surface of the material can appear unattacked, but the mechanical strength of the alloy can deteriorate slowly or rapidly.

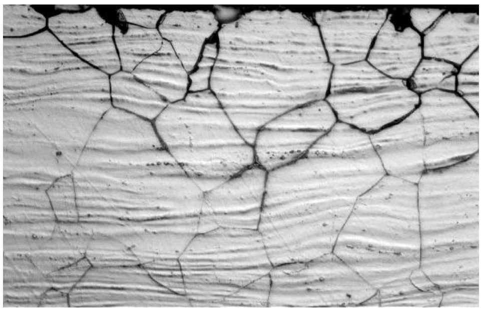

Figure. I. A. 6. Schematic representation of intergranular corrosion **[11].**

I. A. 4. 6. Erosion corrosion

The term "erosion" applies to deterioration due to mechanical force. The rate of deterioration or attack on a metal accelerates or increases due the relative movement between a caustic medium and the surface of metal. Generally, this movement occurs fast, because of involvement of mechanical abrasion. The removal of metal from the surface takes place in the form of dissolved ions, or sometimes in the form of solid corrosion products which are wiped from the metal surface [12]. Erosion corrosion is usually caused by an aqueous or gaseous flow over the metal surface or impinging upon it.

Figure. I. A. 7. Schematic representation of erosion corrosion [11].

I. A. 5. Common corrosive agents

a) Acids

Strong acids such as sulfuric acid, halogen acids and nitrous oxide compounds, will severely corrode most of the alloys [13].

b) Alkalies

Although alkalies, are generally not as corrosive as acids, aluminum and magnesium alloys are exceedingly prone to corrosive attack by many alkaline solutions unless the solutions contain a corrosion inhibitor [13].

c) Salts

Most salt solutions are good electrolytes and can promote corrosive attack. Some stainless-steel alloys are resistant to attack by salt solutions but aluminum alloys, magnesium alloys, and other steels are extremely vulnerable [13].

d) The Atmosphere

The major atmospheric corrosive agents are oxygen and airborne moisture, both of which are in abundant supply. Corrosion often results from the direct action of atmospheric oxygen and moisture on metal, and the presence of additional moisture often accelerates corrosive attack, particularly on ferrous alloys. However, the atmosphere may also contain other corrosive gases and contaminants, particularly industrial and marine environments, which are unusually corrosive [13].

- In areas where there are chemical industrial plants, other corrosive atmospheric contaminants may be present in large quantities, the most common of which are partially oxidized sulfur compounds. When these sulfur compounds combine with moisture, they form sulfur-based acids that are highly corrosive to most metals, but such conditions are usually confined to a specific locality.
- Marine atmospheres contain chlorides in the form of salt particles or droplets of salt saturated water. Since salt solutions are electrolytes, they attack metals and alloys and caused a sever corrosion.

e) Water

The corrosivity of water will depend on the type and quantity of dissolved and organic impurities and dissolved gasses (particularly oxygen) in the water. One characteristic of water which determines its corrosivity is the conductivity or its ability to act as an electrolyte and conduct a current.

I. A. 6. The consequences and costs of corrosion

Corrosion process becomes a problem of worldwide significance that causes a huge economic and security damages in developed and developing countries, which often more serious than the simple loss of mass of metal **[14-16]**. Along with the economic and safety losses, corrosion also causes environmental problems due to leakage of toxic chemicals and solvents through corroded metallic equipments **[17]**. The national association of corrosion engineers (NACE) proclaimed $2.5 trillion as yearly expenditure of corrosion, which is the comparable amount to about 2–4% of the gross national product GDP. In South Africa, Australia, China, India and Japan cost of corrosion are US $ 9.6 billion (R130-billion), US $ 32 billion, US $ 310 billion (2127.8 billion RMB; 3.34% GDP), US $100- billion and US $ 9.2 billion (2.5 trillion Yen; 2.0% GDP), respectively **[18, 19]**. Thus, corrosion should be given highest attention and adequate preventive measures to avoid economic loss and loss of living beings. Some of the major harmful effects of corrosion can be summarized as follows **[20-22]**:

- The reduction of metal thickness affects the physical, chemical, and mechanical properties of the metals.
- Shutdowns of industrial plants such as nuclear plants, process plants, and refineries lead to severe problems for industry and consumers.
- Loss of time involved in the repair of industrial equipment due to corrosion.

- Loss of efficiency: Accumulated corrosion products on pipelines and heat exchanger tubing reduce the heat transfer and piping capacity.
- Product contamination: Corrosion products may spoil chemical preparations of dyes, soap, packaged goods, and pharmaceuticals.
- The unexpected failure of equipment or component affects safety which may result in fire, explosion, or release of toxic products where human safety will be questionable.

1. A. 7. Importance of corrosion studies

The importance of corrosion studies is two folds. The first is economic, including the reduction of material losses resulting from the wasting away or sudden failure of piping, tanks, metal components of machines, ships, hulls, marine, structures…etc. The second is conservation, applied primarily to metal resources, the world's supply of which is limited, and the wastage of which includes corresponding losses of energy and water resources accompanying the production and fabrication of metal structures

Nowadays it is necessary to pay more attention to metallic corrosion than as it was done earlier due to many causes **[23-25]**:

- High usage of metals in different manufacturing and engineering industries.
- Use of high strength alloys, which are more vulnerable to certain types of corrosive attack.
- Use of rare and costly metals whose protection needs special precautions.
- Increase of pollution in both air and water leading to a more corrosive environment.
- Corrosion contaminates products such as pharmaceuticals, food, and dairy products.
- Strict safety standards of operating equipment which may fail in a catastrophic manner as a result of corrosion.

I. A. 8. Corrosion rate

When exposed to a corrosion medium, metals tend to enter into a chemical union with the elements of the corrosion medium, forming stable compounds similar to those found in nature. When metal loss occurs in this manner, the compound formed is referred to as the corrosion product and the surface is referred to as having been corroded and the corrosion rates for materials can be expressed in many different ways depending on the application and personal preferences [11]:

- as a mass loss per unit of surface and per unit of time (ex: $mg/h.cm^2$)
- as corroded depth per unit of time (ex: mm/year)
- as a current density (ex:mA/cm^2)

I. A. 9. Causes and factors influencing corrosion rate

Corrosion is a complex phenomenon and influenced by numerous factors such as temperature, pressure, aggressiveness of the electrolytic medium and presence of metallic impurities. Generally, pure metals and most of the metallic alloys are chemically unstable thereby react with the constituents of the surrounding environment by chemical or/ and electrochemical reactions to form more stable corrosion products. Therefore, corrosion is an electrochemical, thermo-dynamical and spontaneous process of slow conversion of less stable form of metallic materials into more stable forms. The major influencing factors which may influence the corrosion process are [26]:

I. A. 9. 1. Nature of the metal

Some metals have high tendency to corrode compared to others. In general, the metal with lower electrode potential is more reactive and is more susceptible for corrosion and metal with high electrode potential is less reactive and less susceptible for corrosion. For example, metals like Fe, Mg, Zn etc., have low electrode potential and undergo corrosion very easily whereas noble metals like Ag, Au, and Pt have higher electrode potential. Their corrosion rates are negligible. But there are few exceptions for this general trend as some metals show the property of passivity like Al, Cr, Ti, etc. Variations in size and shape of metal can indirectly affect the corrosion resistance property of the metal. The geometry of the material also influences the corrosion [27].

I. A. 9. 2. External material on the surface

Presences of foreign materials such as: soil, atmospheric dust, oil and grease on the surface of the metal greatly influence the corrosive nature of the metal.

I. A. 9. 3. Relative areas of anode and cathode

The ratio of the anodic and cathodic area also affects corrosion. If anodic area is small, localized and rapid, corrosion occurs because of high current density in a smaller anodic area and the demand for electrons of the large cathodic area can be met by smaller anodic areas by increasing corrosion rate **[28]**.

I. A. 9. 4. Temperature and pH

The impact of the temperature on the corrosion rate of the material is usually very high, because the speed of electrochemical attack is increased with temperature and moist climate. The corrosion rate is maximum when the environment is more acidic ($pH<5$) and minimum when the environment is more alkaline ($pH>11$). In general, acidic medium is more corrosive than alkaline or neutral medium **[29, 30]**.

I. A. 9. 5. Nature of the electrolyte

The nature of the electrolyte also affects the rate of corrosion. The presence of chloride ions destroys the protective film formed on the surface of the metal and increase corrosion.

I. A. 10. Corrosion of carbon steel

Steel is a metal alloy whose major component is iron, with carbon content between 0.02% and 1.7% by weight. Carbon steel, the most widely used engineering material, accounts for approximately 85 %, of the annual steel production worldwide. Despite its relatively limited corrosion resistance, carbon steel is used in large tonnages in marine applications, nuclear power and fossil fuel power plants, transportation, chemical processing, and petroleum production and refining, pipelines mining, construction and metal-processing equipment. The cost of metallic corrosion to the total economy must be measured in hundreds of millions of dollars per year. Because carbon steel represents the largest single class of alloys in use, both in terms of tonnage and total cost, it is easy to understand that the corrosion of carbon steel is a problem of enormous practical importance. This is the reason for the existence of entire industries devoted to provide protective systems for iron and steel **[31]**.

I. A. 11. Aqueous corrosion of carbon steel

Carbon steel pipes and vessels are often required to transport water or submerged in water to some extent during service. This exposure can be under conditions of varying temperature, flow rate, pH and other factors all of which can alter the rate of corrosion. At low pH, the evolution of hydrogen tends to eliminate the possibility of protective film formation so that steel continues to corrode. But in alkaline solutions, the formation of protective films greatly reduces the corrosion rate. The greater the alkalinity, the slower the rate of attack. In neutral solutions, other factors such as aeration became determining, so that generalization becomes more difficult. The corrosion of steels in aerated well-water is about the same overall as in aerated fresh water, but this is somewhat misleading because the improved electrical conductivity of seawater can lead to increased pitting. The concentration cells can operate over long distance, and this leads to a more non-uniform attack than in fresh water. Alternate cycling through immersion and exposure to air produces more pitting attack than continuous immersion. There is a need to protect the carbon steel from corrosion which led to many studies in the past **[31]**.

I. A. 12. Corrosion prevention methods

Corrosion is destructive and silent operating processes. Corrosion control is a process aimed at decreasing the corrosion rate and increasing the inhibition efficiency in corrosive environment to a tolerable level. Hence, prevention of corrosion of substrate was achieved by changing the substrate (metal), varying the environment or isolating the substrate from the corrosive species or by altering the substrate electrode potential. There are many different

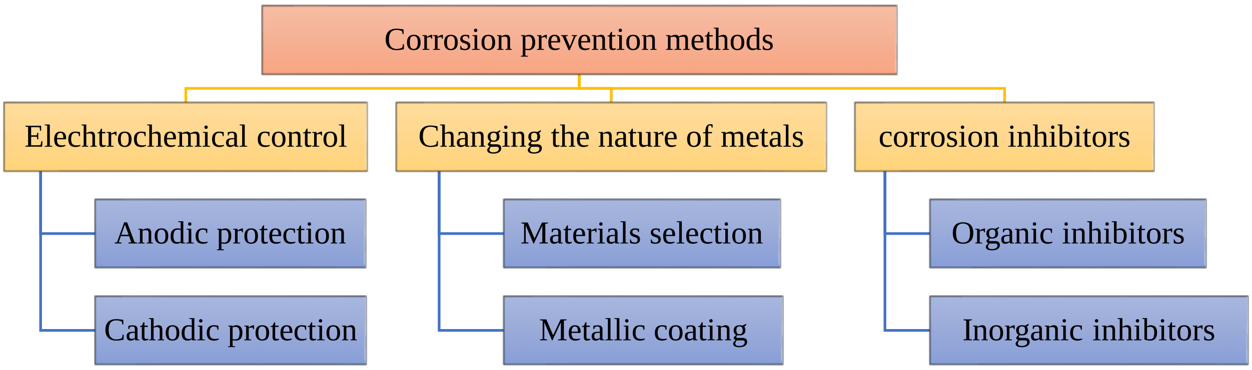

methods of corrosion prevention and control. Each offers its own complexities and purposes. In general, the approach to control most corrosion is to understand the corrosion mechanism involved and remove one or more of the elements of the corrosion cell. The techniques adopted to prevent corrosion can be classified under following headlines **[11]** (**Figure I. A. 8**):

Figure. I. A. 8. Corrosion prevention methods

I. A. 12. 1. Electrochemical control

It well known that the corrosion is an electrochemical process and the rate of corrosion may be controlled by changing the electrode potential of the metal surface including cathodic protection and anodic protection.

- ✓ **Anodic protection**

The application of anodic protection in preventing the corrosion is an old method, which based on the formation of a protective film on the metal by applying an extern anodic current and controlling the electrode potential in a zone where the metal is passive. Generally, the dissolution rate of the metal increase when a metal is made as anode and current is applied, which make it applicable for only those metals and alloys that exhibit active – passive behavior such as nickel, iron and titanium. This method is most often used in highly corrosive environment to protect metal immersed in solution with uncommonly acidic or basic qualities **[32]**.

- ✓ **Cathodic protection**

The technique of cathodic protection is used to control the corrosion of a metal surface by making it cathode of an electrochemical cell, i.e., making it completely cathodic allowing no site of it to act as anode. Cathodic protection is effected by forcing the potential to a negative region where the metal is completely stable. This can be done by using a sacrificial anode made from a more reactive metal, or using an external power supply to change the amount of charge on the metal surface. The principle involved in cathodic protection is to change the electrode potential of the metallic article or structure so that it lies in the immunity region.

Within this region the metal is in the stable form of the element and corrosion reactions are therefore impossible. Cathodic protection may be regarded as the most elegant form of corrosion protection as it renders the metal completely unreactive. It can, however, be fairly expensive due to the consumption of electric power or the extra metals involved in controlling the potential within this region **[33]**.

I. A. 12. 2. Changing the nature of metals

- ✓ **Material Selection**

- The use of noble metal like gold, platinum, titanium is first choice in accordance to material selection. These metals are most resistant to corrosion. But these metals are precious and cannot be used for general purpose.

- We should use pure metal to avoid corrosion because impurities in metal are the main reason for heterogeneity that decreases corrosion resistance of metal. Therefore, the corrosion resistance of any metal can be improved by its purity. But it is not possible to produce a metal of high purity in many cases and the pure metals has high cost and have some disadvantage of insufficient mechanical properties like low strength and softness, although a less amount of impurity leads to corrosion.

- Therefore the use of metal alloys is the better choice to prevent the corrosion. We can increase the corrosion resistance of most metals by alloying them with suitable element. But alloys should be completely homogeneous for maximum corrosion resistance such as: **(a)** Stainless steel containing chromium in iron. Chromium in stainless steel produces an oxide film which protects the steel from further attack, **(b)** Nimonic Alloys (Ni Cr-Mo-alloy) are used in gas turbines, and **(c)** Cubro Nickel alloys (70% Cu + 30% Ni) are used for condenser tubes.

- ✓ **Protective coating**

Metal can be protected from corrosion by covering the surface by means of protective coating which acts like a barrier film between metal surface and atmospheric oxygen and humidity. Protective coatings can be classified into the following two classes: organic and inorganic coatings.

I. A. 12. 3. Corrosion inhibitors

Inhibitors are chemicals that react with a metallic surface, or the environment this surface is exposed to, giving the surface a certain level of protection. Inhibitors often work by adsorbing themselves on the metallic surface, protecting the metallic surface by forming a film. Inhibitors slow corrosion processes by:

- ✓ Increasing the anodic or cathodic polarization behavior (Tafel slopes)
- ✓ Reducing the movement or diffusion of ions to the metallic surface
- ✓ Increasing the electrical resistance of the metallic surface

Table I. A. 1. Some Corrosive Systems and the Inhibitors Used to Protect Them [34]

system	Inhibitor	Metals	Concentration
acids			
HCl	Ethylaniline	Fe	0.5%
	MBT*	Fe	1%
	Pyridine + phenylhyrazine	Fe	0.5% + 0.5%
	Rosin amine + ethylene oxide	Fe	0.2%
H_2SO_4	Phenylacridine	Fe	0.5%
H_3PO_4	Nal	Fe	200 ppm
Others	Thiourea	Fe	1%
	Sulfonated castor oil	Fe	0.5 – 1.0%
	As_2O_3	Fe	0.5%
	Na_3AsO_4	Fe	0.5%
Water			
Drinking Water	$Ca(HCO_3)_2$	Steel , cast iron	10ppm
	Polyhosphate	Fe, Zn, Cu,Al	5 – 10 ppm
	$Ca(OH)_2$	Fe, Zn, Cu	10 ppm
	Na_2SiO_3	Fe	10 – 20 ppm
Cooling	$Ca(HCO_3)_2$	Steel , cast iron	10 ppm
	Na_2CrO_4	Fe, Zn, Cu	0.1%
	$NaNO_2$	Fe	0.05%
Boilers	NaH_2PO_4	Fe, Zn, Cu	10 ppm
	Polyhosphate	Fe, Zn, Cu	10 ppm
	Morpholine	Fe	Variable
	Hydrazine	Fe	O_2 scavenger
	Ammonia	Fe	Neutralizer
	Octadecylamine	Fe	Variable
Seawater	Na_2SiO_3	Zn	10 ppm
	$NaNO_2$	Fe	0.5%
	$Ca(HCO_3)_2$	All	pH dependent
	NaH_2PO_4 + $NaNO_2$	Fe	10 ppm + 0.5 %

More details about the corrosion inhibitors will be found in the next section

I. A. 13. References

[1] W.v. Baeckmann, The History of Corrosion Protection, Handbook of Cathodic Corrosion Protection, Elsevier1997, pp. 1-26.

[2] C. Verma, M. Quraishi, E.E. Ebenso, I. Bahadur, A green and sustainable approach for mild steel acidic corrosion inhibition using leaves extract: experimental and DFT studies, Journal of Bio-and Tribo-Corrosion 4(3) (2018) 33.

[3] C. Fiaud, C. Lemaitre, N. Pébère, Corrosion et anticorrosion, chapitre 13, Lavoisier, Paris (2002).

[4] K. Heusler, D. Landolt, S. Trasatti, Electrochemical corrosion nomenclature (Recommendations 1988), Pure and applied chemistry 61(1) (1989) 19-22.

[5] A. Norma, G15, Standard Terminology Relating to Corrosion and Corrosion Testing Corrosion and Corrosion Testing. Designation: G 15 7.

[6] M. Chakravarthy, Synthesis and corrosion inhibition study of isoniazide nicotinamide and dapsone derivatives for mild steel in acid media.

[7] T. Chaitra, Synthesis and corrosion inhibition behaviour of some new heterocyclic derivatives on mild steel in acid media.

[8] R.W. Revie, Corrosion and corrosion control: an introduction to corrosion science and engineering, John Wiley & Sons2008.

[9] M.G. Fontana, N. Greene, Corrosion Engineering McGraw Hill, New York (1987) 5-30.

[10] B. Wiersma, A Structural Integrity Assessment of the Tank Farm Waste Transfer System, (2006).

[11] G. Palanisamy, Corrosion inhibitors, Corrosion inhibitors (2019) 1-24.

[12] S. Abd El-Maksoud, A. Fouda, Some pyridine derivatives as corrosion inhibitors for carbon steel in acidic medium, Materials chemistry and physics 93(1) (2005) 84-90.

[13] J. Sathiyabama, Dyes as corrosion inhibitors for carbon steel in sea water.

[14] A. OO, C. NWAOKOCHA, A. ADESANYA, Evaluation of Corrosion Cost of Crude oil Processing Industry, Journal of Engineering Science and Technology 7(4) (2012) 517-528.

[15] Z. Zhang, H. Ba, Z. Wu, Y. Zhu, The inhibition mechanism of maize gluten meal extract as green inhibitor for steel in concrete via experimental and theoretical elucidation, Construction and Building Materials 198 (2019) 288-298.

[16] M. Ouakki, M. Galai, Z. Benzekri, C. Verma, E. Ech-chihbi, S. Kaya, S. Boukhris, E.E. Ebenso, M.E. Touhami, M. Cherkaoui, Insights into corrosion inhibition mechanism of mild steel in 1 M HCl solution by quinoxaline derivatives: electrochemical, SEM/EDAX, UV-

visible, FT-IR and theoretical approaches, Colloids and Surfaces A: Physicochemical and Engineering Aspects (2020) 125810.

[17] K.E. Perumal, Corrosion risk analysis, risk based inspection and a case study concerning a condensate pipeline, Procedia Engineering 86 (2014) 597-605.

[18] M. Goyal, S. Kumar, I. Bahadur, C. Verma, E.E. Ebenso, Organic corrosion inhibitors for industrial cleaning of ferrous and non-ferrous metals in acidic solutions: A review, Journal of Molecular Liquids 256 (2018) 565-573.

[19] C. Verma, E.E. Ebenso, I. Bahadur, M. Quraishi, An overview on plant extracts as environmental sustainable and green corrosion inhibitors for metals and alloys in aggressive corrosive media, Journal of molecular liquids 266 (2018) 577-590.

[20] J.C. Scully, The fundamentals of corrosion. 2, (1978).

[21] Z. Ahmad, Principles of corrosion engineering and corrosion control, Elsevier2006.

[22] S. Umoren, Polymers as corrosion inhibitors for metals in different media-A review, The open corrosion journal 2(1) (2009).

[23] P.R. Roberge, Corrosion inspection and monitoring, John Wiley & Sons2007.

[24] H. Kanematsu, D.M. Barry, Corrosion control and surface finishing, Springer2016.

[25] D. Landolt, Corrosion and surface chemistry of metals, CRC press2007.

[26] R. Piere, Corrosion Engineering-Principles and Practice, TheMcGraw-Hill Companies Inc. USA, 2008.

[27] D. Gurudatt, Synthesis of some novel nitrogen containing heterocycles and study of their antioxidant activity and corrosion inhibition performance on mild steel.

[28] P. Preethi Kumari, Aromatic hydrazide derivatives as corrosion inhibitors for mild steel in hydrochloric acid medium.

[29] M. Pourbaix, Lectures on electrochemical corrosion, Springer Science & Business Media2012.

[30] D. Singh, R. Chaudhary, B. Prakash, C. Agarwal, Inhibitive efficiency of some substituted thioureas for the corrosion of aluminium in nitric acid, British Corrosion Journal 14(4) (1979) 235-239.

[31] E. Dharmaraj, C. Pragathiswaran, P. Govindhan, P.A. Sahayaraj, A.J. Amalraj, V. Dharmalingam, Natural Plants as a Source of Green Corrosion Inhibitors on Mild Steel in Hydrochloric Acid.

[32] D. Angeline Sakila, New benzotriazole derivatives as corrosion inhibitors for copper in aqueous media by electro analytical and surface characterization studies.

[33] S. Masroor, Studies on some new surfactants as corrosion inhabitors, Aligarh Muslim University, 2014.
[34] B. Rani, B.B.J. Basu, Green inhibitors for corrosion protection of metals and alloys: an overview, International Journal of corrosion 2012 (2012).

Section B

Inhibitors of Corrosion

"Research is to see what everybody has seen and think what nobody has thought."
Albert Szent-Gyorgyi

I. B. 1. Definition of inhibitors

An inhibitor is a substance which retards corrosion when added to an environment in small concentrations [1]. Inhibitors may also be defined on electrochemical basis as substances that reduce the rates of either partial anodic (metal dissolution) or cathodic (H^+ or O_2 reduction) reaction or both, which minimize the loss of metal, by either acting as a barrier by forming an adsorbed layer or retarding the cathodic, the anodic, or both processes [2]. A very large number of inhibitors are reported in the literature for various metals in different environments. Inhibitors are often easy to apply and offer the advantage of in-situ application without causing any significant disruption to the process. A schematic representation of inhibitor process is shown in **Figure. I. B. 1.**

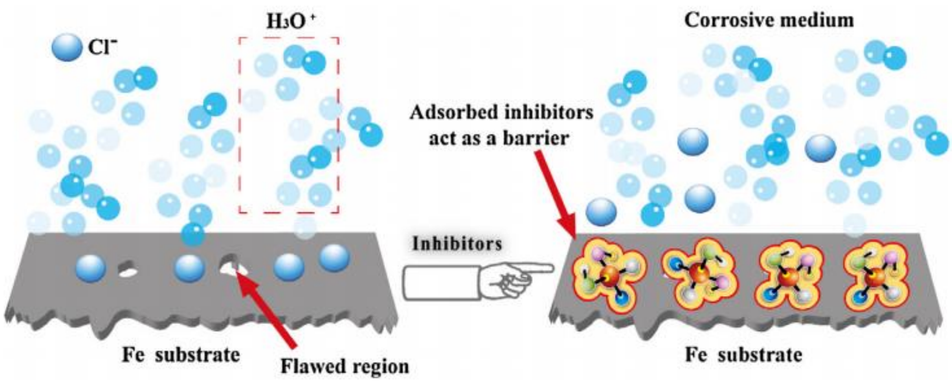

Figure. I. B. 1. Schematic diagram of the corrosion inhibition mechanism [3].

An efficient corrosion inhibitor must satisfy the following conditions [4]:

- It must effective at very low concentration .
- It must effective at higher temperatures
- It should be effective over long range
- Stable in the presence of other constituents
- Compatible with non-toxicity standards
- Easy availability and low cost

Inhibitors increase inhibition efficiency and decrease the corrosion rate by [5]:

- Adsorption of ions/molecules onto the metal surface
- Increasing or decreasing the anodic and/or cathodic reaction
- Decreasing the diffusion rate for reactants on the surface ofthe metal
- Decreasing the electrical resistance ofthe metal surface

I. B. 2. Global demand of corrosion inhibitors

Currently, corrosion inhibitors are attracting a lot of attention and they become of top priority in several fields especially in the industrial application or during any project design and operation especially in areas where metals are used, for the simple reason that the use of these inhibitors can extend the life of the materials and thus increase earnings. The corrosion inhibitors market has thus observed an increase in demand. Corrosion inhibitors market is grouped based on application, functionality, and geography. The application segment include: power generation, paper, oil and gas industries, metal and mining, chemical processing, and the others. By functionality, corrosion inhibitors market is divided into organic and inorganic inhibitors. Geographically, the market is segmented into North America, Europe, Asia-Pacific, and the rest of the world. According to the report of Transparency Market Research, corrosion inhibitors demand globally stood at 4,425.9 kilo in 2012 with the cost pinned at US$ 5.20 billion. The organic corrosion inhibitors led the market by almost 70% and Asia-Pacific held the largest share (>35%) in terms of demand while the North American and European corrosion inhibitors market jointly held more than 50%. In 2013, inhibitors demand increased to 4,659.8 kilo and is predicted that the global inhibitors' market would grow at 5% during 2015-2022 market year with the cost estimated to be US$9.2 billion by 2022 [6].

I. B. 3. Utilization conditions [7]

A corrosion inhibitor can be used as method of protection:

- ✓ As ***a permanent protection***, the inhibitor allows the use of metallic materials (non-alloyed ferrous example) under satisfactory conditions of resistance to corrosion.
- ✓ As a ***temporary protection*** during a period when the piece or installation is particularly susceptible to corrosion (storage, stripping, cleaning).

- ✓ As a ***supplementary protection*** to improve the resistance against the corrosion, in the case of the surface coating.

I. B. 4. Classification of corrosion inhibitors

Corrosion inhibitors can be classified based on mechanism, environment and mode of protection **[8-11].**

I. B. 4. 1. Based on electrode process

a. Anodic inhibitors

Anodic inhibitors are often called passivating inhibitors cause a large anodic shift of the corrosion potential of the metal in the noble direction with the formation of a passive film (slow the anodic reaction) **Figure. I. B. 2.** There are two types of passivating inhibitors: oxidizing anions, such as chromate, nitrite, and nitrate, that can passivate steel in the absence of oxygen and the nonoxidizing ions, such as phosphate, tungstate, and molybdate that require the presence of oxygen to passivate steel **[12]**. Anodic inhibitors build a thin protective film along the anode and increasing their potential and thus slow down the corrosion reaction **[13]**. Anodic inhibitors are also known as "dangerous" inhibitors because insufficient inhibitor concentration can cause pitting corrosion **[14]**.

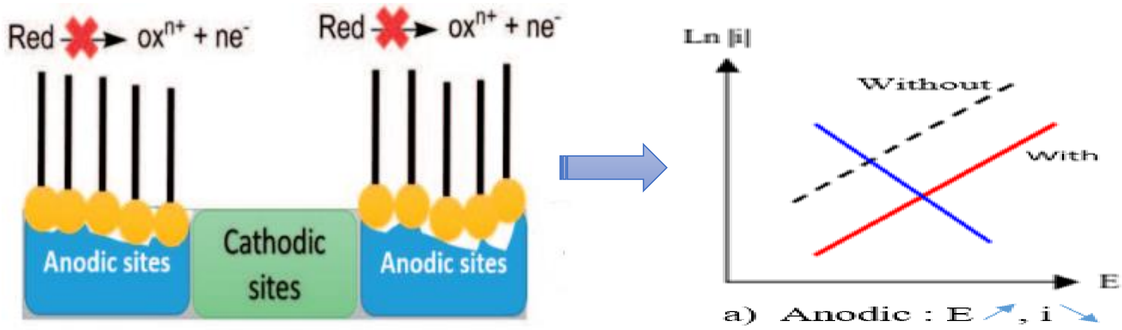

Figure. I. B. 2. Effect of addition of the anodic inhibitor **[7]**.

b. Cathodic inhibitors

Cathodic inhibitors control corrosion by either decreasing the reduction rate or by precipitating selectively on the cathodic sites (cathodic precipitators). Cathodic inhibitors are effective when they slow down the cathodic reaction. Cathodic inhibitors shift the corrosion potential to the anodic direction **[15, 16]**. Here the cations migrate towards the cathode surfaces where they are precipitated chemically or electrochemically and thus block these surfaces. The inhibiting action of cathodic inhibitors takes place by three mechanisms:

- ✓ ***Cathodic poisons:*** The cathodic reduction process is suppressed by impeding the hydrogen recombination and mode of protection discharge but increase the tendency of the metal to be susceptible to hydrogen induced cracking.
- ✓ ***Cathodic precipitates*:** Compounds such as calcium, magnesium will precipitate as oxides to form a protective layer which acts as a barrier on the metal surface.
- ✓ ***Oxygen scavenger*:** These compounds react with oxygen present in the system to form a product and reduce corrosion.

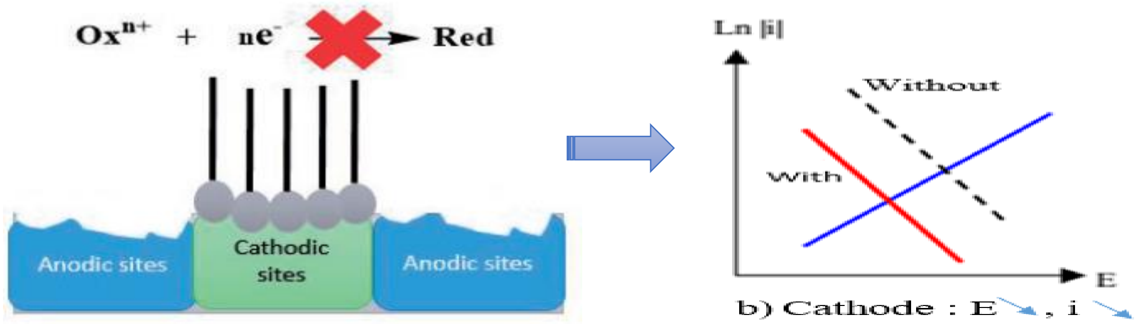

Figure. I. B. 3. Effect of addition of the cathodic inhibitor **[7].**

c. Mixed inhibitors

These inhibitors retard both the anodic and cathodic processes involved in the corrosion process at the same time (*via* **Figure. I. B. 4**) because they affect the oxidation and reduction reaction, with little change in the corrosion potential (less than 85 mV) **[17, 18]**.

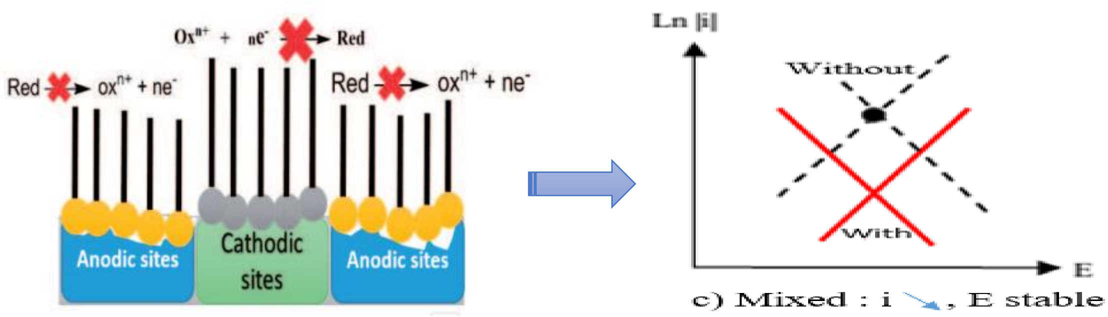

Figure. I. B. 4. Effect of addition of the mixed inhibitor **[7].**

Mixed inhibitors protect the metal in three possible ways: physical adsorption, chemisorption and film formation. Physical (or electrostatic) adsorption is a result of electrostatic attraction between the inhibitor and the metal surface. When the metal surface is positively charged, adsorption of negatively charged (anionic) inhibitors is facilitated (**Figure. I. B. 5**).

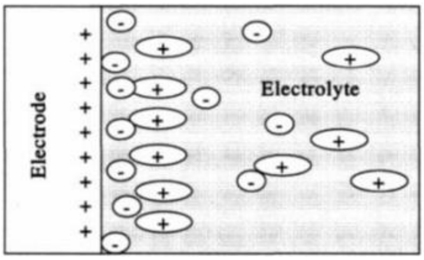

Figure. I. B. 5. Adsorption of negatively charged inhibitor on a positively charged metal surface **[19]**.

Positively charged molecules acting in combination with a negatively charged intermediate can inhibit a positively charged metal. Anions, such as halide ions, in solution are adsorbed on the positively charged metal surface, and organic cations subsequently are adsorbed on the dipole (**Figure. I. B. 6**).

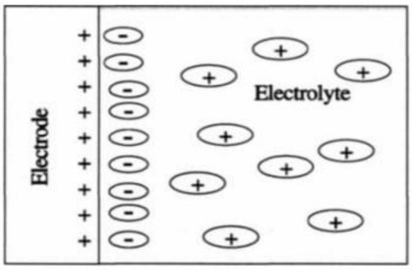

Figure. I. B. 6. Synergistic adsorption of positively charged inhibitor and anion on a positively charged metal surface **[19]**.

Physically adsorbed inhibitors interact rapidly, but they are also easily removed from the surface. Increase in temperature generally facilitates desorption of physically adsorbed inhibitor molecules. The most effective inhibitors are those that are chemically adsorbed (chemisorb), a process that involves charge sharing or charge transfer between the inhibitor molecules and the metal surface.

I. B. 4. 2. Based on environment

a. Acidic environment inhibitors

- ***Inorganic inhibitors:*** The oxides such as As_2O_3, Sb_2O_3 have been reported as inhibitors in acid media. These substances get deposited in the form of metal oxide and increase the hydrogen over-voltage and subsequently reduce the corrosion rate **[20]**. The addition of heavy metal ions like Pb^{2+}, Mn^{2+}, Cd^{2+} inhibit corrosion of iron in acids, due to deposition of these metal ions over the iron surface **[21].**

- ***Organic inhibitors:*** Organic inhibitors are substances, which possess at least one functional group considered as the reaction center for the adsorption process. Organic compound containing oxygen, nitrogen, sulfur with multiple bonds have been reported as good corrosion inhibitors **[22-24]**. Organic inhibitors can be anodic, cathodic and mixed type based on their reaction at the metal surface and potential. Cruz et *al*. **[25]** have shown that the effectiveness of an organic inhibitor is related to its adsorption properties, which depend on the nature and surface condition of the metal, as well as the corrosive environment.

b. Alkaline inhibitors

Metals are prone to corrosion in alkaline solutions. Many organic compounds are often used as inhibitors for metals in basic solution. Compounds such as thiourea, substituted phenols, naphthol, β-diketone, etc., have been used as effective inhibitors in basic solutions due to the formation of metal complexes.

c. Neutral inhibitors

Inhibitors which are effective in acidic solutions do not function effectively in neutral solutions, since the mechanism is different in the two solutions **[26-28]**. In neutral solutions, the interaction of inhibitors with oxide covered metal surface and prevention of oxygen reduction reaction at the cathodic sites takes place. Such inhibitors protect the surface layers from aggressiveness. Some surface active chelating inhibitors have been found to be efficient inhibitors in near-neutral solutions **[29]**.

d. Vapor phase inhibitors

Vapor-phase corrosion inhibitors or volatile corrosion inhibitors (VCIs) are similar to organic adsorption type inhibitors and possess very high vapor pressure. In use, such inhibitors are placed in the vicinity of the metal to be protected, as they are transferred to the metal surface by sublimation followed by condensation and the adsorption of the inhibitor takes place **Figure. I. B. 7**. For example, dicyclohexyl ammonium nitrite and benzothiazole are used for protecting copper whereas phenylthiourea and cyclohexylamine chromate are used for protecting brass. Dicyclohexylamine nitrite protects both ferrous and non-ferrous metals/alloys **[7]**.

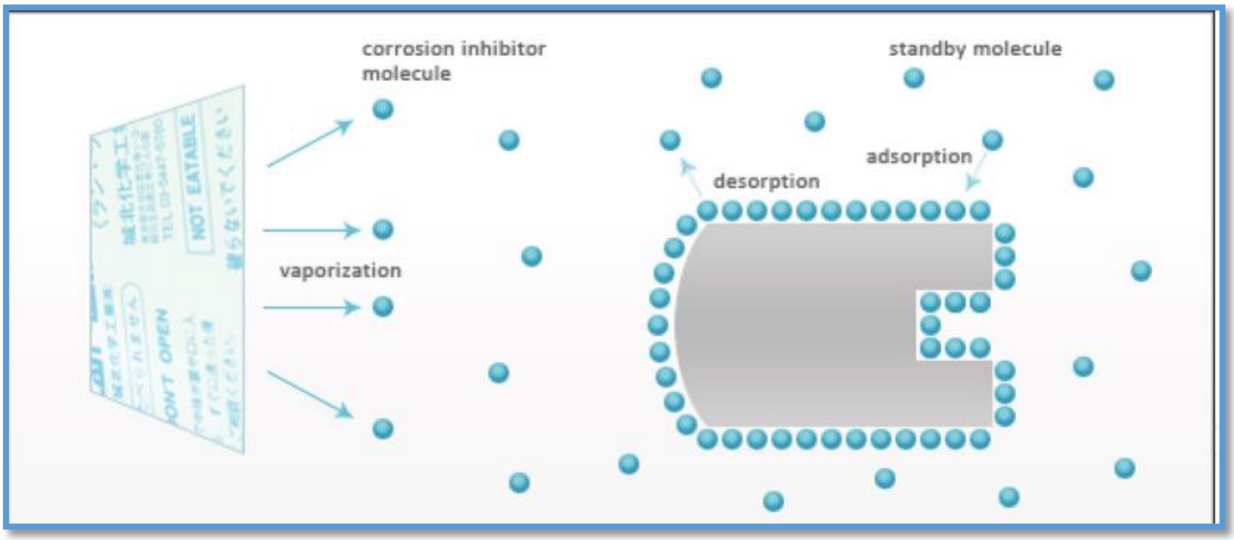

Figure. I. B. 7. Schematic representation of volatile inhibitors [7].

I. B. 4. 3. Based on mode of protection

a. Adsorption inhibitors

This class of inhibitors represents the largest class of corrosion inhibiting substances. In general, they are organic compounds which are adsorbed on the metal surface and suppress metal dissolution and reduction reaction. Generally, they effect both cathodic and anodic reactions equally [7]. Examples: Compounds containing lone pairs of electrons such as nitrogen sulfur and oxygen atoms.

b. Pickling inhibitors

Generally pickling inhibitors function by forming an adsorbed layer on the metal surface, which essentially blocks the discharge of H^+ ion and dissolution of metal ions. Compounds serving as pickling inhibitors require, by and large, a favorable polar group or groups by which the molecule can attach itself to the metal surface.

c. Precipitation inhibitors

These are compounds that forms precipitates on the metal surface, and hence provide a protective film [30]. Hard water is less corrosive compared to soft water because hard water is high in calcium and magnesium so their salts precipitate on the metal surface to form a protective film. The most common precipitation inhibitors are the silicates and the phosphates.

d. Synergistic inhibitors

Single inhibitors are very rarely used in systems such as cooling water systems. More often, a combination of anodic and cathodic inhibitors is used to obtain better corrosion protection properties. Synergistic inhibitors are the blends which are produced by mixing of multi-inhibitors **[21]**. Examples include chromate-phosphates, polyphosphate-silicate, zinc-tannins and zinc-phosphates.

e. Environment friendly or green corrosion inhibitors

The use of traditional corrosion inhibitors, is now limited because of increasing concept of "green chemistry" in field of science, technology and engineering **[31-33]**. In practice, corrosion inhibition studies have become oriented towards human health and safety considerations. For this purpose, the researchers are concentrating on the use of eco-friendly compounds such as plant extracts which contain many organic compounds. Alkaloids, amino acids, pigments and tannins are used as green alternatives for the toxic and hazardous compounds. Due to biodegradability, Eco friendliness, low cost and easy availability the extracts of some common plants and plant products have been studied as corrosion inhibitors for various metals and alloys under different environments **[33, 34]**.

I. B. 5. Action mode of the corrosion inhibitors in liquid phase

Although different inhibition mechanisms have been identified for inhibitors, inhibition usually results from one or more of the following mechanisms:

I .B. 5. 1. Formation of the diffusion barrier

In this type of inhibition of corrosion, an adsorbed inhibitor may form a surface layer which acts as a physical barrier to restrict the diffusion of ions or molecules into the metal surface and retard the corrosion reactions. This effect occurs particularly when the inhibiting molecules are large. A surface film of these types of inhibitors affects both anodic and cathodic reactions **[21].**

I .B. 5. 2. Blocking reaction sites

The interaction of the adsorbed inhibitor with surface metal atoms may prevent the metal atoms from participating in either anodic or cathodic reactions of corrosion. Blocking effect can decrease the number of surface metal atoms at which these reactions can occur. During this, mechanisms of the reactions are not affected, and the Tafel slopes of the polarization curves remain unchanged **[21]**.

I .B. 5. 3. Adsorption of corrosion inhibitors onto metals

The inhibitive efficiency is usually proportional to the fraction of the surface θ covered with adsorbed inhibitor. However, at low surface coverage ($\theta<0.1$), the effectiveness of adsorbed inhibitor species in retarding the corrosion reactions may be greater than at high surface coverage. Adsorption type corrosion inhibitors (mainly organic compounds) are widely used for the corrosion inhibition process. Most of the organic compounds possessing electron rich species such as nitrogen, phosphorus, oxygen and sulfur in their moieties are called as adsorption centers, which plays an important role to inhibit the metal corrosion. They inhibit the metal corrosion process by forming a thin adsorption layer on the electrode (metal) surface through chemical or physical adsorption mode **[21].**

a. Physical adsorption (physisorption)

Physical adsorption is the result of electrostatic attractive forces between inhibiting organic ions or dipoles and the electrically charged surface of the metal. The interaction between the inhibitor and the metal surface is weak (Van der Waals forces) and process is rapid because it involves relatively low, almost temperature-independent activation energies. Moreover, it is reversible, as it is characterized by low adsorption energy (typically 20 kJ/mol), which tends to decrease at increasing temperature **[35, 36]**.

b. Chemical adsorption (chemisorption)

This type of adsorption involves charge transfer or sharing from the organic corrosion inhibitor with a metal, which leads to the formation of a coordinate covalent bond. The chemisorption process takes place more slowly than electrostatic adsorption and with higher activation energy. It is essentially irreversible, with free adsorption energies as high as 40 kJ/mol or more. **[37]**. This type of absorption takes place when there are heteroatoms such as S, N and O present with lone pair electrons and/or aromatic rings in the adsorbed molecules. The adsorption strength is dependent on the electron density and polarity of the corrosion inhibitor. Increase in temperature may increase the protection efficiency of the corrosion inhibitor. Due to irreversibility of chemisorption, these inhibitors can act as prefilming substances which form protective films capable to persist in uninhibited solutions. Some inhibiting molecules may offer coupled physical and chemical adsorption with enhanced inhibiting effects.

The factors that influence the adsorption of inhibitor ions on metal surfaces are [38]:

- **Surface charge on the metal**: Adsorption may occur because of the electrostatic attractive forces between the ionic charges or dipoles on the adsorbed inhibitor and the electric charge on the metal at the metal-solution interface.
- **The functional groups and structure of inhibitor**: Inhibitors get attached to the metal surface by electron transfer and form a coordinate type of linkage leading to strong binding and effective inhibition. Species containing relatively loosely bound electrons in anions, neutral molecules, lone pair of electrons, π-electron systems associated with triple bonds or organic ring systems and the functional groups containing elements of group V or VI of the periodic table favors facile electron transfer and stronger bond formation and hence effective inhibition. The tendency to form stronger coordinate bond increases with decreasing electronegativity and follow the order, $O < N < S < P$.
- **The interaction between adsorbed inhibitor species (synergism)**: Adsorbed species may enter into various interactions on the surface of an electrode that may significantly influence their inhibitive properties and the mechanism of their action.
- **Reaction of adsorbed inhibitors**: The adsorbed inhibitor species may react usually by electrochemical reduction to form a product which is also inhibitive. Inhibition due to the added substance is termed as primary inhibition and that due to reaction products as secondary inhibition.

I. B. 6. Factors influencing inhibitor efficiency

Several structural and chemical factors determine the effectiveness of an inhibitor. For organic inhibitors the following characteristics were identified.

- If chemisorption is involved in the inhibition process its contribution to the inhibition efficiency will increase as the electronic density or electron donation ability of the reaction center increases [39].
- An increase in the carbon chain length of an amine inhibitor will enhance the inhibition efficiency [40]. This could be attributed to an increase in the electronic density due to

inductive effects, an increase in the coverage ability, hydrophobicity, and polarizability and a decrease in the solubility of the inhibitor **[41, 42]**.

- Inhibition efficiency will be affected by the ability of the inhibitor to complex with the metal or the corrosion products **[41, 43]**.

I. B. 7. Adsorption isotherm

In order to understand the corrosion adsorption processes occur onto the metal surface, the adsorption isotherm gives necessary information about the interaction between inhibitor molecules and a metal surface **[44].** It defines the degree of surface coverage (θ) of an adsorbate on the adsorbent at a given temperature. Generally, it is assumed that the degree of the metal surface covered by the inhibitor is directly proportional to the concentration of the inhibitor. That is, the surface coverage increases as the concentration of the inhibitor in the bulk solution increases. Adsorption isotherms are mathematical models that describe the distribution of adsorbate species among adsorbent. For evaluation of the nature and strength of adsorption, the experimental data are fitted to isotherm, and from the best fit, the thermodynamic data for adsorption are calculated. From the plot, the free energy of adsorption of the organic inhibitor can be obtained. Adsorption data are generally described by different adsorption isotherms, which have been listed as follow:

Langmuir: $$\boldsymbol{C/\theta = 1/K_{ads} + C} \qquad \textbf{(I. B. 1)}$$

Temkin : $$\boldsymbol{\theta = \frac{1}{\alpha}\ln K_{ads} + \frac{1}{\alpha}Ln\ C} \qquad \textbf{(I. B. 2)}$$

Freundlich: $$\boldsymbol{\ln\theta = \ln K_{ads} + \alpha\ lnC} \qquad \textbf{(I. B. 3)}$$

Where C represents the concentration of the inhibitor, θ is the fraction of the surface covered by the inhibitor, K_{ads} is the adsorption equilibrium constant and $\boldsymbol{\alpha}$ is the lateral interaction constant.

I. B. 8. References

[1] C.C. Nathan, Corrosion inhibitors, C. C. Nathan, Editor, published 1973 by NACE, 260 (1973).

[2] C.G. Dariva, A.F. Galio, Corrosion inhibitors–principles, mechanisms and applications, Developments in corrosion protection 16 (2014) 365-378.

[3] L. Guo, I.B. Obot, X. Zheng, X. Shen, Y. Qiang, S. Kaya, C. Kaya, Theoretical insight into an empirical rule about organic corrosion inhibitors containing nitrogen, oxygen, and sulfur atoms, Applied Surface Science 406 (2017) 301-306.

[4] N.O. Eddy, Green corrosion chemistry and engineering: opportunities and challenges, John Wiley & Sons2011.

[5] B. Rani, B.B.J. Basu, Green inhibitors for corrosion protection of metals and alloys: an overview, International Journal of corrosion 2012 (2012).

[6] S. Umoren, M. Solomon, Application of polymer composites and nanocomposites as corrosion inhibitors, Corrosion inhibitors, principles, mechanisms, and applications, Nova Science Publishers Inc. New York2017, pp. 27-58.

[7] S. Abbout, Green inhibitors to reduce the corrosion damage, Corrosion, IntechOpen2020.

[8] ISO8044, "Corrosion des métaux et alliages Termes principaux et définitions, Norme internationale,, Suisse, 1999.

[9] C. Fiaud, C. Lemaitre, N. Pébère, Corrosion et anticorrosion, chapitre 13, Lavoisier, Paris (2002).

[10] D. Landolt, Corrosion et chimie de surfaces des métaux, PPUR presses polytechniques1997.

[11] M.G. Fontana, W. Stactile, Corrosion Science and Technology, Plenum Press, London 1 (1970) 149.

[12] S. Frolenkova, T. Overchenko, T. Motronyuk, V. Vorobyova, I. Miroshnychenko, M. Panchenko, Passivating anions effect on the anodic behavior of steel in a converting acetate solution, Journal of Chemical Technology and Metallurgy 54(2) (2019) 443-446.

[13] A. Al-Mayout, A. Al-Suhybani, A. Al-Ameery, Corrosion inhibition of 304SS in sulfuric acid solutions by 2-methyl benzoazole derivatives, Desalination 116(1) (1998) 25-33.

[14] B. Popov, Corrosion inhibitors, Corrosion engineering. Amsterdam: Elsevier (2015) 581-97.

[15] F. Touham, A. Aouniti, Y. Abed, B. Hammouti, S. Kertit, A. Ramdani, New pyrazolic compounds as corrosion inhibitors for Iron Armco in HCI media, Bulletin of Electrochemistry 16(6) (2000) 245-249.

[16] S. Abd El-Rehim, M.A. Ibrahim, K. Khaled, 4-Aminoantipyrine as an inhibitor of mild steel corrosion in HCl solution, Journal of Applied Electrochemistry 29(5) (1999) 593-599.

[17] C. Verma, M. Quraishi, E. Ebenso, I. Obot, A. El Assyry, 3-Amino alkylated indoles as corrosion inhibitors for mild steel in 1M HCl: Experimental and theoretical studies, Journal of Molecular Liquids 219 (2016) 647-660.

[18] Y. El Aoufir, Y. El Bakri, H. Lgaz, A. Zarrouk, R. Salghi, I. Warad, Y. Ramli, A. Guenbour, E. Essassi, H. Oudda, Understanding the adsorption of benzimidazole derivative as corrosion inhibitor for carbon steel in 1 M HCl: experimental and theoretical studies, J Mater Environ Sci 8 (2017) 3290-3302.

[19] R.W. Revie, Uhlig's corrosion handbook, John Wiley & Sons2011.

[20] A. El Rehim, Corrosion inhibition and adsorption behaviour of 4-aminoantipyrine on mild steel in H_2SO_4, Corrosion Prevention and Control 46(6) (1999) 157-62.

[21] G. Palanisamy, Corrosion inhibitors, Corrosion inhibitors (2019) 1-24.

[22] V. Srivastava, J. Haque, C. Verma, P. Singh, H. Lgaz, R. Salghi, M. Quraishi, Amino acid based imidazolium zwitterions as novel and green corrosion inhibitors for mild steel: Experimental, DFT and MD studies, Journal of Molecular Liquids 244 (2017) 340-352.

[23] A. Chaouikia, H. Lgaza, R. Salghib, S.L. Gaonkarc, K.S. Bhatc, S. Jodehd, K. Toumiate, H. Ouddaa, New Benzohydrazide Derivative as Corrosion Inhibitor for Carbon Steel in a 1.0 M HCl Solution: Electrochemical, DFT and Monte Carlo Simulation Studies, Portugaliae Electrochimica Acta 37(3) (2019) 147-165.

[24] M. Chafiq, A. Chaouiki, M.R. Albayati, H. Lgaz, R. Salghi, S.K. AbdelRaheem, I.H. Ali, S.K. Mohamed, I.-M. Chung, Unveiled understanding on corrosion inhibition mechanisms of hydrazone derivatives based on naproxen for mild steel in HCl: A joint experimental/theoretical study, Journal of Molecular Liquids (2020) 114442.

[25] J. Cruz, R. Martınez, J. Genesca, E. Garcıa-Ochoa, Experimental and theoretical study of 1-(2-ethylamino)-2-methylimidazoline as an inhibitor of carbon steel corrosion in acid media, Journal of Electroanalytical Chemistry 566(1) (2004) 111-121.

[26] B. Mistry, N. Patel, S. Sahoo, S. Jauhari, Experimental and quantum chemical studies on corrosion inhibition performance of quinoline derivatives for MS in 1N HCl, Bulletin of Materials Science 35(3) (2012) 459-469.

[27] K. Khaled, Molecular simulation, quantum chemical calculations and electrochemical studies for inhibition of mild steel by triazoles, Electrochimica Acta 53(9) (2008) 3484-3492.

[28] S. Umoren, Y. Li, F. Wang, Synergistic effect of iodide ion and polyacrylic acid on corrosion inhibition of iron in H2SO4 investigated by electrochemical techniques, Corrosion Science 52(7) (2010) 2422-2429.

[29] S. Aejitha, P. Asthuri, Geethamani,"Inhibition effect of Antigonon leptopus extract on mild steel in sulphuric acid medium," Indian Journal of Applied Research 4(12) (2014) 51-53.

[30] S.H. Kumar, S. Karthikeyan, Amoxicillin as an efficient green corrosion inhibitor for mild steel in 1M sulphuric acid, J. Mater. Environ. Sci 4(5) (2013) 675-984.

[31] S.A. Umoren, U.M. Eduok, Application of carbohydrate polymers as corrosion inhibitors for metal substrates in different media: a review, Carbohydrate polymers 140 (2016) 314-341.

[32] K. Hu, J. Zhuang, C. Zheng, Z. Ma, L. Yan, H. Gu, X. Zeng, J. Ding, Effect of novel cytosine-l-alanine derivative based corrosion inhibitor on steel surface in acidic solution, Journal of Molecular Liquids 222 (2016) 109-117.

[33] C. Verma, E.E. Ebenso, I. Bahadur, M. Quraishi, An overview on plant extracts as environmental sustainable and green corrosion inhibitors for metals and alloys in aggressive corrosive media, Journal of molecular liquids 266 (2018) 577-590.

[34] C. Verma, M. Quraishi, E.E. Ebenso, I. Bahadur, A green and sustainable approach for mild steel acidic corrosion inhibition using leaves extract: experimental and DFT studies, Journal of Bio-and Tribo-Corrosion 4(3) (2018) 33.

[35] M. Ferro-Garcia, J. Rivera-Utrilla, I. Bautista-Toledo, C. Moreno-Castilla, Adsorption of humic substances on activated carbon from aqueous solutions and their effect on the removal of Cr (III) ions, Langmuir 14(7) (1998) 1880-1886.

[36] K. Khaled, Experimental and atomistic simulation studies of corrosion inhibition of copper by a new benzotriazole derivative in acid medium, Electrochimica Acta 54(18) (2009) 4345-4352.

[37] N. Hackerman, A. Makrides, Action of polar organic inhibitors in acid dissolution of metals, Industrial & Engineering Chemistry 46(3) (1954) 523-527.

[38] L. Sheir, R. Jarman, G. Burstein, Corrosion: Metal/Environment Reactions, Newnes-Butterworths, London 8 (1994) 3-8.

[39] H. Kaesche, N. Hackerman, Corrosion inhibition by organic amines, Journal of the electrochemical society 105(4) (1958) 191.

[40] P. Dupin, D. Viloria-vera, A. De savignac, A. Lattes, B. Sutter, P. Haicour, th European Symposlum on Corrosion lnhibztors, Ferrara (Italie) 301 1980.

[41] G. Trabanelli, V. Carassiti, Mechanism and phenomenology of organic inhibitors, Advances in corrosion science and technology, Springer1970, pp. 147-228.

[42] S. Raicheva, E. Sokolova, Influence of inhibitor structure and metal/solution interface on the corrosion resistance of the protected metal, Russian Journal of Electrochemistry 42(11) (2006) 1213-1223.

[43] P. Cox, R. Every, O. Riggs Jr, Study of aromatic amine inhibitors by nuclear magnetic resonance, Corrosion 20(9) (1964) 299t-302t.

[44] K. Abderrahim, T. Chouchane, I. Selatnia, A. Sid, P. Mosset, Evaluation of the effect of Tetramethylammonium hydroxide on the corrosion inhibition of A9M steel in industrial water: an experimental, morphological and MD simulation insights, Chemical Data Collections (2020) 100391.

Section C

Literature review

"Curiosity is a delicate little plant which, aside from stimulation, stands mainly in need of freedom"
Albert Einstein

I. C. 1. Introduction

Up to now numerous types of inhibitors have been developed and used for effective inhibition of metallic corrosion those can be divided into several classes or groups depending upon their nature. The utmost frequently used corrosion inhibitors are organic compounds, comprising moieties with π and non-bonding electrons, heteroatoms (N, O, S, …) and/or polar functional groups **[1, 2]**, which are of paramount importance during adsorption process of inhibitors on metal surfaces **[3, 4]**. Over the years, a vast variety of organic compounds has been tested, especially those including nitrogen "N" such as azine derivatives **[5]**, amino acids **[6]**, imines **[7]**, Schiff bases **[8]**, aminobenzonitrile **[9]** and hydrazine **[10]**. Hydrazone and its derivatives are azomethines characterized by the presence of the triatomic grouping >C=N-N<, which represent an important family of organic compounds possessing a wide variety of properties due to their both hard and soft base characters **[11]**. Due to these promising features, hydrazones are recently getting more and more interest as corrosion inhibitors **[12-15]**. Various researchers have recently reported the effectiveness of nitrogenous compounds especially hydrazone derivatives as inhibitors of corrosion in acidic medium. A review of literature on this study is presented here.

I. C. 2. Some nitrogenous compounds as inhibitors of corrosion in acidic medium

Verma *et al.* **[16]** studied the influence of three indole derivatives on corrosion inhibition of mild steel in hydrochloric acid media using gravimetric, electrochemical and morphological techniques. Quantum chemical calculations and molecular dynamics simulations were used to justify the results. One of the derivatives showed the IE (%) of 97 at optimum concentration.

R. Laggoun *et al.* **[17]** investigated the adsorption effect of a new inhibitor "p-toluenesulfonylhydrazide "p-TSH" on copper corrosion in 0.5 M HCl solution was studied by weight loss, electrochemical methods, morphological characterization and quantum chemical calculations. Electrochemical impedance spectroscopy and Potentiodynamic polarization produced the same results, indicating that "p-TSH" reduces the corrosion rate of copper as its concentration increases in acidic solutions, provided that the adsorption mechanism of the inhibitor obeyed the Langmuir isotherm.

The corrosion inhibition behavior of N80 carbon steel in CO_2^- saturated oilfield produced water using three thiadiazole derivatives with different substituent groups,

2(benzylthio)-5-methyl-1,3,4-thiadiazole"BMT",2-(benzylthio)-5-(butylthio)-1,3,4 thiadiazole "BBT", and 5-(benzylthio)-1,3,4-thiadiazole-2-thiol "BTT" using weight loss, electrochemical methods, morphological characterization (SEM, XPS and contact angle), and quantum chemical calculations were reported at various temperatures ranging from 40°C to 60 °C by **Q.H. Zhang *et al*. [18] .** The corrosion inhibition performance is in the order: BTT > BBT > BMT with maximum inhibition efficiency of 99 % at optimum concentration.

Corrosion inhibition activity of 2-amino-4-(5-hydroxy-3-methyl-1H-pyrazole-4-yl)-4H-chromene-3-carbonitrile "PCP" on N80 steel in 15% HCl was thoroughly investigated by **A. Singh *et al*. [19].** Electrochemical impedance spectroscopy, Potentiodynamic polarization, density functional theory, and molecular dynamics simulation were used to study the mechanism of formation of iron-inhibitor complex. SEM, AFM, UV-vis spectroscopy and contact angle were used to confirm the formation of protective inhibitory film. The results confirmed that "PCP" is a mixed type inhibitor and reduces the corrosion process effectively at 400 mg/L concentration with 98.4% efficiency.

Y. Boughoues *et al*. [20] synthesized two nitrogenous compounds namely, N-[(2E)-3-phenylprop-2-en-1-yl] aniline "PPA-1" and 4- [(2E)-3-phenylprop-2-en-1-yl] amino phenol "PPAP-2", and studied their inhibiting effect on mild steel in HCl medium. The experimental studies such as electrochemical impedance spectroscopy, potentiodynamic polarization and surface analysis were performed. Furthermore, theoretical studies by density functional theory and molecular dynamic simulation were used to corroborate the electrochemical results and to establish the adsorption mechanism and the orientation of the two aniline derivatives at the interface mild steel/ aggressive solution. Langmuir adsorption isotherm model was used to explain the adsorption of the two molecules in HCl solution. "PPAP-2" showed better inhibition effect (97%) compared to "PPAP-1" (87%).

The adsorption and inhibition effects of quinoline derivatives such as 2-amino-7-hydroxy-4-phenyl-1,4-dihydroquinoline-3-carbonitrile "Q-1", 2-amino-7-hydroxy-4- (p-tolyl)-1,4-dihydroquinoline-3-carbonitrile "Q-2", 2-amino-7-hydroxy-4-(4- methoxyphenyl)-1,4-dihydroquinoline-3-carbonitrile "Q-3" and 2-amino-4-(4 (dimethylamino)phenyl)-7-hydroxy-1,4-dihydroquinoline-3-carbonitrile "Q-4" on mild steel have been analyzed by **Singh *et al.* [21]** using gravimetric, EIS and PDP techniques. Among the studied inhibitors, "Q-4" exhibited maximum IE of 98.09 % at 150 mg/L. Surface morphology was studied using SEM, atomic force microscopy (AFM) and X-ray photoelectron spectroscopy (XPS) techniques.

2,6-Dimethylpyrimidine-2-amine and two of its derivatives have been investigated by **G.Y. Elewady [22]** as corrosion inhibitors for carbon steel in 2M HCl solution using electrochemical impedance spectroscopy (EIS) and weight loss techniques. The efficiency of the inhibitors increases with increase in the inhibitor concentration. Results obtained reveal that the used pyrimidine derivatives perform as corrosion inhibitors for C-steel in 2M HCl.

The inhibition behavior of three 5-(phenylthio)-3H-pyrrole-4-carbonitriles namely, 2-amino-3-(4-hydroxyphenyl)-3-methyl-5-(phenylthio)-3H-pyrrole-4- carbonitrile "PPCI", 2-amino-3-methyl-3-phenyl-5-(phenylthio)-3H-pyrrole-4-carbonitrile "PPC II" and 2-amino-3-(2,4-dihydroxyphenyl)-3-methyl-5-(phenylthio)-3H-pyrrole-4-carbonitrile "PPC III" on mild steel corrosion in hydrochloric acid was studied by **Verma *et al.* [23]** using gravimetric, EIS, PDP, SEM, AFM and Monte-Carlo simulations. Highest IE of 98 % was obtained at optimum concentration. Experimental results are in good co-relation with theoretical calculations.

A. Boutouil *et al.* [24] investigated the corrosion inhibition effect of a new synthesized heterocycle 1,2,3-triazole, namely(1-p-tolyl-1H-1,2,3-triazol-4-yl) methanol "TTM" was studied in 1 M hydrochloric acid solution by using both experimental and theoretical techniques. The inhibitory action of the "TTM" was investigated by potentiodynamic polarization (PDP) at various temperatures (298–333 K). PDP experiments revealed that the "TTM" behaved as mixed type inhibitor by decreasing both anodic and cathodic corrosion densities. Electrochemical impedance spectroscopy (EIS) measurements confirmed that the studied inhibitor can suppress mild steel corrosion effectively in acidic solution with an inhibition efficiency of 90% after 60 min of immersion. The formed protective layer is confirmed by SEM/EDX investigation and FT-IR spectroscopy.

Y. Feng *et al.* [25] synthesized the 3,3-((4-(methylthio)phenyl)methylene)bis(1H-indole) "TPBI" through the reaction of indole "ID" with 4-(methylthio)benzaldehyde, and tested them as corrosion inhibitor of copper in acidic medium. The electrochemical investigation showed that "TPBI" served as mixed-type inhibitor to protect copper against corrosion more efficiently than "ID", which was further demonstrated by comprehensive characterizations. Quantum calculations results further confirmed that the inhibitory effect of "TPBI" was better than "ID".

Abboud *et al.* [26] checked 2, 2'-bis (benzimidazole) for its corrosion inhibition efficiency on mild steel using various corrosion monitoring techniques. IE (%) increased with increase in concentration of benzimidazole to reach maximum IE of 97.8 % at 10^{-4} M concentration.

A. Singh el *al.* [27] investigated the corrosion inhibition of imidazoline based ionic liquid, namely 1-Decyl-3-methylimidazolium chloride "DMIC" on P110 steel in 15% HCl. The influence of KI addition was also examined over the inhibition performance. EIS results reveal that R_{ct} increase with increases in "DMIC" concentration. PDP suggests that the inhibition action of "DMIC" is a mixed type inhibitor. The inhibitive performance of "DMIC" is less, and its maximum inhibition efficiency is 68.61% at 400 mg/L. Addition of KI (0.5 mM) + "DMIC" (400 mg/L) enhanced the corrosion inhibition efficiency to 90.15%. The performance of "DMIC" and DMIC+KI decreases with an increase in temperature.

Corrosion inhibition activity of bis-1, 2, 4-triazole precursors on mild steel in nitric acid medium was investigated by **John *et al.* [28]** using EIS, PDP and gravimetric techniques, supported by theoretical studies. As the substitution increased, IE also increased because of increased electronic density. One of the triazole derivatives exhibited IE of 97.3 % at 100 ppm concentration.

I. C. 3. Hydrazone derivatives as inhibitors of corrosion in acidic medium

A.S. Fouda el *al.* [29] have investigate and assess the inhibitive properties of some hydrazone derivatives namely, Thiophene-2-carboxaldehyde-[N-(3-hydroxy-2-naphthoyl)]hydrazone "H_2THNH", Ethylacetoacetate-[N-(3-hydroxy-2-naphthoyl)]hydrazone "H_2EHNH", Salicylaldehyde-[N-(3-hydroxy-2-naphthoyl)]hydrazone "H_2SHNH", *p*-Anisaldehyde-[N-(3-hydroxy-2-naphthoyl)]hydrazone "H_2-*p*-AHNH", and 4-Acetylpyridine-[N-(3-hydroxy-2-naphthoyl)]hydrazone "H_2APHNH" for nickel in 2 mol.L^{-1} HCl solution. The inhibition efficiency has been determined using weight loss and galvanostatic polarization techniques. The inhibition efficiency increases with increasing the inhibitor concentration and decreases with increasing temperature. Polarization studies indicate that the compounds act as mixed- type inhibitors. The addition of iodide ions enhances the inhibition efficiency to a considerable extent.

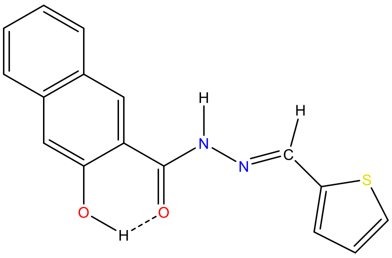

"H_2THNH"

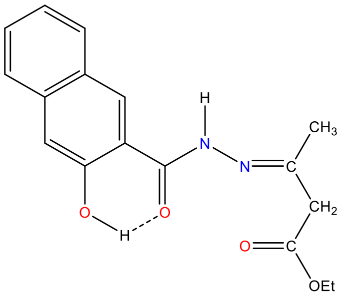

"H_2EHNH"

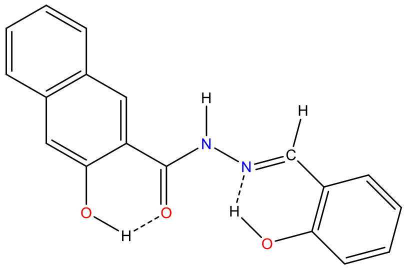

"H_2SHNH"

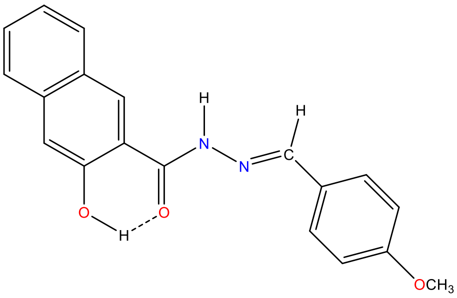

"H_2-*p*-AHNH"

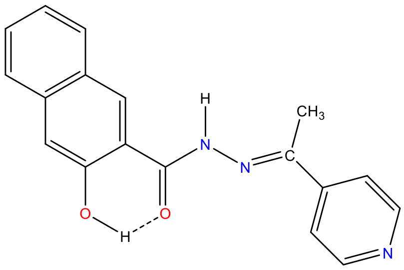

"H_2APHNH"

The anticorrosion behavior of four compounds of N-3-hydroxyl-2-naphthoyl hydrazone derivatives on the corrosion of carbon steel in 0.5 M of H_2SO_4 solution was investigated by **A.S. Fouda and S.A. EL-Sayyad [30].** The effect of various parameters on the behavior of these inhibitors has been studied using the weight loss and polarization measurements. The inhibiting action of the investigated compounds depends primarily on their concentration and molecular size. The compounds act as mixed type inhibitors and function via adsorption on carbon steel surface, which follows Frumkin adsorption isotherm. The addition of KI, KBr and KSCN to N-3-hydroxyl-2-naphthoyl hydrazone derivatives had a synergistic effect in enhancing the efficiency of corrosion inhibition.

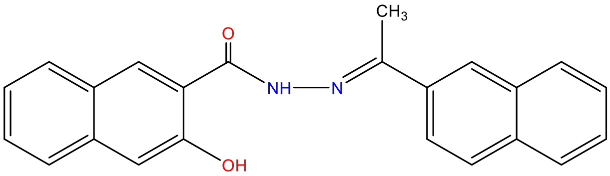

Compound 1

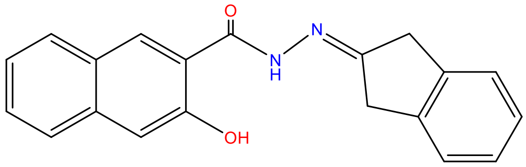

Compound 2

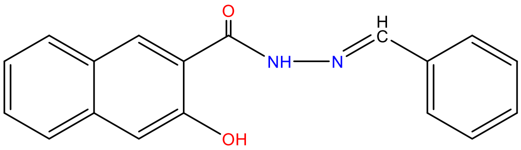

Compound 3

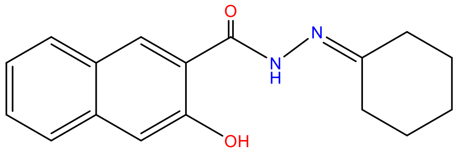

Compound 4

E. S. M. Sherif and A. H. Ahmed [31] synthesized and characterized two hydrazone derivatives namely, o-methoxybenzaldehydebenzoylhydrazone "O-MBH" and bis-(o-methoxybenzaldehyde)-thiocarbodihydrazone "O-MTH", and discussed their corrosion inhibition of copper in aerated 3.5% NaCl solutions under stagnant conditions. Electrochemical and gravimetric techniques were performed for corrosion investigations. Electrochemical results showed that the addition of O-MBH and O-MTH decreased the corrosion parameters of copper in the test solutions. The weight loss experiments indicated that O-MBH and O-MTH decreased the corrosion rate of copper. The data pointed out that O-MBH and O-MTH inhibit the copper corrosion in NaCl solution with inhibition efficiency in the order of O-MTH > OMBH.

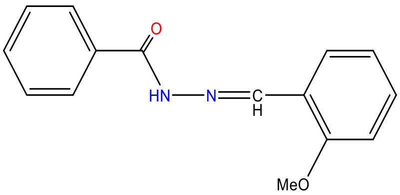

O-MBH

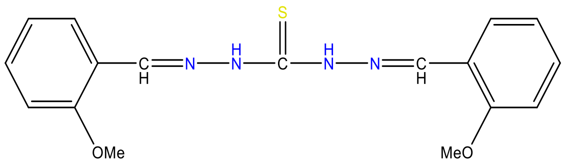

O-MTH

D. K. Singh et *al.* [32] reported the corrosion inhibition of 4(N,N-dimethylamino) benzaldehyde nicotinic acid hydrazone "ABNH" on mild steel in acidic medium using weight loss, potentiodynamic polarization curves, electrochemical impedance, quantum chemical calculation, FE-SEM and AFM techniques. The corrosion rate decreases sharply with an increase in ABNH concentration up to 6 mM in 1M HCl. The polarization study indicates that it acts as a mixed type corrosion inhibitor. The adsorption of inhibitor is spontaneous and obeys the Langmuir's adsorption isotherm. The FE-SEM images and AFM images of mild steel support strong adsorption and high inhibition efficiency of the inhibitor. Quantum chemical parameters are also in agreement with experimental obtained efficiency.

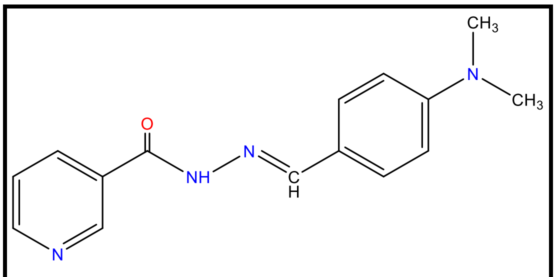

ABNH

H. Lgaz et *al*. [12] evaluated the inhibition potential of four hydrazone derivatives (HDZs) namely, 2- ((2,3-dimethylphenyl)amino) -N′- ((1E,2E)-3 phenylallylidene) benzohydrazide "HDZ[1]", (E)-2-((2,3-dimethylphenyl)amino)-N′-(4-hydroxybenzylidene) benzohydrazide "HDZ[2]", (E)-2-((2,3-dimethylphenyl)amino)-N′-(1 phenylethylidene) benzohydrazide "HDZ[3]" and N′-cyclohexylidene-2- ((2,3 dimethylphenyl)amino) benzohydrazide "HDZ[4]" on mild steel in 1.0 M HCl using chemical, electrochemical and surface characterization techniques. All results show that the inhibitor molecules form a stable layer on steel surface through chemical and physical interactions. HDZs adsorption onto the steel surface was found to follow Langmuir model. Furthermore, electrochemical results demonstrated that the inhibitors act as mixed-type inhibitors. X-ray diffraction and scanning electron microscope were used to study corrosion products phases and surface morphology of mild steel samples.

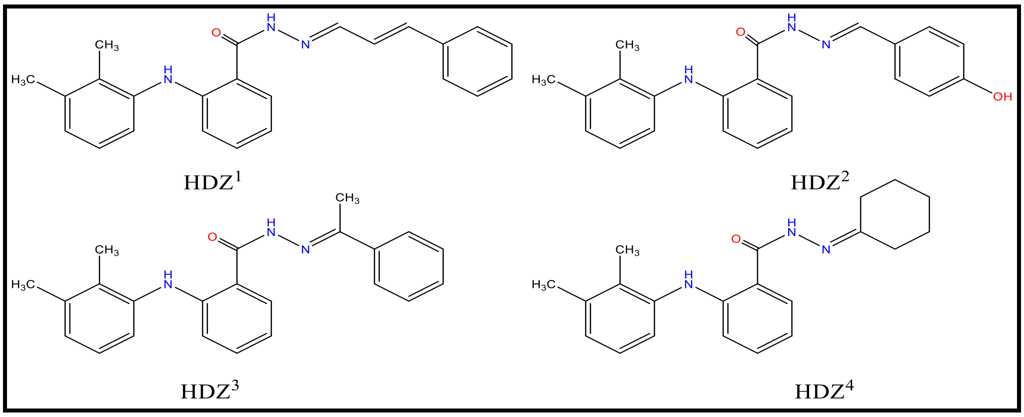

Carbon steel corrosion inhibition in 0.5 M H_2SO_4 solution using a new aromatic hydrazone derivative namely (E)-1-(3-nitrobenzylidene)-2-(p-tolyl)hydrazine "E-NBPTH" was studied by **N. Chafai el *al.*** [13]. The molecular structure of E-NBPTH has been identified and analyzed by spectroscopic methods such as UV-vis, IR, ^{1}H NMR and ^{13}C NMR. The corrosion inhibition behavior was investigated by gravimetric, electrochemical and theoretical methods. According to the polarization study, E-NBPTH acts as a mixed type of inhibitor. The adsorption of E-NBPTH on the iron surface follows the Langmuir isotherm. The optimized molecular structure and some quantum chemical parameters of the synthesized compound have been calculated using the density functional method (DFT). The results obtained from theoretical study are well supported by the experimental results.

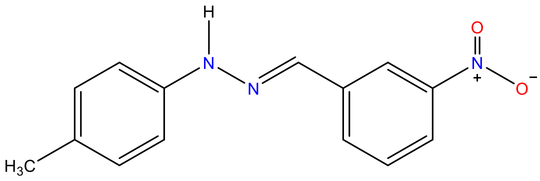

E-NBPTH

Experimental and theoretical study on the inhibition performance of thiazole hydrazones, namely 4-(4-methoxy-phenyl)- thiazole-2-carboxylic acid benzylidene-hydrazide "TH-1", 4-(4-methoxy-phenyl)-thiazole-2-carboxylic acid (3-hydroxy-benzylidene)-hydrazide "TH-2" and 4-(4-methoxy-phenyl)-thiazole-2-carboxylic acid (4- hydroxy-benzylidene)-hydrazide "TH-3" in 0.5 M hydrochloric acid for mild steel corrosion was examined by **T. K. Chaitra et *al*. [15].** Thermodynamic parameters were evaluated for activation and adsorption processes. Adsorption of the inhibitors followed Langmuir isotherm. Electrochemical measurements showed that addition of inhibitors simultaneously decreased corrosion current density and double layer capacitance but increased charge transfer resistance. Potentiodynamic polarization studies revealed that thiazole hydrazones effectively suppressed both the anodic and cathodic processes of mild steel corrosion in acid solution and hence acted as mixed-type inhibitors. SEM analysis confirm the formation of the protective film on mild steel surface.

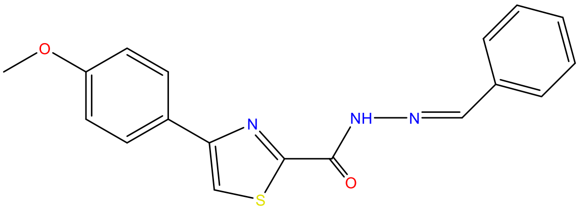

TH-1

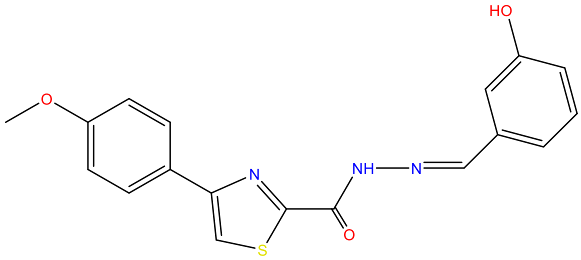

TH-2

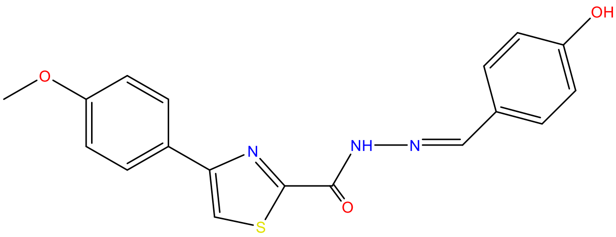

TH-3

Two newly synthesized heterocyclic aromatic hydrazone compounds, 3-(cyanodimethyl-methyl)-benzoic acid thiophen-2-ylmethylene-hydrazide "CBTH" and 3-(cyano-dimethylmethyl)-benzoic acid furan-2-ylmethylene-hydrazide "CBFH" as inhibitors for mild steel corrosion in acidic medium by gravimetric, electrochemical and morphological techniques and correlated with quantum chemical calculations were reported by **K. Chaitra et *al.*** **[33].** At optimum concentration (2 mM), CBTH and CBFH showed the highest inhibition efficiency of 87.1 % and 85.3 % respectively. Impedance study revealed that simultaneous increase in polarization resistance and decrease in double layer capacitance with increasing inhibitor concentration is due to adsorption phenomenon of hydrazones. Quantitative structure activity relationship (QSAR) results showed good correlations between a number of quantum chemical parameters and the experimentally determined inhibition efficiency. SEM and EDX analyses confirmed the formation of protective inhibitory film.

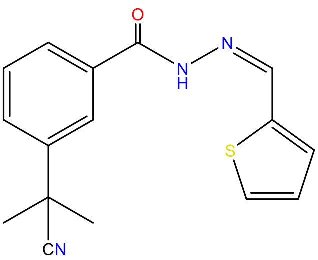

CBTH

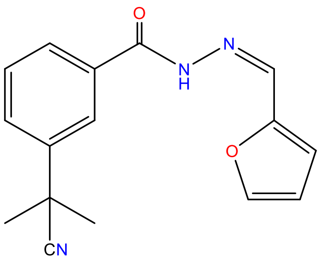

CBFH

An extensive work on the inhibiting effects of three hydrazone derivatives (HDZs), namely, (E)-N'-(4-(dimethylamino) benzylidene)-2-((2,3- dimethylphenyl) amino)benzohydrazide “HDZ-1”, (E)-2-((2,3-dimethylphenyl)amino)- N'-(4-methylbenzylidene) benzohydrazide, “HDZ-2” and (E)-N'-benzylidene-2-((2,3- dimethylphenyl) amino) benzohydrazide “HDZ-3” on the corrosion of mild steel in hydrochloric acid solution have been carried out by **H. Lgaz et *al*.** **[14].** The interaction of HDZs and the metal surface was investigated using electrochemical techniques, X-ray photoelectron spectroscopy (XPS), DFT and molecular dynamic (MD) simulations. The electrochemical measurement results demonstrated that our developed inhibitors act as of mixed-type and followed Langmuir isotherm. XPS and SEM confirm the presence of the protective layer.

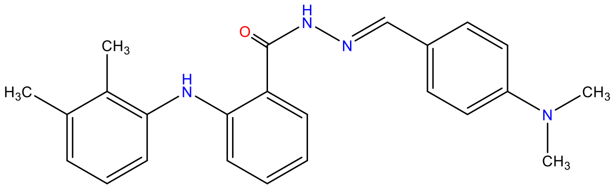

HDZ-1

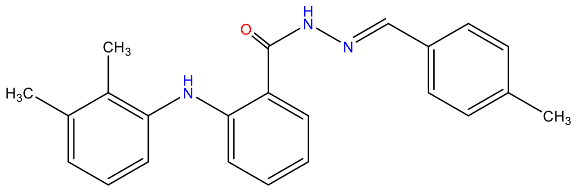

HDZ-2

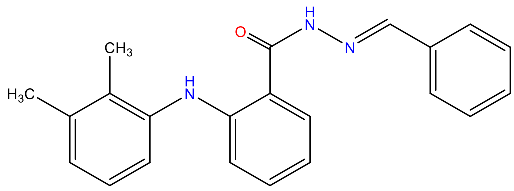

HDZ-3

A. Chaouiki et *al.* **[34]** studied the corrosion inhibition of mild steel in 1 M HCl by two hydrazone derivatives (HDZs), namely, (E)-N′-(2,4-dimethoxybenzylidene)-2-(6-methoxynaphthalen-2-yl)propanehydrazide “HYD-1” and N′-cyclohexylidene-2-(6 methoxynaphthalen-2-yl)propanehydrazide “HYD-2” using weight loss measurements and electrochemical techniques. Results showed that hat the hydrazone derivatives exhibited a high inhibition performance, which increases with increasing their concentrations. HYD-1 and HYD-2 presented maximum inhibition efficiencies of 96% and 84%, respectively, at an optimal concentration of 5×10^{-3} M and the both compound act as mixed type inhibitors in the acidic corrodent. Their microscopic and compositional features had been analyzed using SEM and EDS spectra. The results showed that the protective layer had formed.

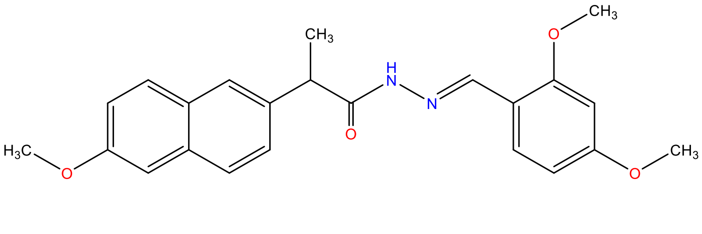

HYD-1

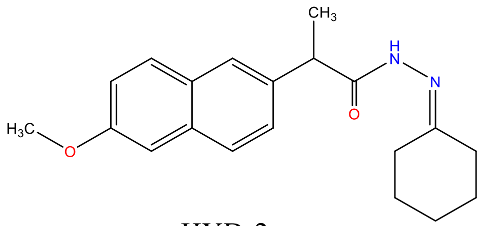

HYD-2

M. Chafiq et *al.* **[35]** reported the inhibition ability of two environmentally friendly hydrazones derivatives namely (E)-2-(6-methoxynaphthalen-2-yl)-N'-(1 phenylethylidene) propanehydrazide “PHD-H” and (E)-N'-(1-(4-bromophenyl) ethylidene)-2-(6-methoxynaphthalen-2- yl)propanehydrazide “PHD-Br” on a mild steel surface in 1.0 M HCl solution. The weight loss and electrochemical measurement indicated high efficiency (91 and 96%, respectively) with mixed type inhibition mechanism. Besides, their adsorption followed the Langmuir isotherm model. The stability of the PHD-Br at higher temperatures (303K to 333K) was investigated by weight loss measurements. In addition, the study revealed that a protective barrier was formed by adsorption of the investigated compounds on the surface of the MS, which is confirmed by scanning electron microscopy with energy-dispersive x-ray (SEM-EDX) analysis.

These authors also assessed the inhibition impacts of two other hydrazones compounds namely, (E)-N'-(1-(4-chlorophenyl)ethylidene)-2-(6-methoxynaphthalen-2 yl) propanehydrazide “PHD-Cl” and (E)-N'-(1-(4-hydroxyphenyl)ethylidene)-2-(6-methoxynaphthalen-2-yl) propanehydrazide “PHD-OH” using a combined electrochemical and theoretical approach. The observed results indicated that these compounds behave as a strong inhibitors for steel in acidic medium and reached a higher inhibition efficiency of 96% for PHD-OH and 91% for PHD-Cl **[36]**.

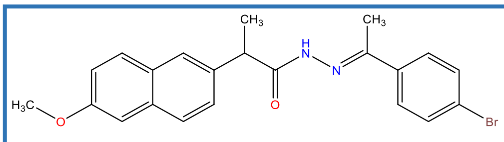

PHD-Br

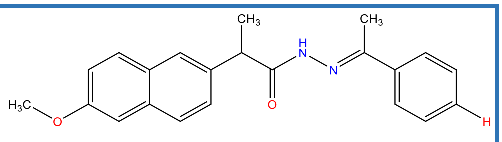

PHD-H

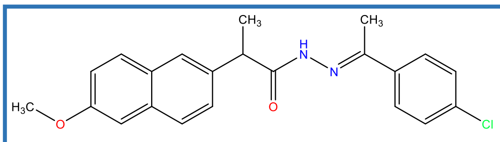

PHD-Cl

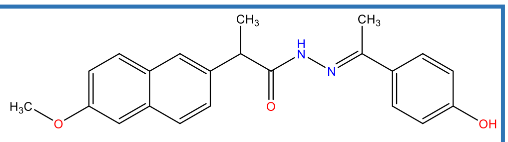

PHD-OH

I. C. 4. References

[1] Y. Qiang, S. Zhang, S. Xu, W. Li, Experimental and theoretical studies on the corrosion inhibition of copper by two indazole derivatives in 3.0% NaCl solution, Journal of colloid and interface science 472 (2016) 52-59.

[2] S. Ralkhal, T. Shahrabi, B. Ramezanzadeh, Synthesis and construction of a highly potent hybrid organic/inorganic anti-corrosive pigment for effective corrosion control of mild steel in simulated seawater, Construction and Building Materials 222 (2019) 400-413.

[3] C. Zhang, J. Zhao, Synergistic inhibition effects of octadecylamine and tetradecyl trimethyl ammonium bromide on carbon steel corrosion in the H2S and CO2 brine solution, Corrosion Science 126 (2017) 247-254.

[4] B.J. Usman, S.A. Umoren, Z.M. Gasem, Inhibition of API 5L X60 steel corrosion in CO2-saturated 3.5% NaCl solution by tannic acid and synergistic effect of KI additive, Journal of Molecular Liquids 237 (2017) 146-156.

[5] K. Abderrahim, I. Selatnia, A. Sid, P. Mosset, 1, 2-bis (4-chlorobenzylidene) Azine as new and effective corrosion inhibitor for copper in 0.1 N HCl: A combined experimental and theoretical approach, Chemical Physics Letters 707 (2018) 117-128.

[6] K. Khaled, Corrosion control of copper in nitric acid solutions using some amino acids–a combined experimental and theoretical study, Corrosion Science 52(10) (2010) 3225-3234.

[7] H.M.A. El-Lateef, Experimental and computational investigation on the corrosion inhibition characteristics of mild steel by some novel synthesized imines in hydrochloric acid solutions, Corrosion Science 92 (2015) 104-117.

[8] H.M.A. El-Lateef, A.M. Abu-Dief, L.H. Abdel-Rahman, E.C. Sañudo, N. Aliaga-Alcalde, Electrochemical and theoretical quantum approaches on the inhibition of C1018 carbon steel corrosion in acidic medium containing chloride using some newly synthesized phenolic Schiff bases compounds, Journal of Electroanalytical Chemistry 743 (2015) 120-133.

[9] G. Sığırcık, T. Tüken, M. Erbil, Inhibition efficiency of aminobenzonitrile compounds on steel surface, Applied Surface Science 324 (2015) 232-239.

[10] A. Fouda, A.E.-M. SA, A. El-Hossiany, A. Ibrahim, Evolution of the corrosion-inhibiting efficiency of novel hydrazine derivatives against corrosion of stainless steel 201 in acidic medium, Int J Electrochem Sci 14 (2019) 2187-2207.

[11] S. Rollas, S. Küçükgüzel, Biological activities of hydrazone derivatives, Molecules 12(8) (2007) 1910-1939.

[12] H. Lgaz, A. Chaouiki, M.R. Albayati, R. Salghi, Y. El Aoufir, I.H. Ali, M.I. Khan, S.K. Mohamed, I.-M. Chung, Synthesis and evaluation of some new hydrazones as corrosion inhibitors for mild steel in acidic media, Research on Chemical Intermediates 45(4) (2019) 2269-2286.

[13] N. Chafai, S. Chafaa, K. Benbouguerra, A. Hellal, M. Mehri, Synthesis, spectral analysis, anti-corrosive activity and theoretical study of an aromatic hydrazone derivative, Journal of Molecular Structure 1181 (2019) 83-92.

[14] H. Lgaz, I.-M. Chung, M.R. Albayati, A. Chaouiki, R. Salghi, S.K. Mohamed, Improved corrosion resistance of mild steel in acidic solution by hydrazone derivatives: an experimental and computational study, Arabian Journal of Chemistry 13(1) (2020) 2934-2954.

[15] T.K. Chaitra, K.N. Mohana, D.M. Gurudatt, H.C. Tandon, Inhibition activity of new thiazole hydrazones towards mild steel corrosion in acid media by thermodynamic, electrochemical and quantum chemical methods, Journal of the Taiwan Institute of Chemical Engineers 67 (2016) 521-531.

[16] C. Verma, M. Quraishi, E. Ebenso, I. Obot, A. El Assyry, 3-Amino alkylated indoles as corrosion inhibitors for mild steel in 1M HCl: Experimental and theoretical studies, Journal of Molecular Liquids 219 (2016) 647-660.

[17] R. Laggoun, M. Ferhat, B. Saidat, A. Benghia, A. Chaabani, Effect of p-toluenesulfonyl hydrazide on copper corrosion in hydrochloric acid solution, Corrosion Science 165 (2020) 108363.

[18] Q. Zhang, B. Hou, G. Zhang, Inhibitive and adsorption behavior of thiadiazole derivatives on carbon steel corrosion in CO2-saturated oilfield produced water: Effect of substituent group on efficiency, Journal of colloid and interface science 572 (2020) 91-106.

[19] A. Singh, K. Ansari, D.S. Chauhan, M. Quraishi, H. Lgaz, I.-M. Chung, Comprehensive investigation of steel corrosion inhibition at macro/micro level by ecofriendly green corrosion inhibitor in 15% HCl medium, Journal of colloid and interface science 560 (2020) 225-236.

[20] Y. Boughoues, M. Benamira, L. Messaadia, N. Ribouh, Adsorption and corrosion inhibition performance of some environmental friendly organic inhibitors for mild steel in HCl solution via experimental and theoretical study, Colloids and Surfaces A: Physicochemical and Engineering Aspects 593 (2020) 124610.

[21] P. Singh, V. Srivastava, M. Quraishi, Novel quinoline derivatives as green corrosion inhibitors for mild steel in acidic medium: electrochemical, SEM, AFM, and XPS studies, Journal of Molecular Liquids 216 (2016) 164-173.

[22] G. Elewady, Pyrimidine derivatives as corrosion inhibitors for carbon-steel in 2M hydrochloric acid solution, Int. J. Electrochem. Sci 3(10) (2008) 1149.

[23] C. Verma, E. Ebenso, I. Bahadur, I. Obot, M. Quraishi, 5-(Phenylthio)-3H-pyrrole-4-carbonitriles as effective corrosion inhibitors for mild steel in 1 M HCl: experimental and theoretical investigation, Journal of Molecular Liquids 212 (2015) 209-218.

[24] A. Boutouil, M.R. Laamari, I. Elazhary, L. Bahsis, H. Anane, S.-E. Stiriba, Towards a deeper understanding of the inhibition mechanism of a new 1, 2, 3-triazole derivative for mild steel corrosion in the hydrochloric acid solution using coupled experimental and theoretical methods, Materials Chemistry and Physics 241 (2020) 122420.

[25] Y. Feng, L. Feng, Y. Sun, J. He, The inhibition mechanism of a new synthesized indole derivative for copper in acidic environment via experimental and theoretical study, Journal of Materials Research and Technology 9(1) (2020) 584-593.

[26] Y. Abboud, A. Abourriche, T. Saffaj, M. Berrada, M. Charrouf, A. Bennamara, A. Cherqaoui, D. Takky, The inhibition of mild steel corrosion in acidic medium by 2, 2′-bis (benzimidazole), Applied surface science 252(23) (2006) 8178-8184.

[27] A. Singh, K. Ansari, M. Quraishi, P. Banerjee, Corrosion inhibition and adsorption of imidazolium based ionic liquid over P110 steel surface in 15% HCl under static and dynamic conditions: Experimental, surface and theoretical analysis, Journal of Molecular Liquids (2020) 114608.

[28] S. John, A. Joseph, Electroanalytical and Theoretical Investigations of the Corrosion Inhibition Behavior of Bis-1, 2, 4-Triazole Precursors EBATTand BBATT on Mild Steel in 0.1 N HNO3, Industrial & engineering chemistry research 51(51) (2012) 16633-16642.

[29] A. Fouda, H. Mostafa, S. Ghazy, S. Farah, Use of hydrazone derivates as inhibitors for the corrosion of nickel in hydrochloric acid solution, Int. J. Electrochem. Sci 2 (2007) 182-194.

[30] A. Fouda, S. EL-Sayyad, M. Abdallah, N-3-hydroxyl-2-naphthoyl hydrazone derivatives as inhibitors for corrosion of carbon steel in H2SO4 acid solution, Anti-Corrosion Methods and Materials (2011).

[31] E.-S.M. Sherif, A.H. Ahmed, Synthesizing new hydrazone derivatives and studying their effects on the inhibition of copper corrosion in sodium chloride solutions, Synthesis and Reactivity in Inorganic, Metal-Organic, and Nano-Metal Chemistry 40(6) (2010) 365-372.

[32] D.K. Singh, S. Kumar, G. Udayabhanu, R.P. John, 4 (N, N-dimethylamino) benzaldehyde nicotinic hydrazone as corrosion inhibitor for mild steel in 1 M HCl solution: An experimental and theoretical study, Journal of molecular liquids 216 (2016) 738-746.

[33] T.K. Chaitra, K.N. Mohana, H.C. Tandon, Evaluation of newly synthesized hydrazones as mild steel corrosion inhibitors by adsorption, electrochemical, quantum chemical and morphological studies, Arab Journal of Basic and Applied Sciences 25(2) (2018) 45-55.
[34] A. Chaouiki, M. Chafiq, H. Lgaz, M.R. Al-Hadeethi, I.H. Ali, S. Masroor, I.-M. Chung, Green corrosion inhibition of mild steel by hydrazone derivatives in 1.0 M HCl, Coatings 10(7) (2020) 640.
[35] M. Chafiq, A. Chaouiki, M.R. Al-Hadeethi, R. Salghi, I.-M. Chung, A Joint Experimental and Theoretical Investigation of the Corrosion Inhibition Behavior and Mechanism of Hydrazone Derivatives for Mild Steel in HCl Solution, Colloids and Surfaces A: Physicochemical and Engineering Aspects (2020) 125744.
[36] M. Chafiq, A. Chaouiki, M.R. Albayati, H. Lgaz, R. Salghi, S.K. AbdelRaheem, I.H. Ali, S.K. Mohamed, I.-M. Chung, Unveiled understanding on corrosion inhibition mechanisms of hydrazone derivatives based on naproxen for mild steel in HCl: A joint experimental/theoretical study, Journal of Molecular Liquids (2020) 114442.

Part II

Experimental methodology

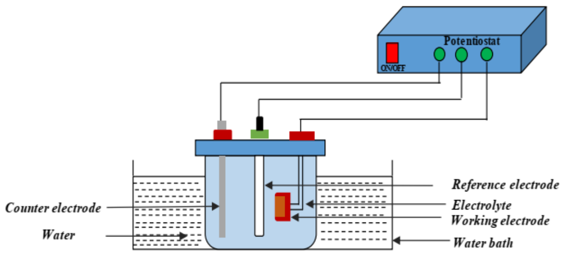

Used Products

- **Solvents:**

- Ethyl acetate
- Acetone
- Chloroform
- Dichloromethane
- Methanol

- **Reagents:**

- Hydrochloric acid
- Benzaldehyde derivatives
- Sulfuric acid
- 2,4-dinitrophenylhydrazine “DNPH ”

Analysis equipment's

- ✓ The IR spectra of the synthesized products are established in the range (400-4000 cm^{-1}) with the use of VERTEX 70 spectrometer in the form of a clean powder.
- ✓ The Visible Ultraviolet spectra of these products are carried out using a spectrophotometer type SHIMADZU UV 16A.
- ✓ NMR spectra are performed using a typical spectrophotometer BRUKER (300, 400 MHz) for the proton and of BRUKER type (75, 100 MHz) for carbon 13. The chemical shifts δ are expressed in parts per million (ppm) relative to tetramethylsilane (TMS) taken as internal reference. The J coupling constants are expressed in Hertz (Hz). The following notations express the different types of coupling: s: singlet; d: doublet; dd: doublet of doublet; ddd: doublet of doublet of doublet; m: multiplet
- ✓ The measurement of the melting point of solids required the use of a standard device BÜCHI 510, T (0-300° C) and a BRONSTED ELECTROTHERMAL device.
- ✓ Mechanical stirring is accomplished by means of a HEIDOLPH stirer type device (RZR O / RZR 1).
- ✓ The electrochemical measurements are carried out with an assembly comprising a potentiostat, type PZG301 (Voltalab), controlled by the Voltamaster4 software.
- ✓ The SEM observations were carried out using an SEM type device (JEOL-JSM-6360LV).
- ✓ Water contact angle measurements were measured by the sessile drop method with the DSA100 Kruss instrument.
- ✓ XPS measurements were carried out on a Kratos Axis Ultra using AlKα (1486.6 eV) radiation.

"Science is a wonderful thing as long as you don't have to make a living from it!"
Albert Einstein

II. A. Corrosion monitoring techniques

Corrosion monitoring techniques play a key role in efforts to fight corrosion, which has major economic implication. The most important corrosion monitoring methods are:

II. A. 1. Non electrochemical methods

II. A. 1. 1. Weight loss method [1]

It is one of the oldest, simplest and most widely used technique of monitoring corrosion rate (C_R), but does not allow to determine the mechanisms involved during corrosion but it will give baseline to the electrochemical impedance spectroscopy and linear polarization methods. This method is carried out by exposing the weighed metal coupons in the test media for a predetermined period of time and temperature. Later the coupons removed and cleaned according to ASTM G1-03 [2] to remove corrosion products and is reweighed. The average weight loss of the coupons was recorded.

Advantages of weight loss technique are that:

- The technique is applicable to all environments- gases, liquids, and solids/ particulate flow.
- Visual inspection can be undertaken.
- Corrosion deposits can be observed and analyzed.
- Weight loss can be readily determined and corrosion rate easily calculated.
- Localized corrosion can be identified and measured.
- Inhibitor performance can be easily assessed.

The disadvantage of the coupon technique is that:

- If a corrosion upset occurs during the period of exposure, the coupon alone will not be able to identify the time of occurrence of the upset, and depending upon the peak value of the upset and its duration, may not even register a statistically significant increased weight loss

Therefore, coupon monitoring is most useful in environments where corrosion rates do not significantly change over long time periods.

II. A. 2. Electrochemical methods

Electrochemical methods are used widely in inhibitor testing, the most commonly used techniques are:

II. A .2. 1. Open Circuit Potential measurement

The measurement of Open Circuit Potential (OCP) is used for monitoring corrosion, though the corrosion potential itself is difficult to interpret. In this method the metal is covered with 1mL of the electrolyte solution and measured OCP for an hour. The corrosion potential is used to predict the behavior of metals.

II. A. 2. 2. Potentiodynamic polarization method

This technique generally used to evaluate the corrosion current density of the substrate. The polarization character of the substrate (any metal/material) was analyzed by using current and applied potential relationship. This method is also used in the investigation of rate of instantaneous reaction in substrate/electrolyte interface. This method is also called as potentiodynamic polarization technique. In this technique, the metal sample is polarized ± 250 mv (vs. open circuit potential (OCP)) by anodic and cathodic direction with a scan rate. Corrosion current density (i_{corr}) can be obtained from the plot of applied potential vs. log (current density) (*via* **Figure II. A. 1**). This technique can also be used for the determination of the nature of corrosion inhibitor in various corrosive systems. The anodic/ cathodic/ mixed mode of corrosion inhibitors can be understood by corrosion potential, anodic and cathodic slope values obtained from the plot of potential vs log (current density).

Advantages:

- This technique yields better results in conducting medium.
- This technique applicable for the reactions which are in activated control.
- It measures the lowest corrosion rate of the metal samples with accuracy.
- This technique monitors the rate of corrosion of metal samples continuously.

Disadvantages:

- This technique applicable only for a reduction process.
- Time needed for data of the single polarization curve (Tafel curve) requires more time compared to gravimetric (weight loss) method.
- This technique is insensitive to localized corrosion.

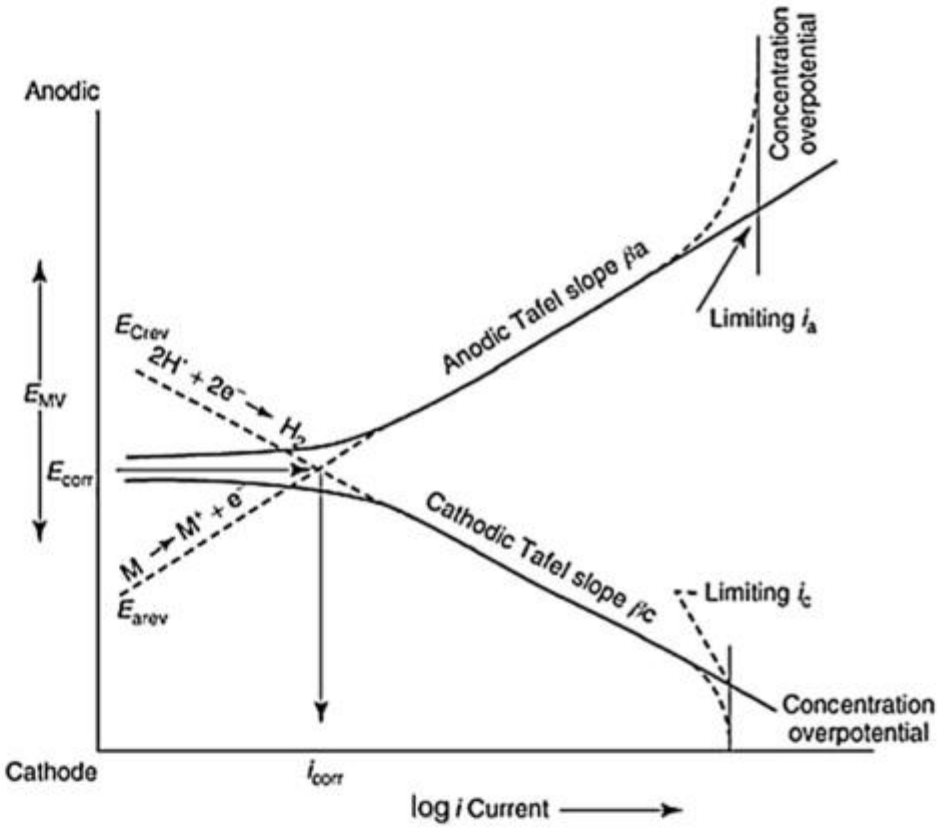

Figure. II. A. 1. Potentiodynamic polarization curve (Tafel plot)

II. A. 2. 3. Electrochemical impedance spectroscopy method

The Electrochemical Impedance Spectroscopy (EIS) method is the most widely used technique for studying corrosion and corrosion protection processes (inhibitors or coatings) because it is not destructive **[3]**. Electrochemical impedance measurement consists of studying the response of the electrochemical system, following a disturbance which is, in most cases, a low amplitude alternating signal. The strength of this technique is to differentiate the reaction phenomena by their relaxation time. Only fast processes are characterized at high frequencies; when the applied frequency decreases, the contribution of slower steps, such as transport or diffusion in solution, will appear **[4, 5]**. Different electrochemical processes are observed at the metal / electrolyte interface, the charge transfer that takes place between the interface and the metal is defined as a rapid phenomenon and the material transport that takes place between the interface and the electrolyte is defined as a rather slow phenomenon **[6]**. The interface is also the link where the corrosion products are formed, it is thus possible to separate among others the effects of the currents involved in the stationary dissolution of the metal from those related to currents involved in surface state modifications:

- In the liquid (double layer capacity in contact with the metal);
- On the solid (adsorbate, growth of a film).

Its principle is to impose on a constant potential E_0, a sinusoidal potential ΔE (t) of low amplitude and to follow the current response for different frequencies of the disturbing signal. Conversely ΔI(t) can be imposed on the current I_0 and the potential recorded **[7]**. (*via* **Figure . II. A. 2**)

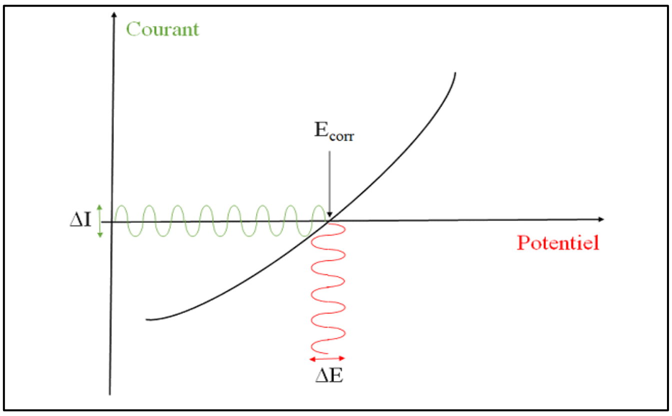

Figure. II. A. 2. Disturbance of a nonlinear electrochemical system at E_{corr} with $I_0 = 0$ **[7]**.

Electrochemical spectroscopy impedance can be represented in two different ways **[8]**. In Nyquist's representation, the imaginary part of the impedance is plotted against the real part. In Bode's representation, we report the modulus and phase shift angle of the impedance as a function of the logarithm of the frequency (**Figure. II. A. 3**).

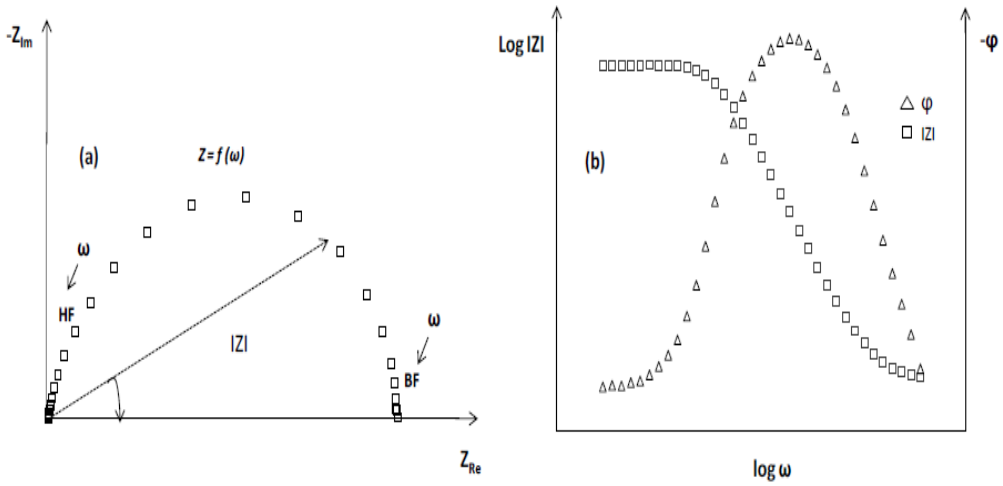

Figure. II. A. 3. Representation of the electrochemical impedance in Nyquist (a) and Bode (b) **[8]**.

The impedance of an electrochemical system can be likened by analogy to an electrical impedance. The different processes taking place at the electrode / electrolyte interface can be modeled by constructing an equivalent electrical circuit.

However, the interpretation of experimental impedance diagrams via an equivalent electrical circuit (EEC) must comply with two conditions:

- All the elements of the circuit must have a precise physical meaning, associated with the physical properties of the system.

- The spectrum simulated from the EEC must be the most similar to the experimental spectrum and the error must not be systematic as a function of the frequency.

- **Interpretation of Nyquist diagrams**

a. Charge transfer

The interface can be represented, in the case of disturbances of small amplitudes, by an arc of a circle in the Nyquist plane, and be modeled by an equivalent electrical circuit, called Randles (**Figure II. A. 4**).

The phenomenon of charge transfer at the electrode / electrolyte interface causes the appearance of a capacitive current represented by the noted capacitance (C_d). The charge transfer resistance (R_t) is crossed by the faradic current. In the absence of any reaction other than electron transfer, R_t is identified with the charge transfer resistance **[9].**

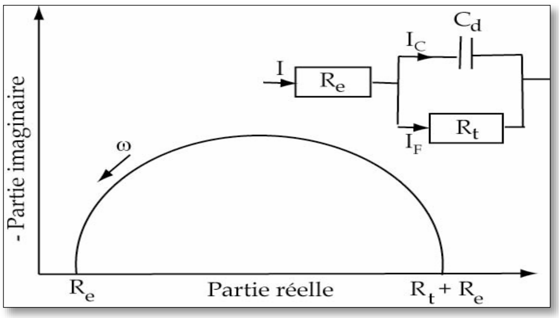

Figure. II. A. 4. Nyquist diagram of the electrochemical impedance, and its equivalent electrical circuit **[9]**.

b. Surface heterogeneity

Due to the heterogeneity and distribution of reaction sites on the surface of the electrode, the semi-circle representing the charge transfer resistance and the capacity of the double layer in the Nyquist plane is often flattened (**Figure II. A. 5**), in this case, a constant phase element CPE, represented by the value n, is introduced in the modeling of the equivalent circuit.

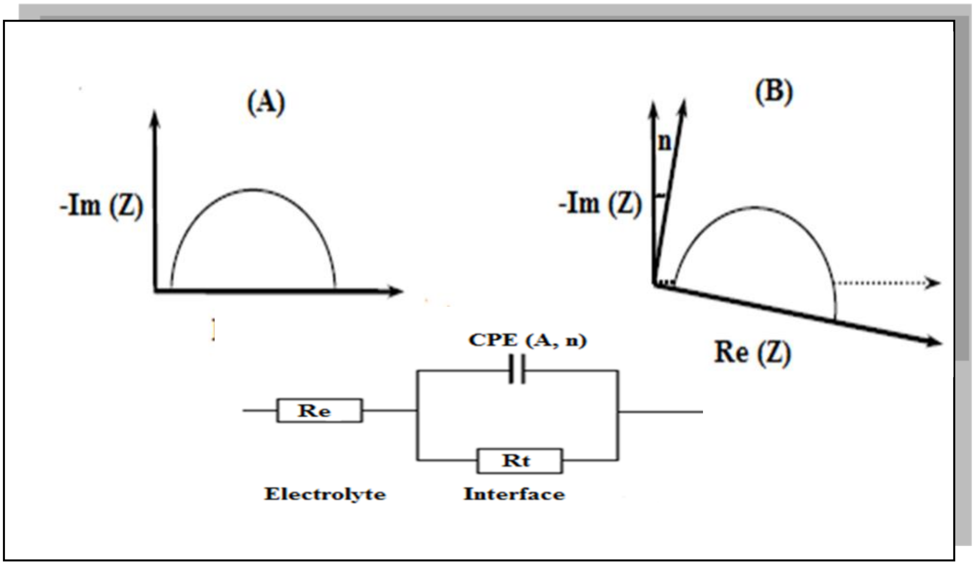

Figure. II. A. 5. Nyquist diagram: (A) ideal case; (B) experimental spectrum and its equivalent electrical circuit **[9]**.

Advantages:

- This method is more valuable because both charge transfer resistance and capacitance can be determined.
- Error free results can be obtained due to minimum perturbation.
- This technique can also be used in the lower conducting medium.
- This method provides good mechanistic information **[10-12].**

II. A. 3. Computational methods

Inhibition mechanisms have now been deeply explored through investigation of the electron distribution, optimized structure, and the adsorption of molecules onto metal surfaces. Several computational calculations and molecular simulations have been developed to correlate the inhibition efficiency of the organic inhibitors with their molecular properties **[13-16].**

II. A. 3. 1. Quantum chemical calculations

Usually, evaluation of inhibition performance is primarily conducted experimentally. However, in general, these experimental methods are expensive, time consuming and often do not provide any significant insight about the mechanism of metal surface-inhibitor interactions. In order to derive significant insight about the interactions between organic inhibitor and metal surface, computational chemistry methods have been served as powerful tools in the corrosion research **[17]**. In fact, density functional theory (DFT) has become an attractive, theoretical method, because it gives exact, basic, and vital parameter values for even hugely complex molecules at low cost **[18]**, and also enabled corrosion scientist to accurately predict the inhibition efficacies of organic corrosion inhibitors based on electronic/molecular properties and reactivity indices. This technique provide some vital parameters such as energy of highest occupied and lowest unoccupied molecular orbitals (E_{HOMO}, E_{LUMO}), energy band gap (ΔE), electronegativity (χ), global hardness (η) and softness (σ), fraction of electron transfer (ΔN) and diploe moment (μ) etc. that can be used to predict relative order of binding affinities of any given series of organic inhibitors on any metallic surface **[19]**.

II. A. 3. 2. Molecular dynamics simulation

In recent years, molecular simulations have become powerful tools for studying the structure and movements of corrosion inhibitors in presence of simulated aggressive solutions and establishing relationships between molecular structure and inhibition efficiency of organic molecules. Information about the interactions between inhibitor molecule and the metal surfaces becomes apparent and very useful, while they were not easily accessible by other methods. Molecular dynamics is an accurate but computational expensive method. It is very valuable when performing a large simulation system including all concerned species (water, ions, molecules...etc). Additionally, MD simulation technique also provide orientation over the metallic surface which is an important descriptor while analyzing the extent of inhibitor adsorption on metallic surface as an inhibitor with flat orientation would cover larger surface area as compared to the vertical orientation **[20-25]**.

II. B. Experimental and computational Conditions

The experimental protocol used for the synthesis of the different inhibitors, the method of preparation of the carbon steel (CS) samples, the experimental procedures for the corrosion tests and the surface characterization, as well as the theoretical methods employed in this study are described in this section. . The overview of the experimental methodology was presented in **Figure II. B. 1.**

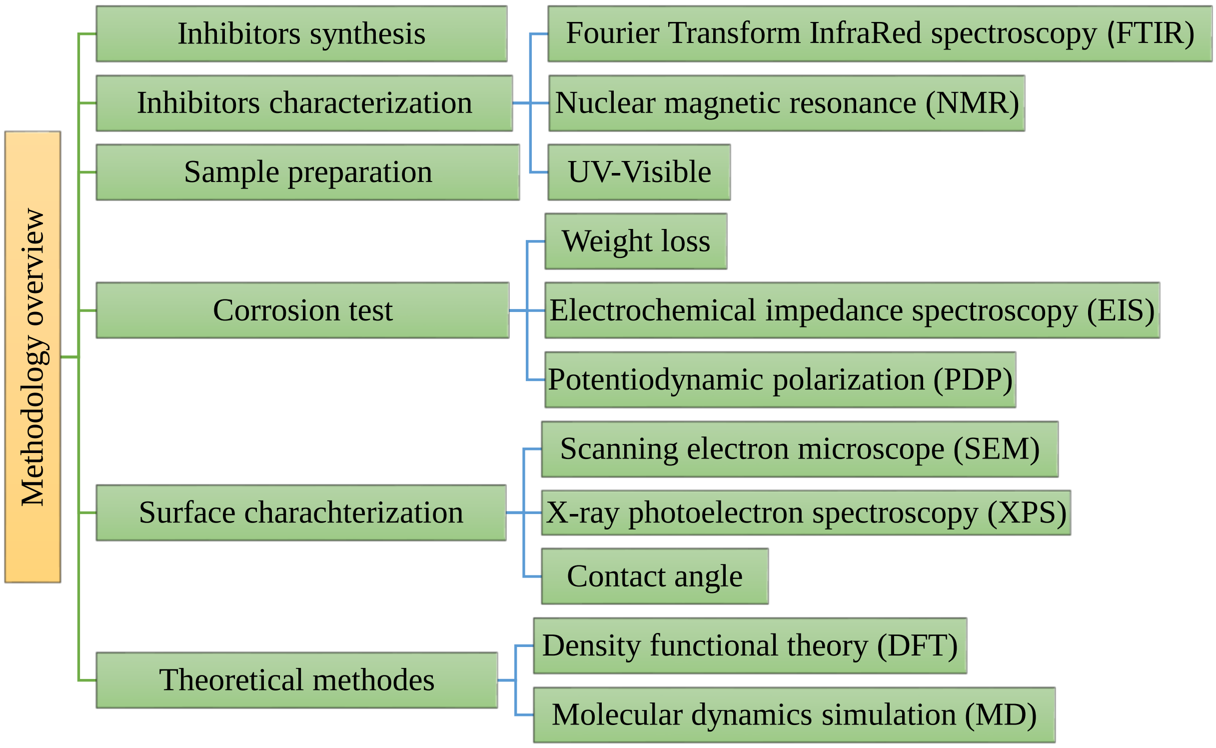

Figure. II. B. 1. Overview of the experimental and theoretical methods used in this work

II .B. 1. Materials

II. B. 1 .1. Synthesis of inhibitors

(*E*) -1- (2,4-dinitrophenyl) -2- (arylidene) hydrazines **(3a-d)** used as a corrosion inhibitors were obtained through equimolar condensation between 2,4-dinitrophenylhydrazine DNPH **(1)** and benzaldehyde derivatives **(2a-d)** in an acid medium (Ethanol / H_2SO_4 (3 drops)) after 4 hours of stirring under reflux **(Scheme II. B. 1).** The molecular structures and the spectral data of tested compounds are listed in **Table II. B. 1.**

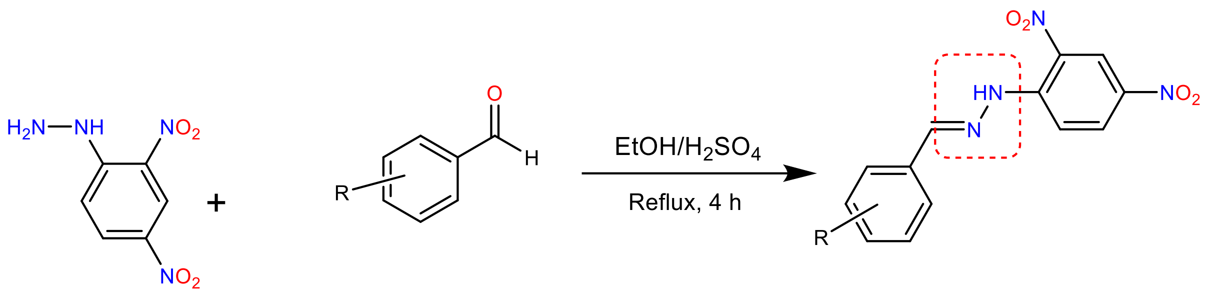

(1) **(2a-d)** **(3a-d)**

2a, 3a: R= 2,4 dihydroxy
2b, 3b: R= 4-isopr
2c, 3c: R= 4-Me
2d,3d: R= 4-Cl

Scheme II. B. 1. Schematic representation of the synthetic pathway for the tested inhibitors

Table II. B. 1. Chemical structures of the synthesized inhibitors.

Chemical structures of inhibitors	Name and abbreviation
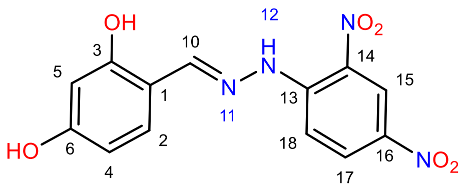	(*E*) -1- (2,4-dinitrophenyl) -2- (2,4-dihydroxy benzylidene) hydrazine **« HYD-OH »** **3a**
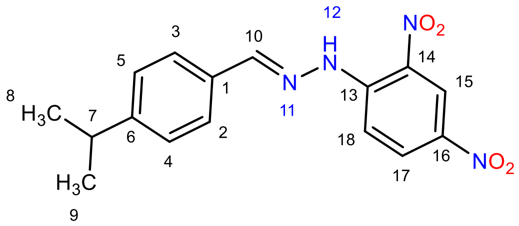	(*E*) -1- (2,4-dinitrophenyl) -2- (4-isopropyl benzylidene) hydrazine **« HYD-iso »** **3b**
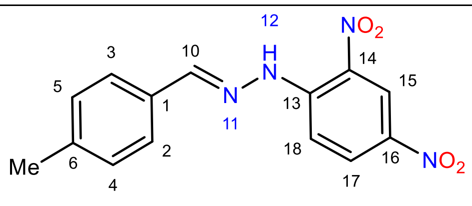	(*E*) -1- (2,4-dinitrophenyl) -2- (4-methyl benzylidene) hydrazine **« HYD-Me »** **3c**
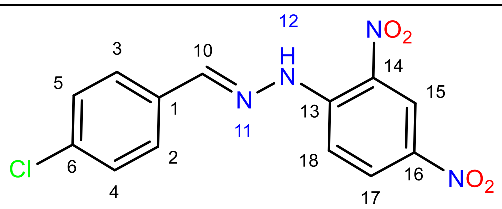	(*E*) -1- (2,4-dinitrophenyl) -2- (4-chloro benzylidene) hydrazine **« HYD-Cl »** **3d**

(*E*) -1- (2,4-dinitrophenyl) -2- (2,4-dihydroxy benzylidene) hydrazine « **HYD-OH** »

^{1}H NMR (300 MHz, in *ppm*, DMSO-*d6*) δ: 11.40 (1H, s, OH); 10.05 (1H, s, OH); 9.66 (1H, s, NH); 8.94 (1H, s, imine CH); 8.57 (1H, s, H-15); 8.24 (1H, d, H-5); 7.71 (2H, d, H-17 and H-2); 6.33 (1H, d, H-18) **[26].**

(*E*) -1- (2,4-dinitrophenyl) -2- (4-isopropyl benzylidene) hydrazine « **HYD-iso** »

^{1}H NMR (300 MHz, in *ppm*, $CDCl_3$): δ: 11.31 (1H, d, -NH), δ 9.15 (1H, d, *J*=2.6 Hz, H-15), 8.36 (1H, ddd , imine CH), 8.10 (2H, m, H-17 and H-18), 7.71 (2H, m, H-2 and H-3), 7.33 (2H, m, H-4 and H-5), 2.9 (1H, hept, H-5) 1.29 (6H, d, *J*=6.9 Hz, H-8 and H-9).

^{13}C NMR-DEPT 135 (75 MHz, in *ppm*, $CDCl_3$): δ: 148.09 (s, 1C, C-10), 130.02 (s, 1C, C-15), 127.78 (s, 2C, C-5 and C-4), 127.19 (s, 2C, C-2 and C-3), 123.56 (s, 1C, C-17), 116.77 (s, 1C, C-18), 34.24 (s, 1C, C-7), 23.77 (s, 2C, C-8 and C-9). Quaternary carbon resonance does not appear in DEPT 135.

(*E*) -1- (2,4-dinitrophenyl) -2- (4-methyl benzylidene) hydrazine « **HYD-Me** »

^{1}H NMR (300 MHz, in *ppm*, $CDCl_3$): δ 11.29 (1H,d, NH), 9.13 (1H, dd, *J* = 15.3, 2.6 Hz, H-15), 8.34 (1H, m, imine CH), 8.10 (2H, m, H-17 and H-18), 7.67 (2H, m, H-2 and H-3), 7.29 (2H, m, H-4 and H-5), 2.42 (3H, s, $C\underline{H_3}$).

^{13}C NMR-DEPT 135 (75 MHz, $CDCl_3$) δ 148.12 (s, 1C, C-10), 130.11 (s, 1C, C-15), 130.01 (s, 1C, C-17), 129.79 (s, 1C, C-4), 127.66 (s, 1C, C-5), 123.78 (s, 1C, C-2), 123.56 (s, 1C, C-3), 116.78 (s, 1C, C18), 21.84 (s, 1C, $\underline{C}H_3$). Quaternary carbon resonance does not appear in DEPT 135.

(*E*) -1- (2,4-dinitrophenyl) -2- (4-Chloro benzylidene) hydrazine « **HYD-Cl** »

^{1}H NMR (500 MHz, in *ppm*, DMSO-*d6*) δ: 11.71 (s, 1H, N-H), 8.87 (1H, d, H-15), 8.70 (s, 1H, imine CH), 8.37 (1H, d, H-17), 8.11 (1H, d, H-18), 7.84 (2H, d, *J* = 8.5 Hz , H-2 and H-3), 7.57 (2H, d, *J* = 8.5 Hz, H-4 and H-5) **[27].**

II. B. 1. 2. Sample preparation and solutions

In the present work, API 5L-X60 carbon steel (CS), obtained from petroleum refining storage tanks in Algeria, with the following chemical composition (wt.%): C (0.26), Mn (1.35), P(0.03), S (0.03) and the rest Fe was used. Rectangular pieces with the same size ($1\times1\times1cm^3$) were used for weight loss and surface analysis. For electrochemical measurements, CS specimens were implanted in epoxy resin with bottom exposed surface area of 1 cm^2**.** The CS specimens were treated according to the ASTM G1-03 standard method **[2].**

II. B. 1. 3. Solutions

The corrosive solution of 1.0 M HCl were prepared by dilution of 37 % HCl in distilled water. The concentration range of the studied inhibitor was fixed between 10^{-4} and 5×10^{-3} M.

II. B. 2. Corrosion tests

II. B. 2. 1. Weight loss measurement (WL)

ASTM G 31-72 standard laboratory methodology was adopted to realize the weight loss measurement **[28].** The CS specimens were immersed for 24 hours in the corrosive solution with and without different concentrations of the hydrazone derivatives **"HYD's"** at different temperatures ranging from 298 to 328 K. After the required immersion time, the CS coupons were taken out of the test solution, rinsed with distilled water, acetone then dried and finally re-weighted. Experiments were repeated thrice to obtain reliable results. The performance of the inhibitors can be evaluated by their inhibiting efficiencies ($\eta_w\%$) and surface coverage, which is calculated using the following equations **[29, 30]:**

$$C_R = \frac{w}{A.t} \qquad (\boldsymbol{II.B.1})$$

$$\eta_w\% = \frac{C_R^0 - C_R}{C_R^0} \times 100 \qquad (\boldsymbol{II.B.2})$$

$$\theta = \frac{\eta_w\%}{100} \qquad (\boldsymbol{II.B.3})$$

II. B. 2. 2. Electrochemical methods

The most commonly used techniques are:

- Electrochemical impedance spectroscopy (EIS) method.
- Potentiodynamic polarization method

A classical electrochemical cell containing three-electrode system was used to perform all electrochemical experiments via Voltalab PGZ 301 Potentiostat/Galvanostat, where 1 cm^2 carbon steel was applied as a working electrode, platinum as the counter electrode and saturated calomel electrode as the reference electrode for all experiments. To establish steady-state corrosion potential, the CS working electrode was immersed in the test solution for 30 min at open circuit potential (E_{ocp}). The schematic diagram of the electrochemical set-up is presented in **Figure II. B. 2.**

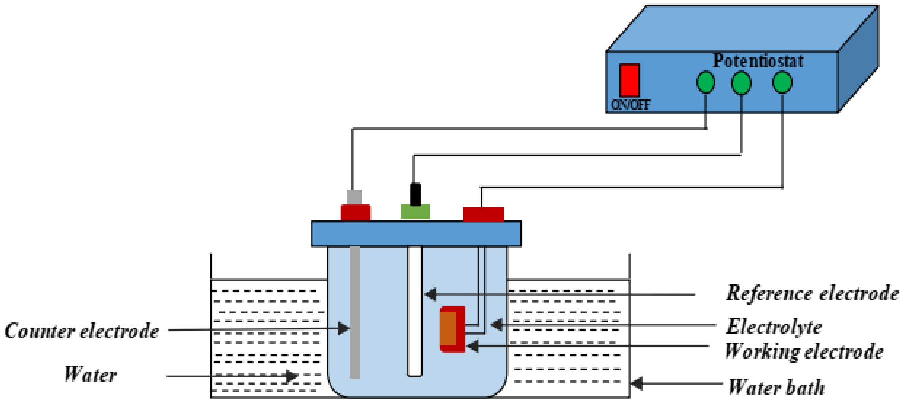

Figure. II. B. 2. A schematic representation of a three-cell electrochemical set-up.

- Electrochemical impedance spectroscopy (EIS) was conducted in a frequency range from 100 KHz to 0.01 Hz with a signal amplitude perturbation of 10 mV. Electrochemical parameters were obtained by fitting the results to an equivalent circuit using Zview software, and the corresponding inhibition efficiency was calculated as **[31]:**

$$\eta_R\% = \frac{R_p - R_p^0}{R_p}.100 \qquad (\boldsymbol{II.B.4})$$

where R_p^0 and R_p are polarization resistances in the absence and presence of the inhibitor, respectively.

- Potentiodynamic polarization curves were obtained by sweeping the electrode potential ± 250 mV versus E_{ocp} with a scan rate of 1 mV/s. Inhibition efficiency ($\eta_p\%$) was defined as below **[32, 33]:**

$$\eta_p(\%) = \frac{i_{corr}^0 - i_{corr}}{i_{corr}^0}.100 \qquad (\boldsymbol{II.B.5})$$

where i_{corr}^0 and i_{corr} are the corrosion current densities in the absence and presence of inhibitor respectively.

II. B. 3. Material characterization

To characterize the characteristic of the formed inhibited film, surface analysis using scanning electron microscope (SEM), contact angle and X-ray photoelectron spectroscopy (XPS) were carried out.

II. B. 3. 1. Scanning electron microscope (SEM)

The surface morphology of the corroded CS after 24 h of immersion in 1 M HCl solution without and with 5×10^{-3} M was observed using a scanning electron microscope QUANTA FEG250 instrument.

II. B. 3. 2. Contact angle

Water contact angle measurements were performed on the steel surfaces uncorroded and corroded in 1 M % HCl solution without and with 5×10^{-3} M for 24 h. The contact angles of a drop of water (2 µL) on the sample surfaces were measured by the sessile drop method with the DSA100 Kruss instrument.

II. B. 3. 3. X-ray photoelectron spectroscopy (XPS)

XPS measurements were carried out on a Kratos Axis Ultra using AlKα (1486.6 eV) radiation. The measurements were carried out at 20 eV pass energy with an energy resolution of 0.9 eV. The C 1s line of 284.4 eV was used as a reference to correct the binding energies for the charge energy shift. A Shirley background was subtracted from the spectra and signals; symmetric Gaussian functions were used in the peak fitting procedure.

II. B. 4. Computational details

II. B. 4. 1. Quantum chemical calculations

For the DFT study, the hydrazone derivatives were geometrically optimized using generalized gradient approximation (GGA) with double numeric plus polarization (DNP) basis set **[34]** in aqueous solution (COSMO solvation model) **[35].** All calculations were performed using the material studio program **[36].** The calculated values of the highest occupied molecular orbital energy (E_{HOMO}) and lowest unoccupied molecular orbital energy (E_{LUMO}) were used to determined several quantum chemical parameters according to the following equations **[37, 38]:**

The energy gap (ΔE)= E_{HOMO}- E_{LUMO} **(II.B.6)**

The ionization energy (I)= - E_{HOMO} **(II.B.7)**

The electron affinity (A)= - E_{LUMO} **(II.B.8)**

Absolute electronegativity (χ)= $\frac{I+A}{2}$ **(II.B.9)**

Global hardness (γ)= $\frac{I-A}{2}$ **(II.B.10)**

The fraction of electron transferred (ΔN) from the inhibitor molecule to the metallic surface is given by the following formula **[39]**:

$$\Delta N = \frac{\varphi - \chi_{inh}}{2(\gamma_{Fe} + \gamma_{inh})} \qquad \textbf{(}\boldsymbol{II.B.}\textbf{11)}$$

Where φ is the work function ($\varphi = 4.82\ eV$ for Fe (110) plan) and the γ_{Fe} is the global hardness of iron ($\gamma_{Fe} = 0$) **[40, 41]**.

The local reactivity of the investigated molecule was analyzed using Fukui function (f_k), which is defined as the first derivative of the electronic density ($\rho\ (\vec{r})$) with respect to the number of electrons N in a constant external potential v($\vec{r}$):

$$f_k = \left(\frac{\partial \rho\ (\vec{r})}{\partial N}\right)_{v(\vec{r})} \qquad \textbf{(}\boldsymbol{II.B.}\textbf{12)}$$

The condensed Fukui function can be calculated as follows:

$$f_k^+ = q_k(N+1) - q_k(N) \qquad \textbf{(}\boldsymbol{II.B.}\textbf{13)}$$

$$f_k^- = q_k(N) - q_k(N-1) \qquad \textbf{(}\boldsymbol{II.B.}\textbf{14)}$$

Where $q_k(N+1), q_k(N)$ and $q_k(N-1)$ are the atomic charges of the anionic, neutral and cationic species, respectively.

II. B. 4. 2. Molecular dynamics simulations

Molecular dynamics simulations were performed to study the adsorption of the investigated hydrazones on iron surface in the presence of a simulated electrolyte **[42-44]**. The simulation box consisted of two layers; surface layer of Fe (110) plan, which is picked up in the present study because it is the most stable among three common Fe substrates **[45]**, and an electrolyte layer contains one inhibitor molecule, 491 water molecules, 9 ions of H_3O^+ and Cl^- balanced with their counter ions. The interaction process between the inhibitor molecule and Fe (110) surface was assumed in a simulation box (24.82×24.82×30.04 Å). The Andersen thermostat was used to control the temperature at 298K. Simulations were conducted under periodic boundary conditions in the NVT ensemble using Ewald sum for electrostatic interactions and COMPASS force field **[46, 47].** Forcite code implemented in Material studio package was used to perform all geometry optimizations and MD simulations. Dynamics simulation was executed for 5000 ps simulation time and 1 fs time step. Interactions between hydrazones and hematite surface are estimated using the following equation:

$$E_{inter} = E_{Fe-inh} - (E_{Fe} + E_{inh}) \qquad \textbf{(}\boldsymbol{II.B.}\textbf{15)}$$

Where E_{Fe-inh}, E_{Fe}, and E_{inh} denote the total energy of Fe-hydrazone complex, iron surface, and inhibitor molecule, respectively.

II. B. 5. References

[1] H.H. Uhlig, R.W. Revie, Corrosion and corrosion control, (1985).

[2] A.S.f. Testing, Materials, ASTM G1-03: Standard Practice for Preparing, Cleaning, and Evaluating Corrosion Test Specimens, ASTM, 2004.

[3] P.M. Monk, R.J. Mortimer, D.R. Rosseinsky, Electrochromism: fundamentals and applications, John Wiley & Sons2008.

[4] J.B. Allen, R.F. Larry, Electrochemical methods fundamentals and applications, John Wiley & Sons2001.

[5] C. Ribaut, Elaboration d'un biocapteur cellulaire impédancemétrique pour la mesure des changements physiologiques affectant la cellule parasitée, Université de Toulouse, Université Toulouse III-Paul Sabatier, 2008.

[6] L. Jaubert, Etude de la corrosion uniforme d'aciers non alliés et inoxydables: utilisation conjointe de l'émission acoustique et des techniques électrochimiques, Lyon, INSA, 2004.

[7] M.E. Orazem, N. Pébère, B. Tribollet, Enhanced graphical representation of electrochemical impedance data, Journal of The Electrochemical Society 153(4) (2006) B129.

[8] F. BEDIOUI, Voltampérométrie. Perfectionnement des techniques, Techniques de l'ingénieur. Analyse et caractérisation 3(P2128) (1999) P2128. 1-P2128. 26.

[9] S. Franger, Synthèse, caractérisation et étude des propriétés électrochimiques de nouveaux oxydes de manganèse pour électrodes positives d'accumulateurs au lithium, 2001.

[10] E. Barsoukov, J.R. Macdonald, Impedance spectroscopy: theory, experiment, and applications, John Wiley & Sons2018.

[11] M.E. Orazem, B. Tribollet, Electrochemical impedance spectroscopy, New Jersey (2008) 383-389.

[12] X.-Z.R. Yuan, C. Song, H. Wang, J. Zhang, Electrochemical impedance spectroscopy in PEM fuel cells: fundamentals and applications, Springer Science & Business Media2009.

[13] C. Verma, L.O. Olasunkanmi, I. Obot, E.E. Ebenso, M. Quraishi, 2, 4-Diamino-5-(phenylthio)-5 H-chromeno [2, 3-b] pyridine-3-carbonitriles as green and effective corrosion inhibitors: gravimetric, electrochemical, surface morphology and theoretical studies, RSC advances 6(59) (2016) 53933-53948.

[14] S.K. Saha, A. Dutta, P. Ghosh, D. Sukul, P. Banerjee, Novel Schiff-base molecules as efficient corrosion inhibitors for mild steel surface in 1 M HCl medium: experimental and theoretical approach, Physical Chemistry Chemical Physics 18(27) (2016) 17898-17911.

[15] H. Shokry, E. Mabrouk, Computational and electrochemical investigation for corrosion inhibition of nickel in molar sulfuric acid by dihydrazide derivatives. Part II, Arabian Journal of Chemistry 10 (2017) S3402-S3411.
[16] H. Shokry, Molecular dynamics simulation and quantum chemical calculations for the adsorption of some Azo-azomethine derivatives on mild steel, Journal of Molecular Structure 1060 (2014) 80-87.
[17] C. Verma, H. Lgaz, D. Verma, E.E. Ebenso, I. Bahadur, M. Quraishi, Molecular dynamics and Monte Carlo simulations as powerful tools for study of interfacial adsorption behavior of corrosion inhibitors in aqueous phase: a review, Journal of Molecular Liquids 260 (2018) 99-120.
[18] J. Zhang, G. Qiao, S. Hu, Y. Yan, Z. Ren, L. Yu, Theoretical evaluation of corrosion inhibition performance of imidazoline compounds with different hydrophilic groups, Corrosion Science 53(1) (2011) 147-152.
[19] I. Obot, D. Macdonald, Z. Gasem, Density functional theory (DFT) as a powerful tool for designing new organic corrosion inhibitors. Part 1: an overview, Corrosion Science 99 (2015) 1-30.
[20] J. Bartley, N. Huynh, S. Bottle, H. Flitt, T. Notoya, D. Schweinsberg, Computer simulation of the corrosion inhibition of copper in acidic solution by alkyl esters of 5-carboxybenzotriazole, Corrosion Science 45(1) (2003) 81-96.
[21] L. Guo, S. Kaya, I.B. Obot, X. Zheng, Y. Qiang, Toward understanding the anticorrosive mechanism of some thiourea derivatives for carbon steel corrosion: A combined DFT and molecular dynamics investigation, Journal of colloid and interface science 506 (2017) 478-485.
[22] L. Guo, S. Zhang, T. Lv, W. Feng, Comparative theoretical study on the corrosion inhibition properties of benzoxazole and benzothiazole, Research on Chemical Intermediates 41(6) (2015) 3729-3742.
[23] X. Wang, L. Liu, P. Wang, W. Li, J. Zhang, Y. Yan, How the inhibition performance is affected by inhibitor concentration: a perspective from microscopic adsorption behavior, Industrial & Engineering Chemistry Research 53(43) (2014) 16785-16792.
[24] C. Verma, L. Olasunkanmi, I. Obot, E.E. Ebenso, M. Quraishi, 5-Arylpyrimido-[4, 5-b] quinoline-diones as new and sustainable corrosion inhibitors for mild steel in 1 M HCl: a combined experimental and theoretical approach, RSC advances 6(19) (2016) 15639-15654.

[25] B. Xu, W. Yang, Y. Liu, X. Yin, W. Gong, Y. Chen, Experimental and theoretical evaluation of two pyridinecarboxaldehyde thiosemicarbazone compounds as corrosion inhibitors for mild steel in hydrochloric acid solution, Corrosion Science 78 (2014) 260-268.

[26] S.D. Gupta, B. Revathi, G.I. Mazaira, M.D. Galigniana, C. Subrahmanyam, N. Gowrishankar, N. Raghavendra, 2, 4-dihydroxy benzaldehyde derived Schiff bases as small molecule Hsp90 inhibitors: Rational identification of a new anticancer lead, Bioorganic Chemistry 59 (2015) 97-105.

[27] S. Ortiz, R. Nelson, V. Kesternich, M. Pérez-Fehrmann, P. Christen, L. Marcourt, Synthesis and antifungal activity of diaryl hydrazones from 2, 4-dinitrophenylhydrazine, Journal of the Chilean Chemical Society 61(3) (2016) 3081-3084.

[28] G. ASTM, G 31-72, Standard practice for laboratory immersion corrosion testing of metals (1990).

[29] N. Djeddi, M. Benahmed, S. Akkal, H. Laouer, E. Makhloufi, N. Gherraf, Study on methylene dichloride and butanolic extracts of Reutera lutea (Desf.) Maire (Apiaceae) as effective corrosion inhibitions for carbon steel in HCl solution, Research on Chemical Intermediates 41(7) (2015) 4595-4616.

[30] K. Orubite, N. Oforka, Inhibition of the corrosion of mild steel in hydrochloric acid solutions by the extracts of leaves of Nypa fruticans Wurmb, Materials letters 58(11) (2004) 1768-1772.

[31] H. Zarrok, A. Zarrouk, B. Hammouti, R. Salghi, C. Jama, F. Bentiss, Corrosion control of carbon steel in phosphoric acid by purpald–weight loss, electrochemical and XPS studies, Corrosion Science 64 (2012) 243-252.

[32] M. Benahmed, I. Selatnia, A. Achouri, H. Laouer, N. Gherraf, S. Akkal, Steel corrosion inhibition by Bupleurum lancifolium (Apiaceae) extract in acid solution, Transactions of the Indian Institute of Metals 68(3) (2015) 393-401.

[33] S. Boudiba, K. Hanini, I. Selatnia, I. Saouane, S. Hioun, M. Benahmed, Experimental, theoretical and mathematical studies of Echium italicum L. extract as a corrosion inhibitor for carbon steel in acidic medium, Materials Research Express (2019).

[34] J.P. Perdew, K. Burke, M. Ernzerhof, Generalized gradient approximation made simple, Physical review letters 77(18) (1996) 3865.

[35] A. Klamt, G. Schüürmann, COSMO: a new approach to dielectric screening in solvents with explicit expressions for the screening energy and its gradient, Journal of the Chemical Society, Perkin Transactions 2 (5) (1993) 799-805.

[36] Materials Studio, Accelrys Inc, San Diego, USA, 2013.

[37] R.G. Pearson, Absolute electronegativity and hardness: application to inorganic chemistry, Inorganic chemistry 27(4) (1988) 734-740.

[38] V. Sastri, J. Perumareddi, Molecular orbital theoretical studies of some organic corrosion inhibitors, Corrosion 53(8) (1997) 617-622.

[39] H. Lgaz, I.-M. Chung, R. Salghi, I.H. Ali, A. Chaouiki, Y. El Aoufir, M.I. Khan, On the understanding of the adsorption of Fenugreek gum on mild steel in an acidic medium: Insights from experimental and computational studies, Applied Surface Science 463 (2019) 647-658.

[40] Z. Cao, Y. Tang, H. Cang, J. Xu, G. Lu, W. Jing, Novel benzimidazole derivatives as corrosion inhibitors of mild steel in the acidic media. Part II: Theoretical studies, Corrosion Science 83 (2014) 292-298.

[41] A. Kokalj, On the HSAB based estimate of charge transfer between adsorbates and metal surfaces, Chemical Physics 393(1) (2012) 1-12.

[42] A. Singh, K.R. Ansari, D.S. Chauhan, M.A. Quraishi, H. Lgaz, I.M. Chung, Comprehensive investigation of steel corrosion inhibition at macro/micro level by ecofriendly green corrosion inhibitor in 15% HCl medium, Journal of Colloid and Interface Science 560 (2020) 225-236.

[43] H. Lgaz, R. Salghi, S. Masroor, S.H. Kim, C. Kwon, S.Y. Kim, Y.J. Yang, I.M. Chung, Assessing corrosion inhibition characteristics of hydrazone derivatives on mild steel in HCl: Insights from electronic-scale DFT and atomic-scale molecular dynamics, Journal of Molecular Liquids 308 (2020).

[44] A. Chaouiki, H. Lgaz, R. Salghi, M. Chafiq, H. Oudda, Shubhalaxmi, K.S. Bhat, I. Cretescu, I.H. Ali, R. Marzouki, I.M. Chung, Assessing the impact of electron-donating-substituted chalcones on inhibition of mild steel corrosion in HCl solution: Experimental results and molecular-level insights, Colloids and Surfaces a-Physicochemical and Engineering Aspects 588 (2020).

[45] L. Guo, I.B. Obot, X. Zheng, X. Shen, Y. Qiang, S. Kaya, C. Kaya, Theoretical insight into an empirical rule about organic corrosion inhibitors containing nitrogen, oxygen, and sulfur atoms, Applied Surface Science 406 (2017) 301-306.

[46] H. Sun, COMPASS: an ab initio force-field optimized for condensed-phase applications overview with details on alkane and benzene compounds, The Journal of Physical Chemistry B 102(38) (1998) 7338-7364.

[47] P.P. Ewald, Die Berechnung optischer und elektrostatischer Gitterpotentiale, Annalen der physik 369(3) (1921) 253-287.

Part III

Results and discussion

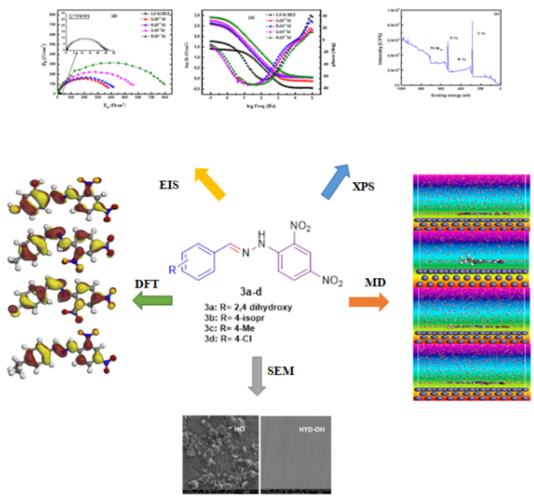

"Chemistry is necessarily an experimental science: its conclusions are drawn from data, and its principles supported by evidence from facts"
Michael Faraday

III. 1. Introduction

Hydrazone and its derivatives have become a center of attraction in recent researches because they possess not only a widespread of pharmaceutical and biological activities but also various applications in industrial chemistry **[1-5]**, due to their reactivity towards both electrophiles and nucleophiles which may be related to the presence of N-N and C=N bonds in their molecular structures **[6, 7]**.

The present part focused on the study of inhibition action of newly prepared hydrazone derivatives on the corrosion of carbon steel (CS) in 1.0 M HCl solution at 298 K. The work is carried out to establish the effective concentration for good inhibition action. Further, the work deals with the study of mechanism of inhibition through adsorption.

The studied four hydrazone derivatives are:

- (*E*) -1- (2,4-dinitrophenyl) -2- (2,4-dihydroxy benzylidene) hydrazine "**HYD-OH"**
- (*E*) -1- (2,4-dinitrophenyl) -2- (4-isopropyl benzylidene) hydrazine "**HYD-iso"**
- (*E*) -1- (2,4-dinitrophenyl) -2- (4-methyl benzylidene) hydrazine "**HYD-Me"**
- (*E*) -1- (2,4-dinitrophenyl) -2- (4-Chloro benzylidene) hydrazine "**HYD-Cl"**

The corrosion inhibition effect of these hydrazone derivatives on carbon steel in 1.0 M HCl has been determined by chemical, electrochemical, X-ray photoelectron spectroscopy (XPS) and theoretical studies. The inhibition efficiencies of these hydrazones in different concentrations and temperatures obtained for carbon steel in 1.0 M HCl were compared. Scanning electron microscope (SEM) and contact angle analyses were performed to examine the surface morphology of inhibited and uninhibited samples.

III. 2. Synthesis

III. 2. 1. Preparation of hydrazone derivatives 3a-d

The reaction leading to hydrazone derivatives (Schiff's base) **3a-d** was carried out quite easily because of the electrophilicity of the carbonyl carbon with good yields of (78-85%). The mechanism of the condensation reaction of 2,4-dinitrophenylhydrazine with the carbonyl compounds (benzaldehyde derivatives); (**Scheme 1**), involves an acid-catalyzed addition-elimination that begins with the nucleophilic addition of DNPH on the carbonyl group giving a carbinol hydrazine. The latter undergoes dehydration catalyzed by sulfuric acid; to form an iminium ion. Regeneration of the acid catalyst leads to hydrazone derivatives.

The synthesized hydrazones **(3a)** and **(3b)** were obtained as red powder while the hydrazone **(3c)** and **(3d)** were obtained as an orange powder having melting points between [140-256°C]. These compounds are soluble in dichloromethane (DCM), acetone and tetrahydrofuran (THF). The powders were recrystallized in the mixture (EtOH / THF) in order to purify them.

The synthesized compounds are stable because of the good distribution of the conjugation.

III. 2. 2. The reaction mechanism

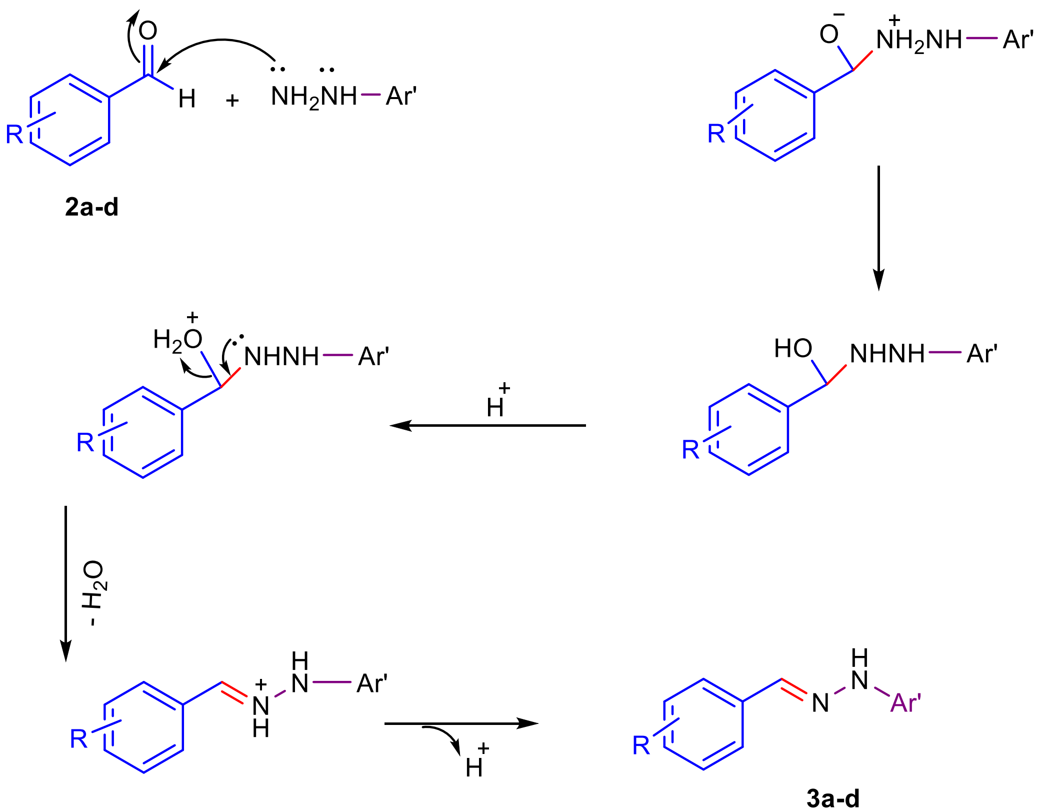

Ar': 2,4-dinitrophényl
2a, 3a: R= 2,4 dihydroxy
2b, 3b: R= 4-isopr
2c, 3c: R= 4-Me
2d,3d: R= 4-Cl

Scheme III. 1. Reaction mechanism of Hydrazone derivatives

III. 2. 3. Physicochemical characteristics of the synthetized hydrazones:

Compound (3a) red powder <$C_{13}H_{10}O_6N_4$>		
MP (°C): 256	R_{dt} : 75%	M=318 g/mol

Compound (3b) red powder <$C_{16}H_{16}O_4N_4$>		
MP (°C): 140	R_{dt} : 85%	M=328 g/mol

Composund (3c) orange powder <$C_{14}H_{12}O_4N_4$>		
MP (°C): 215	R_{dt} : 81%	M=300 g/mol

Compound (3d) orange powder <$C_{13}H_9ClO_4N_4$>		
MP (°C): 244	R_{dt} : 78%	M=320g/mol

III. 2. 4. Spectral analysis

- The examination of the UV-vis spectrum of the obtained hydrazone derivatives (HYD's) in dichloromethane at room temperature indicates the presence of an absorption bands in ultraviolet domain. The spectrum of HYD's shows band at 270-273 nm attributed to $\pi \rightarrow \pi^*$ transitions produced by the imine group (C=N), aromatic rings and nitro group (NO_2) of the synthesized hydrazones.
- The analysis of the obtained IR spectrum of the synthesized HYD's reveals the disappearance of the absorption band due to the functional group (C = O) and the presence of the following bands: the band located at the region between 3266-3455 cm^{-1} is attributed to the N‒H and –OH stretching vibration for HYD-OH . Vibration elongation bands appear at 3111 cm^{-1} are attributed to aromatic CH bonds. Moreover, the bands appeared at 2964-2970 cm^{-1} are assigned to the stretching vibration of aliphatic C‒H bonds. The presence of bands within the range of 1610‒1615 cm^{-1} is mostly due to the bending vibration of the aromatic system. The characteristic band of the synthesized hydrazones is observed as a very intense band within the range 1506-1515 cm^{-1}, which is assigned to the stretching vibration of the imine group (C=N), this fairly low stretching frequency means that nitrogen (C = N) forms a strong hydrogen bond with a proton-donating azomethine group. In addition, the stretching vibration of the aromatic nitro group (Ar‒NO_2) was appeared as an intense band within the range 1314-1360 cm^{-1}.
- The examination of the obtained ^1H NMR spectrum for the synthesized molecules allows determining the main characteristic signals, the characteristic aromatic protons – CH aromatic are assigned to the signals observed in the region of 6.33-8.94 ppm for HYD-OH, 7.33-8.36 ppm for HYD-iso, 7.62-9.13 ppm for HYD-Me and 7.57-8.87 ppm

for HYD-Cl. Moreover, the observed singular signal at 9.66 ppm for HYD-OH, 11.31 ppm for HYD-iso, 11.29 ppm for HYD-Me and 11.71 ppm for HYD-Cl may be referred to the proton of -NH group. The protons appeared as a singular signal at 10.05 ppm and 11.40 ppm are assigned to –OH group for HYD-OH. On the other hand, the interpretation of ^{13}C NMR spectrum of the HYD's derivatives indicates the presence of signals characteristic of the carbons present in the proposed molecular structures, for example aromatic signals between 123 and 130 ppm

III. 3. Corrosion study results

III. 3. 1. Weight loss measurements

III. 3. 1. 1. Effect of concentration on corrosion inhibition

The variation of corrosion rate (C_R) and inhibition efficiencies $\eta_w\%$ with different concentrations of hydrazone derivatives in 1.0 M HCl at 298 K for 24 hours are summarized in **Table III. 1.** Like most organic inhibitors, the obtained results for the four inhibitors indicate that the corrosion rate decreases with the increase of concentration **(***via* **Table III. 1),** leading to an increase of the inhibition efficiency that reaches a maximum at 5×10^{-3} M, which reflects its excellent corrosion inhibition properties. The protection performance follows the order HYD-OH >HYD-iso>HYD-Me > HYD-Cl.

Even though weight loss are primary results, they are of great interest and give basic insights about the performance of tested compounds. Based on this finding, we could obviously assume that the tested hydrazone derivatives act by adsorption on the steel surface and cover the metal surface by the accumulation of more number of molecules leading to the formation of an adsorbed film from the hydrazone compounds, and therefore, isolating it from the corrosive solution **[8]**, which can be favored by the presence of several nonbonding electrons on heteroatoms of functional groups (-NO_2, -NH, -OH), and π-electrons of the aromatic rings. The presence of two (-OH) groups in the position *ortho* and *para*, which is an electron-donating group, seems to be the reason for the higher anti-corrosion performance of HYD-OH (97.83% at 5×10^{-3} M) compared to other inhibitors. It could enhance the adsorption process by increasing the electron charge density on the molecule, thereby increasing the binding affinity with steel surface **[9, 10]**.

Table III. 1. Variation of the corrosion rate of CS and inhibition efficiencies in the absence and presence of different concentrations of hydrazone derivatives for 24 hours at 298 K.

[inhibitor] (M)	HYD-OH			HYD-iso			HYD-Me			HYD-Cl		
	C_R (mg cm^{-2} h^{-1})	η_w (%)	θ	C_R (mg cm^{-2} h^{-1})	η_w (%)	θ	C_R (mg cm^{-2} h^{-1})	η_w (%)	θ	C_R (mg cm^{-2} h^{-1})	η_w (%)	θ
Blank	1.321	-	-	1.321	-	-	1.321	-	-	1.321	-	-
1×10^{-4}	0.0881	93.33	0.9333	0.1247	90.56	0.9056	0.1564	88.16	0.8816	0.2143	83.78	0.8378
5×10^{-4}	0.0592	95.52	0.9552	0.0919	93.12	0.9312	0.1288	90.25	0.9025	0.1759	86.69	0.8669
1×10^{-3}	0.0548	95.85	0.9585	0.0792	94.00	0.9400	0.1129	91.45	0.9145	0.1459	88.96	0.8896
5×10^{-3}	0.0287	97.83	0.9783	0.0486	96.32	0.9632	0.0778	94.11	0.9411	0.1114	91.57	0.9157

III. 3. 1. 2. Effect of temperature on corrosion inhibition

As known, the variation in the temperature of the corrosive medium doesn't affect only the corrosion rate of steel, but also the interaction between the inhibitor and the surface of the steel **[11]**. In this context, the effect of temperature on the corrosion inhibition property of the hydrazone derivatives, weight loss measurement was performed using variable temperatures ranging from 298 to 328 K in the absence and presence of different concentrations of the hydrazone derivatives. The obtained resulted are represented in **Table III. 2** and **Figure III. 1**.

Data in **Table III. 2** suggest that all inhibitors get adsorbed on the carbon steel surface at all studied temperatures and the corrosion rate increases with temperature the increase of in both uninhibited (more obvious) and inhibited solution and the inhibition efficiency decreases with the increase in the temperature, indicating that the hydrazone derivatives is a temperature-dependent inhibitor, which favor the dissolution of CS by decreasing the strength of adsorption process with the increase in temperature, and this is indicative of the physical adsorption mode **[12]**. Actually, the slight decrease in the inhibition efficiency (*via* **Figure III. 1**) from 97.83%, 96.32%, 94.11% and 91.57% at 298 K to 93.24%, 91.25%, 89.15% and 85.48% at 328 k, for HYD-OH, HYD-iso, HYD-Me and HYD-Cl, respectively, indicates the strength of the interactions between the inhibitors and steel surface **[13]**

Table III. 2. Variation of the corrosion rate and inhibition efficiencies in the absence and presence of different concentrations of hydrazone derivatives for 24 hours at different temperatures.

T (K)	Inhibitors /Conc. (M)	HYD-OH			HYD-iso			HYD-Me			HYD-Cl		
		C_R (mg cm^{-2} h^{-1})	η_w (%)	θ	C_R (mg cm^{-2} h^{-1})	η_w (%)	θ	C_R (mg cm^{-2} h^{-1})	η_w (%)	θ	C_R (mg cm^{-2} h^{-1})	η_w (%)	θ
298	,	1.321	-	-	1.3210	-	-	1.321	-	-	1.321	-	-
	1×10^{-4}	0.0881	93.33	0.9333	0.1247	90.56	0.9056	0.1564	88.16	0.8816	0.2143	83.78	0.8378
	5×10^{-4}	0.0592	95.52	0.9552	0.0919	93.12	0.9312	0.1288	90.25	0.9025	0.1759	86.69	0.8669
	1×10^{-3}	0.0548	95.85	0.9585	0.0792	94.00	0.9400	0.1129	91.45	0.9145	0.1459	88.96	0.8896
	5×10^{-3}	0.0287	97.83	0.9783	0.0486	96.32	0.9632	0.0778	94.11	0.9411	0.1114	91.57	0.9157
308	Blank	1.9521	-	-	1.9521	-	-	1.9521	-	-	1.9521	-	-
	1×10^{-4}	0.1638	91.61	0.9161	0.2323	88.10	0.8810	0.3088	84.18	0.8418	0.3812	80.47	0.8047
	5×10^{-4}	0.1284	93.42	0.9342	0.1566	91.98	0.9198	0.2118	89.15	0.8915	0.2819	85.56	0.8556
	1×10^{-3}	0.1148	94.12	0.9412	0.1435	92.65	0.9265	0.1778	90.89	0.9089	0.2471	87.34	0.8734
	5×10^{-3}	0.0779	96.01	0.9601	0.0957	95.10	0.9510	0.1214	93.78	0.9378	0.1864	90.45	0.9045
318	Blank	2.5744	-	-	2.5744	-	-	2.5744	-	-	2.5744	-	-
	1×10^{-4}	0.2775	89.22	0.8922	0.3403	86.78	0.8678	0.4147	83.89	0.8389	0.5702	77.85	0.7785
	5×10^{-4}	0.2304	91.05	0.9105	0.3007	88.32	0.8832	0.4119	84	0.84	0.4593	82.16	0.8216
	1×10^{-3}	0.2021	92.15	0.9215	0.2360	91.22	0.9122	0.3403	86.78	0.8678	0.407	84.19	0.8419
	5×10^{-3}	0.1491	94.21	0.9421	0.1738	93.25	0.9325	0.2749	89.32	0.8932	0.3285	87.24	0.8724
328	Blank	3.1423	-	-	3.1423	-	-	3.1423	-	-	3.1423	-	-
	1×10^{-4}	0.5109	83.74	0.8373	0.4792	84.75	0.8475	0.5911	81.19	0.8119	0.8626	72.55	0.7255
	5×10^{-4}	0.3472	88.95	0.8895	0.4336	86.20	0.8620	0.5056	83.91	0.8391	0.7407	76.43	0.7643
	1×10^{-3}	0.2995	90.47	0.9047	0.3733	88.12	0.8812	0.4475	85.76	0.8576	0.5911	81.19	0.8119
	5×10^{-3}	0.2124	93.24	0.9324	0.2750	91.25	0.9125	0.3409	89.15	0.8915	0.4563	85.48	0.8548

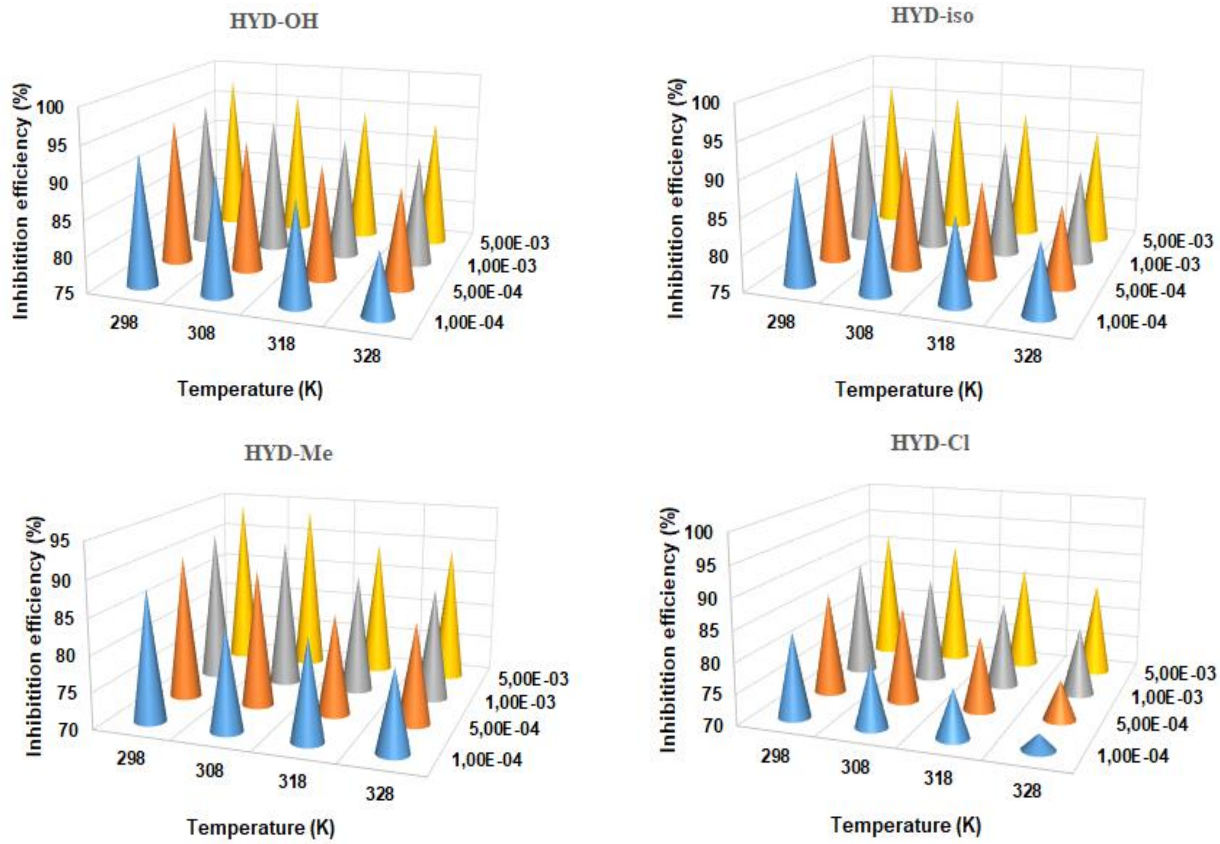

Figure. III. 1. Variation of inhibition efficiencies as a function of temperature after 24 hours of immersion time in 1M HCl with different concentrations of the four hydrazone derivatives.

III. 3. 1. 3. Activation parameters of the corrosion process

The activation energy (E_a) of the corrosion process could be determined according to the Arrhenius formula **[14, 15]**:

$$C_R = A \exp\left(\frac{-E_a}{RT}\right) \qquad \textbf{(III. 1)}$$

Where R is gas constant, T is the absolute temperature (K) and A is pre-exponential constant.

The activation energy (E_a) values calculated from the slopes of the straight lines (*via* **Figure III. 2**) in the absence and presence of different concentrations of hydrazone derivatives are reported in **Table III. 3**. It is obviously in this table that the values of activation energy increased from 23.46 kJ/mol (blank) to 37.60 kJ/mol, 38.93 kJ/mol, 47.17 kJ/mol and 54.37 kJ/mol after the addition of 5×10^{-3} of HYD-Cl, HYD-Me, HYD-iso and HYD-OH, respectively, which is almost in agreement with the order of inhibitory effectiveness. this behavior suggests that the inhibitors was adsorbed on the steel surface and formed an energy barrier which reduces the metallic dissolution [16]. According to Solmaz [17], the change in activation energy cannot be considered a criterion for determining the adsorption type due to some excess activation energy that results from the removal of water particles from the surface. It can be concluded that the adsorption of hydrazone derivatives molecules on the CS surface in HCl solution involves both physical which is the first stage of adsorption, and chemical processes.

Additional, the transition state equation (**eq. III. 2**) was used to deduce the entropy of activation (ΔS_a) and enthalpy of activation (ΔH_a) for the adsorption/desorption process involved in CS corrosion [15].

$$C_R = \frac{RT}{Nh} \exp\left(-\frac{\Delta H_a}{RT}\right) \exp\frac{\Delta S_a}{R} \qquad \textbf{(III. 2)}$$

Where h is the Planck's constant and N is Avogadro's constant. **Figure. III. 3** represent the plots of ln CR/T against 1/T, the slope and intercept were used to obtain the values of ΔH_a and ΔS_a, respectively. The positive values for the enthalpy of activation presented in **Table III. 3** for both uninhibited and inhibited solutions and higher in the presence of inhibitors indicate that the corrosion process is endothermic and an activated complex was formed which making the dissolution of CS difficult leading to higher protection efficiency [18]. Otherwise, the values of entropy of activation increased in the presence of hydrazones, suggesting that the decrease in the disorder during the formation of activated complex by replacement of water molecules from the steel surface by the inhibitors molecules [19].

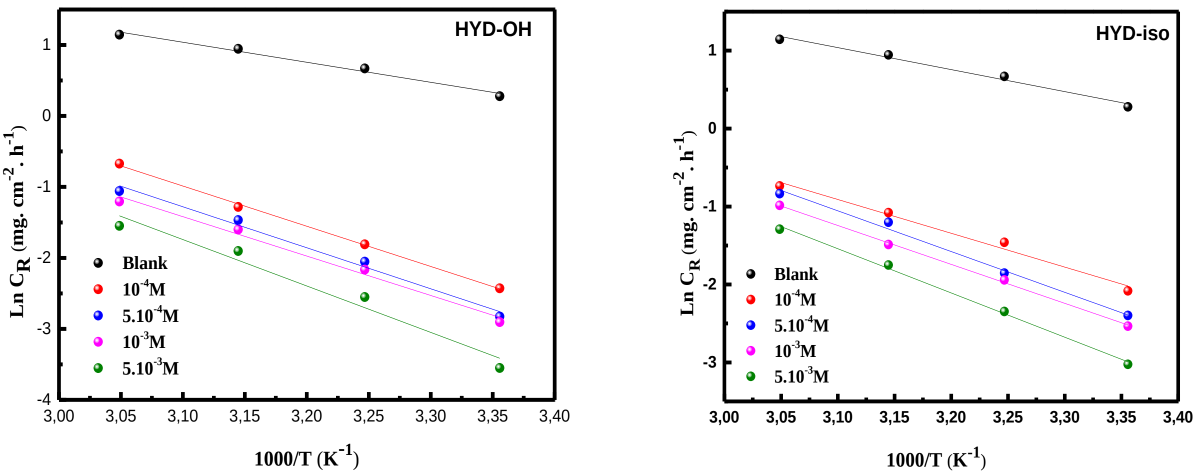

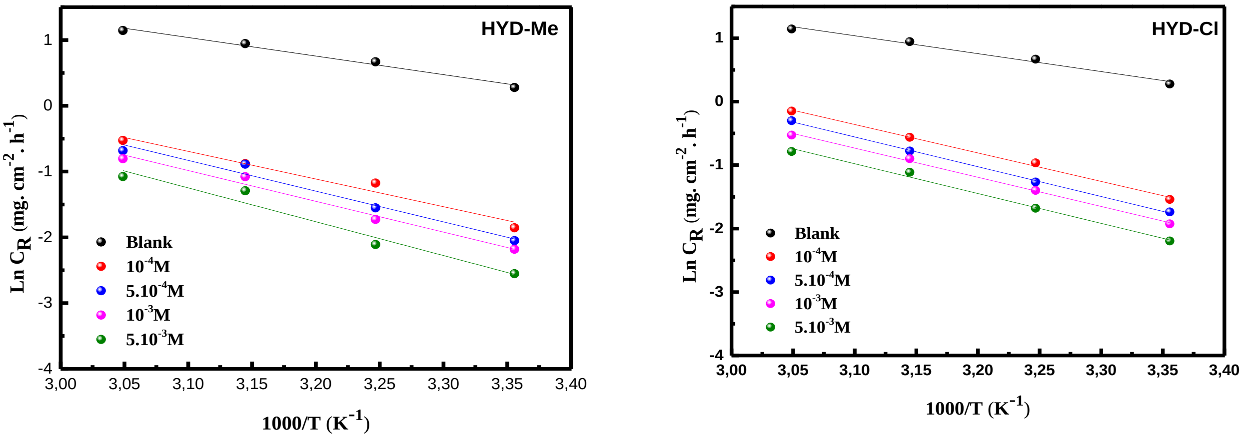

Figure. III. 2. Arrhenius plots for CS with and without different concentrations of hydrazone derivatives.

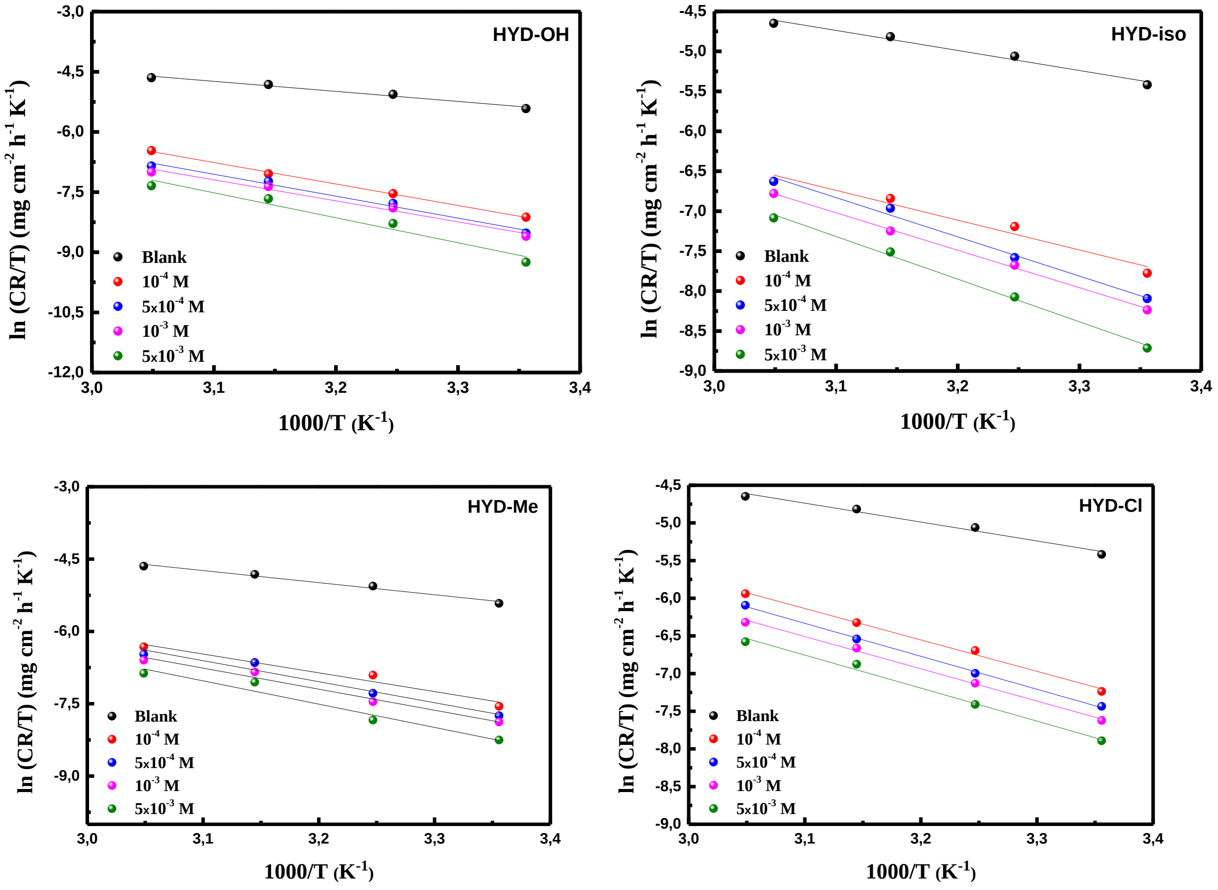

Figure. III. 3. Transition state plots for CS with and without different concentrations of hydrazone derivatives.

Table III. 3. Activation parameters for carbon steel in 1.0 M HCl for different concentrations of hydrazone derivatives at different temperatures.

Inhibitor	C (M)	E_a (kJ mol^{-1})	ΔH_a(kJ mol^{-1})	-ΔS_a(J mol^{-1} K^{-1})
HYD-OH	Blank	23.46	20.86	133.99
	1×10^{-4}	47.11	44.52	77.50
	5×10^{-4}	48.04	45.44	77.06
	1×10^{-3}	46.15	43.56	84.06
	5×10^{-3}	54.37	51.78	61.26
HYD-iso	Blank	23.46	20.86	133.99
	1×10^{-4}	36.04	33.45	111.17
	5×10^{-4}	43.46	40.86	89.39
	1×10^{-3}	41.49	38.90	97.05
	5×10^{-3}	47.17	44.58	81.91
HYD-Me	Blank	23.46	20.86	133.99
	1×10^{-4}	34.96	32.36	112.72
	5×10^{-4}	38.87	36.27	101.75
	1×10^{-3}	38.92	36.31	102.88
	5×10^{-3}	42.75	40.15	93.20
HYD-Cl	Blank	23.46	20.86	133.99
	1×10^{-4}	37.28	34.69	102.75
	5×10^{-4}	38.99	36.39	99.10
	1×10^{-3}	38.22	35.62	102.94
	5×10^{-3}	39.05	36.45	102.41

III. 3. 1. 4. Adsorption isotherm

In order to understand the mechanism of corrosion inhibitor and the type of interaction between hydrazone derivatives and CS surface, various adsorption isotherms such as (Langmuir, Temkin, Freundlich,…) were employed to fit the experimental results. In our present study, Langmuir adsorption isotherm, **Eq. (III. 3)** **[20],** was found to be the most suitable mode to fit experimental data. At all temperatures, the values of regression coefficients (R^2) were almost close to unity (*via* **Table III. 4**), which confirm that the adsorption of the tested hydrazones on the CS surface obeys Langmuir isotherm model.

$$\frac{C}{\theta} = \frac{1}{K_{ads}} + C \qquad \textbf{(III. 3)}$$

where C is the concentration of hydrazones, θ is the surface coverage and K_{ads} is the adsorption equilibrium constant, which is related to the standard Gibbs free energy of adsorption ΔG^0_{ads} as follow **[21]**:

$$\Delta G^0_{ads} = -RT \ln (C_{solvant} \times K_{ads}) \qquad \textbf{(III. 4)}$$

Where $C_{solvant}$ the concentration of water in solution (55.5 mol/l) **[22]**, R is the gas constant (8.314 J K^{-1} mol^{-1}) and T is the absolute temperature (K).

From the **Table III. 4**, the large value of K_{ads} at 298 K for hydrazone derivatives suggesting the strong adsorption of the hydrazones on the CS surface, which implies more efficient adsorption and hence better $\eta_w\%$ but the decrease in K_{ads} value with increases with temperature indicates the tendency of hydrazones to undergo desorption at higher temperature. The calculated value of ΔG^0_{ads} for hydrazones is negative implying spontaneity of their adsorption on CS surface and stability of adsorbed inhibitory film. Generally, values of ΔG^0_{ads} up to -20 kJ mol^{-1} represent interaction between the charged molecules and charged metal (physical adsorption), while value more negative than -40 kJ mol^{-1} involve sharing or transfer of electrons from the inhibitors to the metal surface to form a coordinate type of bond (chemical adsorption) **[22]**. The values of ΔG^0_{ads} for hydrazone derivatives varied between -35.39 and -39.82 kJ mol^{-1}. It can be suggested that the adsorption of these derivatives particularly involves both physical and chemical processes **[23-25]**. Hydrazones shows better inhibition efficiency because their structure contains several numbers of heteroatoms (N and O) and high electron density (aromatic rings), which act as donors of electrons to the vacant *d*-orbital of iron.

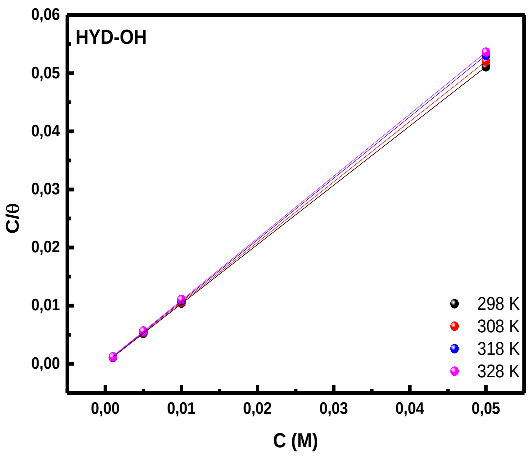

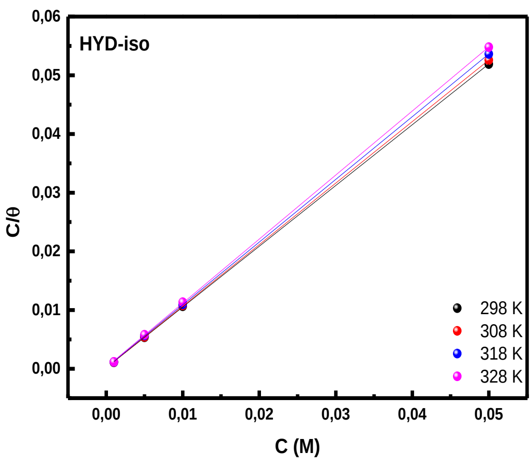

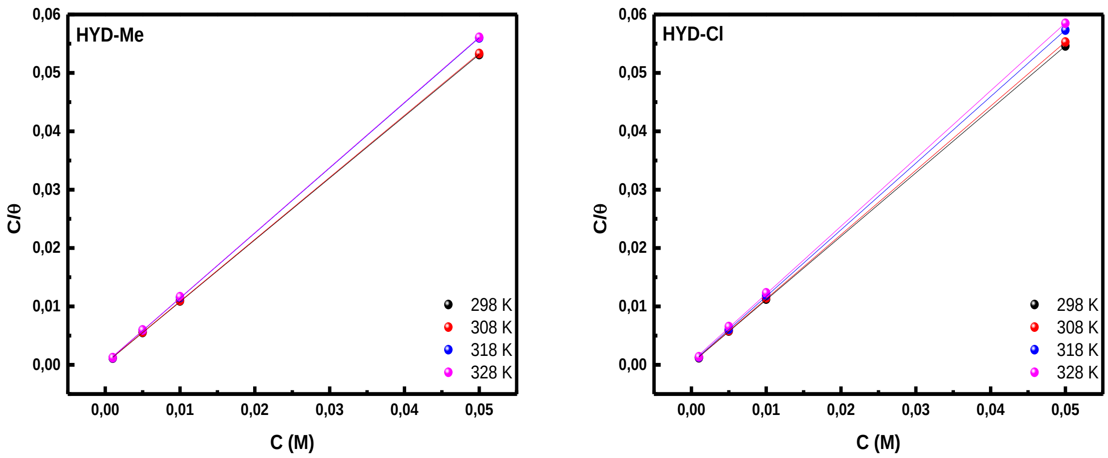

Figure. III. 4. Langmuir plots of hydrazone derivatives at different temperatures

Table III. 4. Standard thermodynamic parameters of hydrazone derivatives in 1.0 M HCl solution at different temperatures.

inhibitor	Temperature (K)	Langmuir isotherm		
		R^2	K_{ads} 10^{-3} (M^{-1})	-ΔG ($KJ\ mol^{-1}$)
HYD-OH	298	0.999	74.51	37.75
	308	0.999	70.60	38.87
	318	0.999	59.04	39.66
	328	0.999	39.63	39.82
HYD- iso	298	0.999	56.80	37.07
	308	0.999	52.55	38.12
	318	0.999	45.17	38.96
	328	0.999	35.80	39.55
HYD-Me	298	0.999	46.94	36.60
	308	0.999	36.39	37.18
	318	0.999	34.95	38.27
	328	0.999	31.21	39.17
HYD-Cl	298	0.999	28.80	35.39
	308	0.999	23.62	36.07
	318	0.999	22.53	37.12
	328	0.999	20.02	37.96

III. 4. 1. Electrochemical measurements

III. 4. 1. 1. Electrochemical impedance spectroscopy (EIS)

The corrosion inhibition process of CS in 1.0 M HCl solution without and with different concentrations of hydrazone derivatives can be explored more thoroughly from electrochemical impedance spectroscopy test [26]. EIS curves (Nyquist and Bode representations) of CS steel in 1 M HCl obtained in the absence and presence of hydrazone derivatives at various concentrations are presented in **Figure III. 5**. As observed, Nyquist plots (**Figure III. 5 a-d**) display imperfect single depressed capacitive loop with almost similar shapes without and with inhibitors characteristic of the corrosion process controlled by a charge transfer with a heterogeneous and irregular surface [27]. However, the diameter of semicircle increased after the addition of inhibitors compared to the capacitive loop of the uninhibited solution, which may be attributed to a higher charge-transfer resistance of the working electrode in the inhibited solution than in the uninhibited solution [28-30], indicating that hydrazones self-assemble on the CS surface to form protective layer [30, 31]. In the bode plots (**Figure III. 5 e-h**), only one-time constant is observed in the phase angle curves, that describes the interfacial impedance, which can be attributed to the relaxation effect resulting by the adsorption of the studied inhibitors on the CS surface [12]. The increase at the low-frequency impedance modulation values (**Figure III. 5 e-h**) with an increase in the inhibitor concentration is mainly attributed to the adsorption of hydrazones molecules on the CS surface [32]. Moreover, the obvious increase in the phase angle value from 65° in the blank solution to approximately 74° in the presence of 5×10^{-3}M of all tested hydrazones can be attributed to the formation of a protective layer on the CS surface. For a deeper analysis of the corrosion inhibition process, EIS plots should be fitted using equivalent circuits. The most appropriate electrical equivalent circuit (EEC) obtained by fitting the experimental data is shown in **Figure III. 6**. It consists of solution resistance (R_s), constant phase element (CPE), polarization resistance that is the sum of all other resistances ($R_p = R_{ct} + R_d + R_f + R_a$) [12], with R_{ct} denotes the charge transfer resistance, R_d is the diffuse layer resistance, R_a refers to the resistance of accumulated species at the metal/solution interface and R_f is the resistance of inhibitor film at the steel, which is considered only in the presence of inhibitors. The constant phase element (CPE) is associated with the double layer capacitance (C_{dl}) by equation **(III. 5)** and impedance is given by equation **(III. 6)** [33]:

$$C_{dl} = (Q \times R_p^{1-n})^{\frac{1}{n}} \qquad \textbf{(III. 5)}$$

$$Z_{\mathrm{CPE}} = \frac{1}{Q(j\omega)^{n}} \qquad \textbf{(III. 6)}$$

Where Q and n are the proportionality coefficient and irregularity parameter, ω is the angular frequency, and j denotes the imaginary unit.

The electrochemical EIS parameters obtained from fitting along with the inhibition efficiencies $\eta_R(\%)$ are recorded in **Table III. 5**.

According to results reported in **Table III. 5**, the values of the polarization resistance R_p increases with increase in the hydrazone derivatives concentration even in small amount 10^{-4}M (399.0, 306.3, 199.2 and 155.2 Ω cm² for HYD-OH, HYD-iso, HYD-Me and HYD Cl, respectively) compared to the acidic solution (24.37 Ω cm²), suggesting the formation of a protective layer over the steel surface. On the other hand, the double layer capacitance (C_{dl}) decreases with the addition of inhibitors, indicating that more organic molecules are adsorbed on the metallic surface by replacing H_2O molecules, thus forming a compact barrier against acid attack at the same time **[34, 35]**. As can be also seen from **Table III. 5**, the inhibition efficiency was increased markedly and reached 97%, 96%, 93% and 91% for HYD-OH, HYD-iso, HYD-Me and HYD Cl, respectively. The presence of OH groups in the phenyl ring of HYD-OH leads a significant increase in the inhibition efficiency compared to the other substituent. It is common knowledge that the organic compounds containing OH group have an obvious role in the corrosion inhibition of metals. The electron donating nature of OH groups imply considerable delocalization of π-electron density at phenyl ring. While the substitution by electron withdrawing groups like Chlorine atoms decreases the inhibition efficiency of tested hydrazones **[27, 36]**.

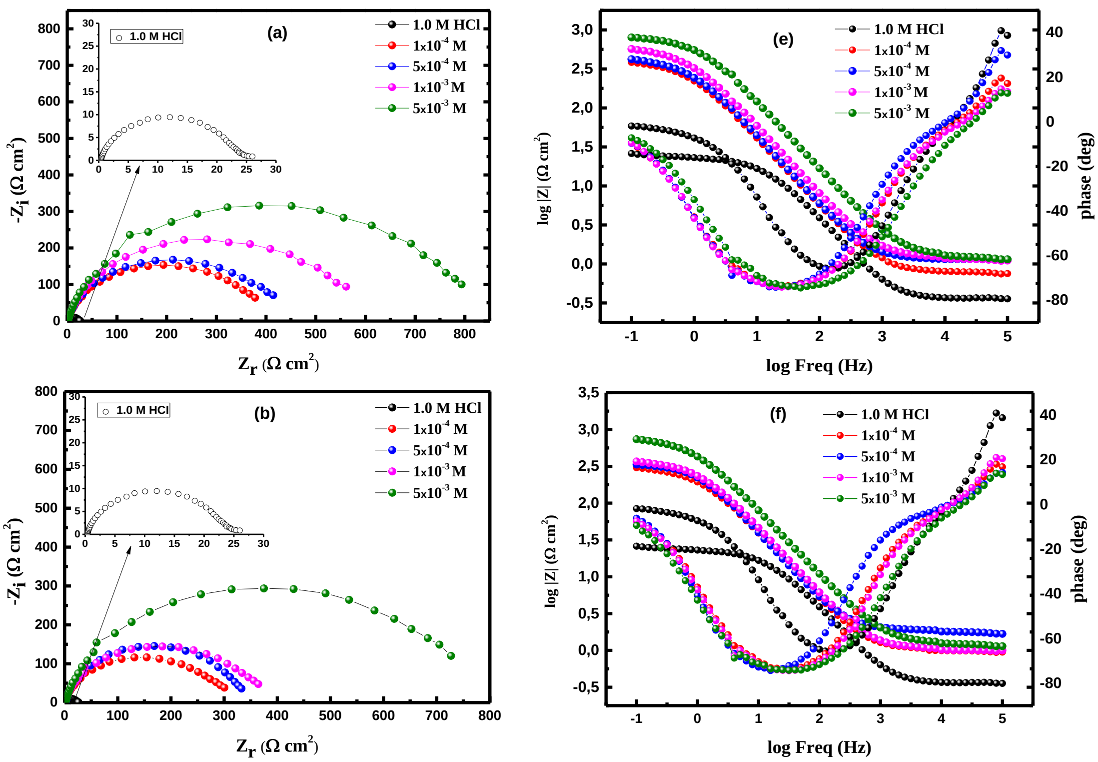

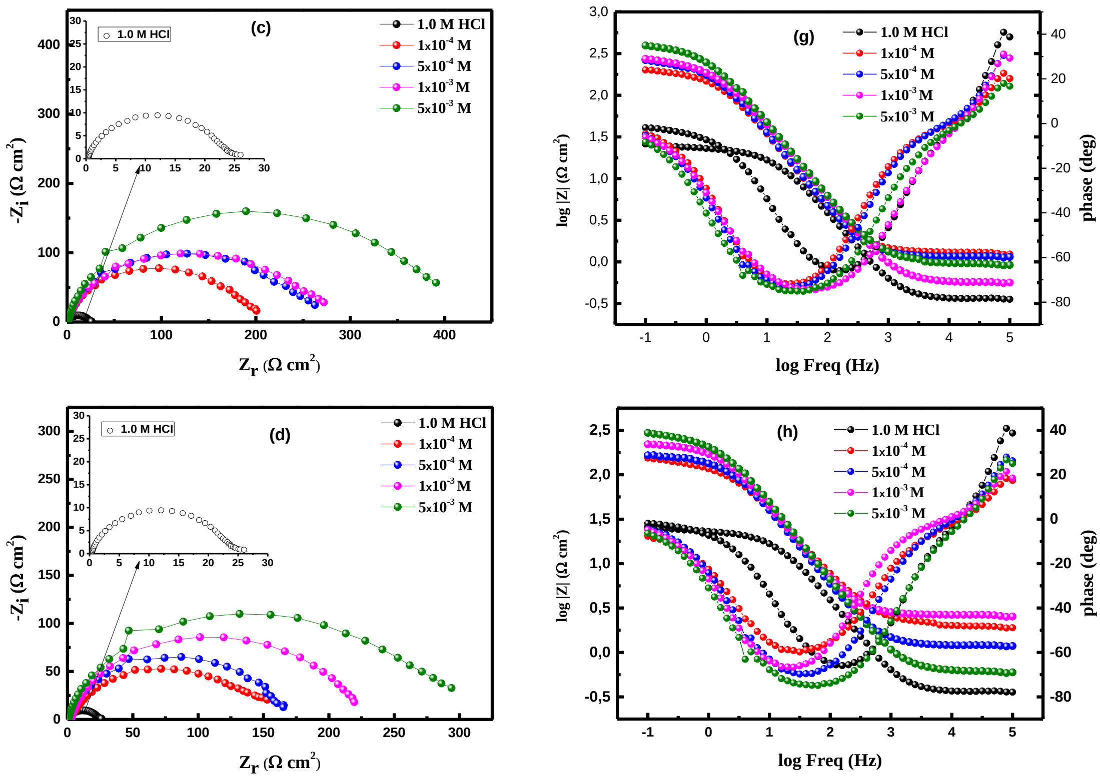

Figure. III. 5. Nyquist, Bode and phase angle plots for CS in 1.0 M HCl with and without the optimum concentrations of HYD-OH (a,e), HYD-iso (b,f), HYD-Me (c,g) and HYD-Cl (d,h).

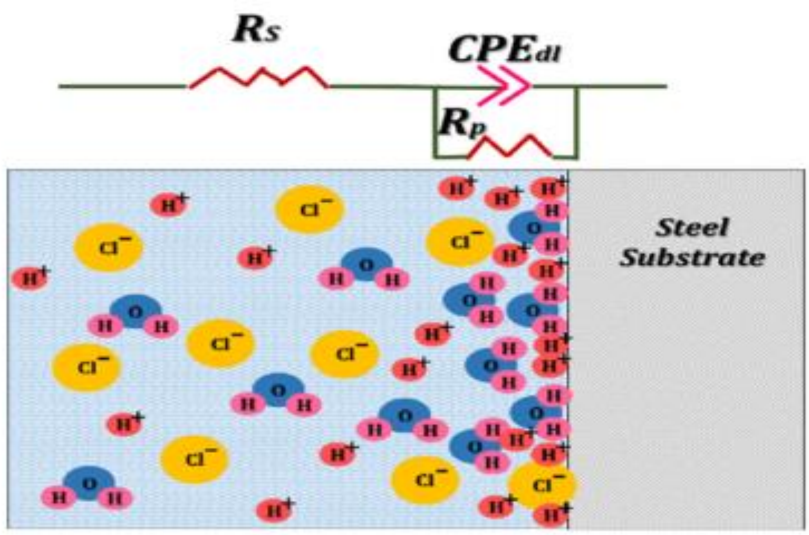

Figure. III. 6. Equivalent circuit plot for fitting the EIS data.

Table III. 5. Electrochemical impedance spectroscopy parameters for CS in 1 M HCl in the absence and presence of different concentrations of HYD's compounds at 298 K.

Inhibitors	C (M)	R_p (Ω cm^2)	R_s (Ω cm^2)	10^{-3} *Q* (F S^{-1})	*n*	C_{dl} (μF cm^{-2})	η_R(%)
HYD-OH	Blank	24.37	0.271	0.893	0.963	522.3	-
	1×10^{-4}	399.0	0.274	0.615	0.997	502.5	93.89
	5×10^{-4}	433.6	0.402	0.539	0.994	462.4	94.38
	1×10^{-3}	588.6	0.203	0.437	0.995	340.6	95.86
	5×10^{-3}	819.1	0.293	0.211	0.996	155.4	97.02
HYD-iso	Blank	24.37	0.271	0.893	0.963	522.3	-
	1×10^{-4}	306.3	0.325	0.619	0.990	519.5	92.04
	5×10^{-4}	335.0	0.174	0.559	0.992	475.0	92.73
	1×10^{-3}	372.9	0.345	0.520	0.993	426.7	93.46
	5×10^{-3}	767.5	0.220	0.328	0.997	261.2	96.82
HYD-Me	Blank	24.37	0.271	0.893	0.963	522.3	-
	1×10^{-4}	199.2	0.808	0.648	0.986	504.8	87.77
	5×10^{-4}	260.6	0.452	0.605	0.983	488.5	90.65
	1×10^{-3}	275.3	0.258	0.516	0.987	462.4	91.15
	5×10^{-3}	402.3	0.327	0.489	0.994	395.6	93.94
HYD-Cl	Blank	24.37	0.271	0.893	0.963	522.3	-
	1×10^{-4}	155.2	1.686	0.798	0.982	512.4	84.30
	5×10^{-4}	165.2	0.998	0.594	0.997	481.5	85.25
	1×10^{-3}	221.1	2.318	0.546	0.997	454.9	88.97
	5×10^{-3}	294.7	0.169	0.472	0.997	432.0	91.73

III. 4. 1. 2. Potentiodynamic polarization curves (PDP)

Polarization curves are a very good and useful approach to study corrosion mechanisms by understanding the kinetics of both anodic and cathodic reactions. Electrochemical parameters like corrosion potential (E_{corr}), corrosion current density (i_{corr}) as well as cathodic and anodic Tafel slopes (β_c, β_a) were extracted from the PDP curves (**Figure III. 7**) and presented in **Table III. 6.** Inspection of **Figure III. 7**and **Table III. 6** shows that there is no substantial change in anodic polarization curves while a slight modification can be noticed in the cathodic branches. The same can be stated for the corrosion potential values, which are moved slightly towards positive directions. In contrast, the comparison between PDP curves in the absence and presence of inhibitors reveals a noticeable decrease in the corrosion current density upon addition of inhibitor concentrations. These observations signify that the hydrazone derivatives act as mixed-type inhibitors with a slight modification of cathodic process mechanism of hydrogen evolution reaction **[37, 38]**. It suggests that, in the presence of all inhibitors, the hydrogen evolution reaction is activation-controlled and inhibitors act by adsorption at the metal/solution interface, blocking active sites of corrosion via a protective layer **[39].**

Besides visual inspection, numerical parameters listed in **Table III. 6** indicate that the corrosion current density in the blank solution (1.2268 mA/cm²) decreases considerably after the addition of all inhibitors (0.1921-0.0332 mA/cm²). This decrease in i_{corr} values is associated with an increase in the inhibition efficiencies, suggesting that these compounds are excellent corrosion inhibitors, might be due to the high electron densities on the molecule resulting from the presence of π-electrons in the aromatic ring and lone pair electrons. Furthermore, PDP results confirm the highest inhibition performance of HYD-OH having an inhibition efficiency of 97.29%, followed by HYD-iso (95.82%), HYD-Me (93.76%), and HYD-Cl (91.07%).

Table III. 6. Potentiodynamic polarization indices and inhibition efficiencies of CS in 1 M HCl without and with the addition of various concentrations of hydrazone derivatives at 298 K.

Inhibitors	C (M)	$-E_{corr}$ (mV/SCE)	i_{corr} (mA cm^{-2})	β_a (mV dec^{-1})	$-\beta_c$ (mV dec^{-1})	η_P(%)
HYD-OH	Blank	454.4	1.2268	107.4	143.8	-
	1×10^{-4}	427.3	0.0862	72.6	115.2	92.97
	5×10^{-4}	431.8	0.0733	71.4	114.8	94.03
	1×10^{-3}	425.7	0.0498	71.0	117.4	95.94
	5×10^{-3}	405.3	0.0332	55.8	126.1	97.29
HYD-iso	Blank	454.4	1.2268	107.4	143.8	-
	1×10^{-4}	449.7	0.1158	95.2	115.8	90.56
	5×10^{-4}	442.6	0.0927	51.1	115.7	92.44
	1×10^{-3}	447.1	0.0719	67.3	109.3	94.13
	5×10^{-3}	438.7	0.0512	48.9	122.8	95.82
HYD-Me	Blank	454.4	1.2268	107.4	143.8	-
	1×10^{-4}	447.2	0.1558	71.9	139.3	87.30
	5×10^{-4}	433.2	0.1185	77.6	165.5	90.34
	1×10^{-3}	429.8	0.1025	79.5	158.6	91.64
	5×10^{-3}	424.5	0.0766	73.0	141.9	93.76
HYD-Cl	Blank	454.4	1.2268	107.4	143.8	-
	1×10^{-4}	426.7	0.1921	85.0	166.2	84.34
	5×10^{-4}	431.4	0.1691	82.0	169.1	86.22
	1×10^{-3}	424.4	0.1572	85.5	165.6	87.19
	5×10^{-3}	427.2	0.1096	80.6	163.4	91.07

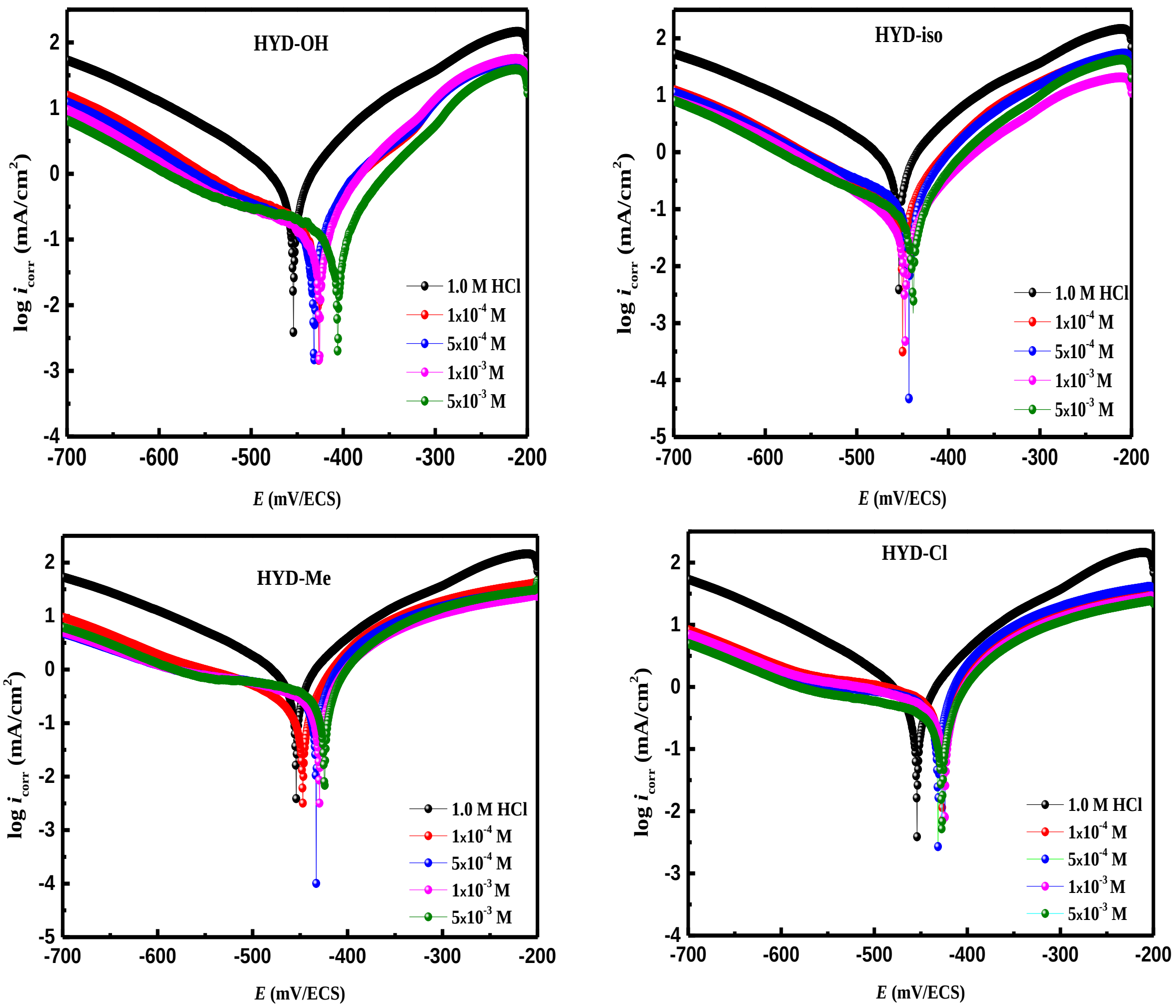

Figure. III. 7. Potentiodynamic polarization curves for CS obtain in 1.0 M HCl in the absence and presence of different concentrations of hydrazone derivatives.

III. 5. 1. Surface analysis

III. 5. 1. 1. Scanning electron microscopy (SEM)

Figure III. 8 displays the surface morphology of CS samples exposed to 1.0 M HCl solution with and without the optimal concentration 5×10^{-3} M of hydrazone derivatives for 24 h at 298 K. **Figure III. 8 (a)** indicate that the surface of CS in the absence of inhibitors is strongly damaged and the corrosion products covered the whole surface due to acceleration of its dissolution in HCl solution. However, the influence of the addition of hydrazone derivatives to the acid solution on the morphology of the steel surface is evident, as observed in **Figure III. 8 (b-e)**. It is apparent that morphology has been a very remarkable change attributed to the decreased the dissolution of the metal substrate, and almost a smoother surface is achieved, suggesting the formation of a protective layer by hydrazones molecules on the iron surface, which prevent the metal from corrosion.

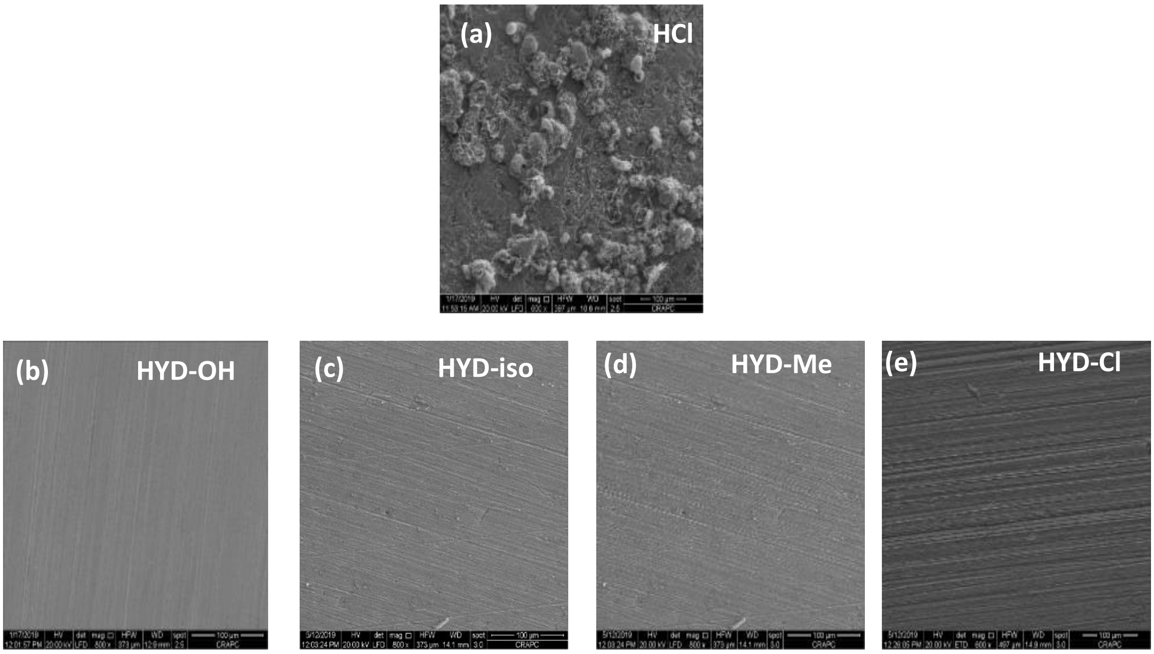

Figure. III. 8. SEM micrographs after 24 h of immersion in 1 M HCl solution without and with the presence of 5.10^{-3} M of hydrazones derivatives.

III. 5. 1. 2. Contact angle

Contact angle tests were performed to confirm the presence of a protective layer by evaluating the hydrophobicity/hydrophilicity of the CS surface. **Figure III. 9** shows the contact angle of the CS coupons after dipping for 24 hours without and with the optimum concentration of tested hydrazones at 298 K. The contact angle in the acid medium alone is 55.0°, which indicates that the carbon steel in the HCl solution has a hydrophilic character, due to the precipitation of a porous layer of iron oxide/hydroxide on its surface. This leads to the condensation of the hydrogen bond formed between the electrolyte and the substrate **[40, 41].** In contrast, the contact angle increases in the presence of 5×10^{-3} M of hydrazone derivatives. It shows 114.9°, 102.4°, 69.0°, and 63.8° in the presence of HYD-OH, HYD-iso, HYD-Me, and HYD-Cl, respectively. These results reveal an improved hydrophobic properties of steel surface, thereby suggesting the formation of a protective layer on the CS surface that prevent the adsorption of water molecules and result in a highest protection from corrosion **[42].**

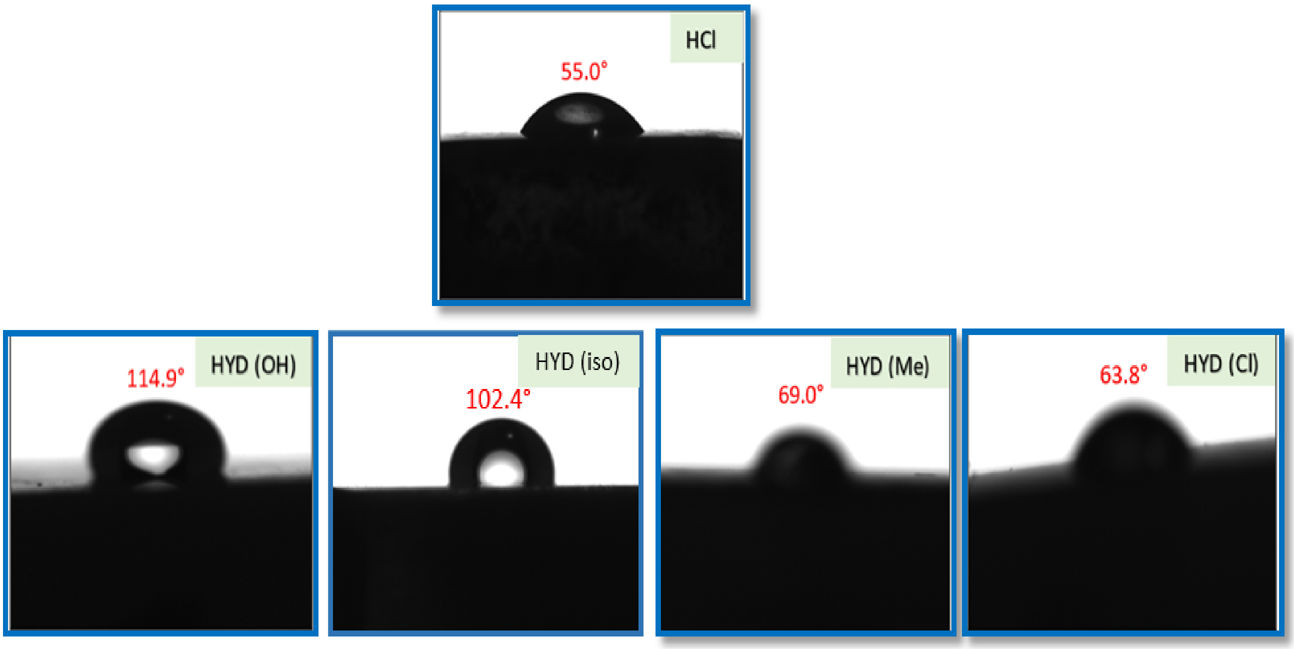

Figure. III. 9. Contact angle micrographs after 24 h immersion of steel in 1.0 M HCl solution without and with the addition of 5×10^{-3} M of the hydrazones derivatives.

III. 5. 1. 3. X-ray photoelectron spectroscopy (XPS)

XPS analysis is known to be an effective device to confirm the protected layer composition formed by the adsorption of inhibitors on the steel surface and to elucidate the corrosion inhibition mechanism. Thus, we performed XPS on CS specimens dipped in 1 M HCl with the optimum concentration (5×10^{-3} M) of the four hydrazones derivatives after 24 hours. The overall XPS survey spectrum **(Figure III. 10 a-d)** shows multiple peaks for different elements Fe 2p, N 1s, O 1s and C 1s. The appearance of peaks of N and O in protected sample surface spectra confirms the adsorption of hydrazones on the CS surface. The high resolution of Fe 2p, N 1s, O 1s and C 1s spectra are represented in **Figure III. 11 a-d.** The Fe 2p spectrum (*via* **Figure III. 11 a-d.** depicts a double peak profile located at a binding energy around 710 eV (Fe $2p_{3/2}$) and 724 eV **(**Fe $2p_{1/2}$**)** together with an associated ghost structure **[43, 44]**. The deconvolution of $Fe2p_{3/2}$ of HYD-OH **(Figure III. 11a)** and HYD-iso **(Figure III. 11b)** consist in four main peaks, while HYD-Me **(Figure III. 11c)** and HYD-Cl **(Figure III. 11d)** consist in three main peaks which may be correspond to iron oxide and hydroxide **[45]**. The peak appear at 706.5 eV **(Figure III. 11a)** reveals to metallic iron (Fe^0) species **[37]**. The peak at ~ 710 eV **(Figure III. 11 a-d)** attributed to Fe^{+3} due to the formation of Fe_2O_3 and/or Fe_3O_4 and FeOOH. These ferric species can be formed a stable and insoluble film which suppress ionic diffusion and protect the steel **[46, 47]**. The peak around 713 eV (**Figure III. 11 a-d**) correspondent to the presence of $FeCl_3$. However the peak at ~715 eV (**Figure III. 11 a-d**) can be ascribed to the satellite of Fe (III) **[47]**. Based on the oxidation state in the literature **[48]**, the peak located at ~ 712 eV (**Figure III. 11b**) is associated to ferryl ions Fe^{+4}, which can lead to the formation of an oxoiron (IV) complex (**Scheme III. 2**) **[48, 49]**. The C 1s spectrum (**Figure III. 12 a-d**) shows three peaks at ~ 284, 285 and 288 eV. The first peak has the major influence and corresponds to C-C, C-H of aromatic rings and C=C **[10, 50]**. The second peak confirms the presence of the C-N and C=N bonds **[46]**. The last peak may be attributed to carbon atom of $C=N^+$ and $C-O^+$ (**Scheme III. 3**) which resulted from protonation of nitrogen atoms and hydroxyl groups of HYD-OH, respectively **[20, 37, 45, 51].** While the peak observed at 286.6 eV (**Figure III. 12a**) attributed to C-OH. The deconvolution of O 1s spectrum consists of three peaks (**Figure III. 13a-d**), the first one at ~ 529 eV due to O_2^- bonded with Fe_3^+, which results from Fe_2O_3 or Fe_3O_4 oxides **[52]**.While, the second peak at ~ 531 eV signifies to OH^- , and can be related to the presence of hydrous iron oxides **[53]**. The lastly one appears at ~534 eV attributed to C-OH and oxygen of adsorbed water molecules on the surface **[46]**. A single peak is observed in the N 1s spectra (**Figure III. 14 a-d**) at binding energy ~399 eV is attributed to N-Fe, confirm that the hydrazone derivatives was adsorbed on the steel surface by forming an organo-metalic complex on the basis of donor-acceptor interactions between N atoms of the hydrazone derivatives and the *d*-orbital of iron **[45]**. Together, these results confirm the effective adsorption of inhibitor molecule on steel surface, which is explained by the presence of all inhibitor parts in the inhibitors film. It also suggests that there are mainly two type of interactions between iron atoms and inhibitor molecules, electrostatic and chemical interactions.

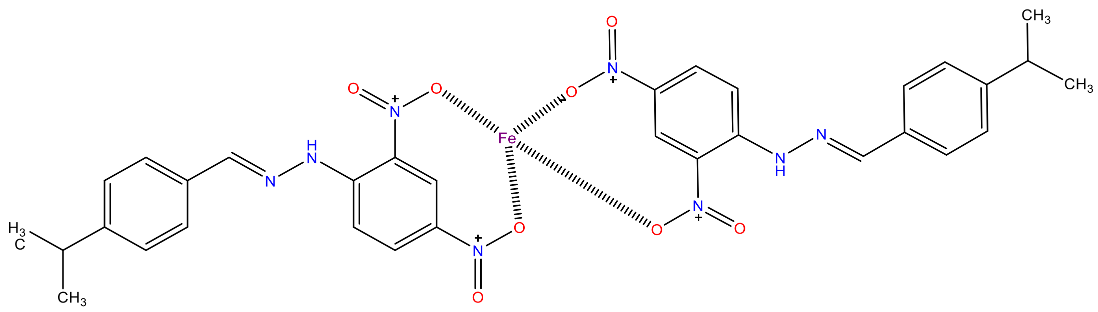

Scheme III. 2. The formation of an oxoiron (IV) complex.

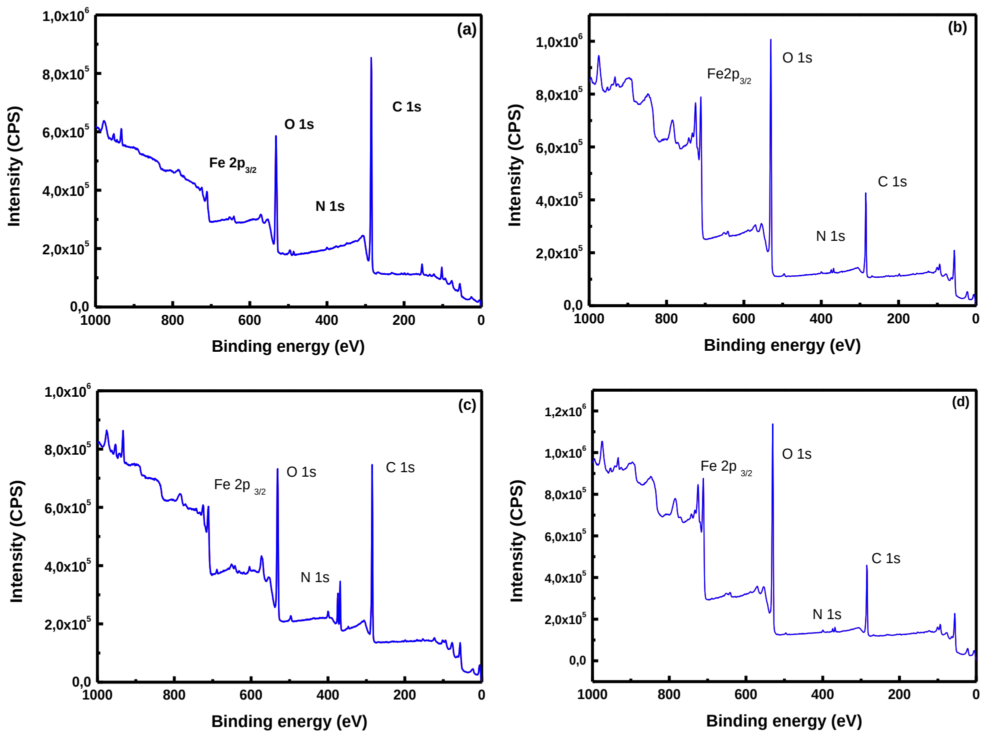

Figure. III. 10. XPS survey spectra of the CS treated for 24 h in 1.0 M HCl solution containing 5. 10^{-3} M of HYD-OH (a), HYD-iso (b), HYD-Me (c) and HYD-Cl (d).

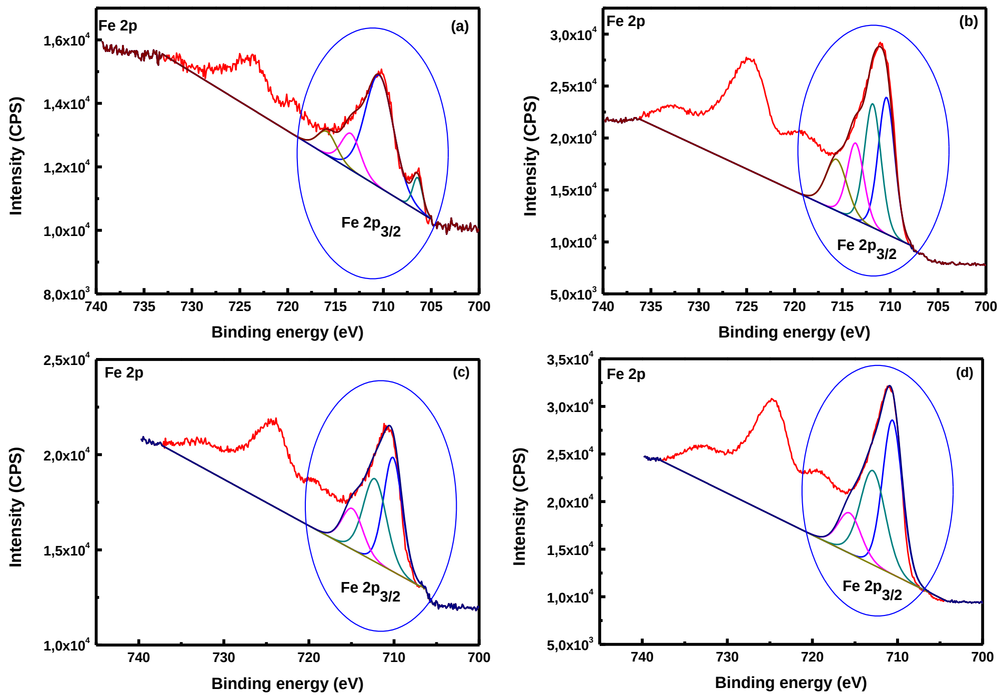

Figure. III. 11. XPS High-resolution deconvoluted profiles of Fe 2p for CS treated for 24 h in 1.0 M HCl solution containing 5. 10^{-3} M of HYD-OH (a), HYD-iso (b), HYD-Me (c) and HYD-Cl (d).

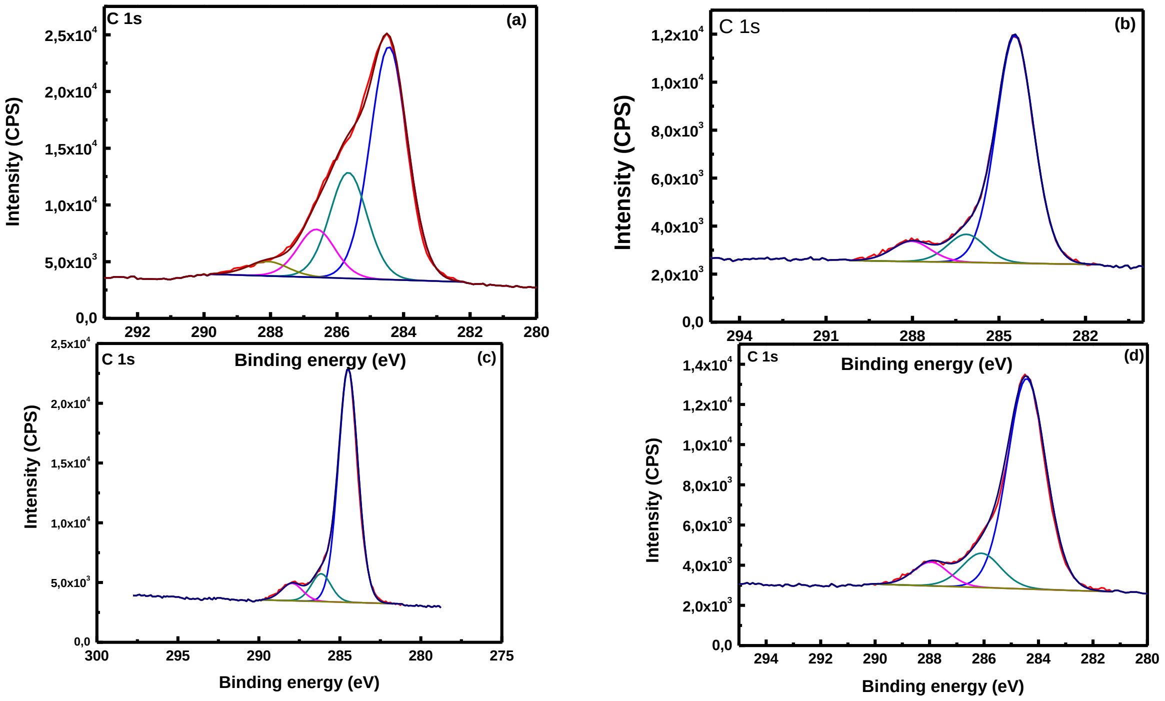

Figure. III. 12. C1s XPS spectra of the CS surfaces covered with 5. 10^{-3} M of HYD-OH (a), HYD-iso (b), HYD-Me (c) and HYD-Cl (d) immersed in 1.0 M HCl solution for 24 h.

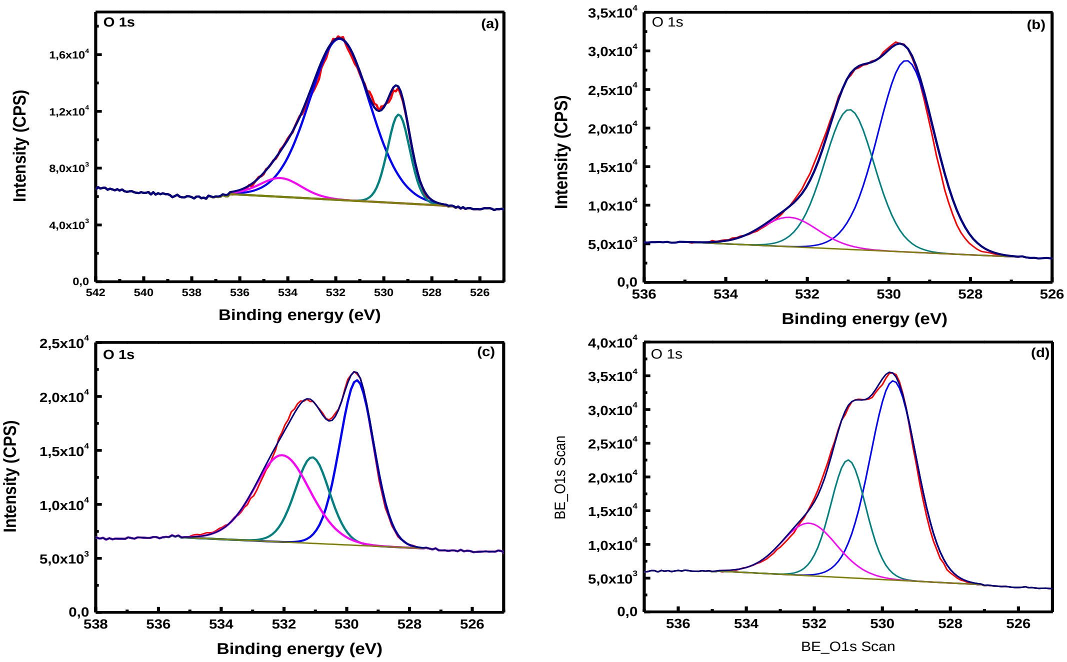

Figure. III. 13. O 1s XPS spectra of the CS surfaces covered with 5. 10^{-3} M of HYD-OH (a), HYD-iso (b), HYD-Me (c) and HYD-Cl (d) immersed in 1.0 M HCl solution for 24 h.

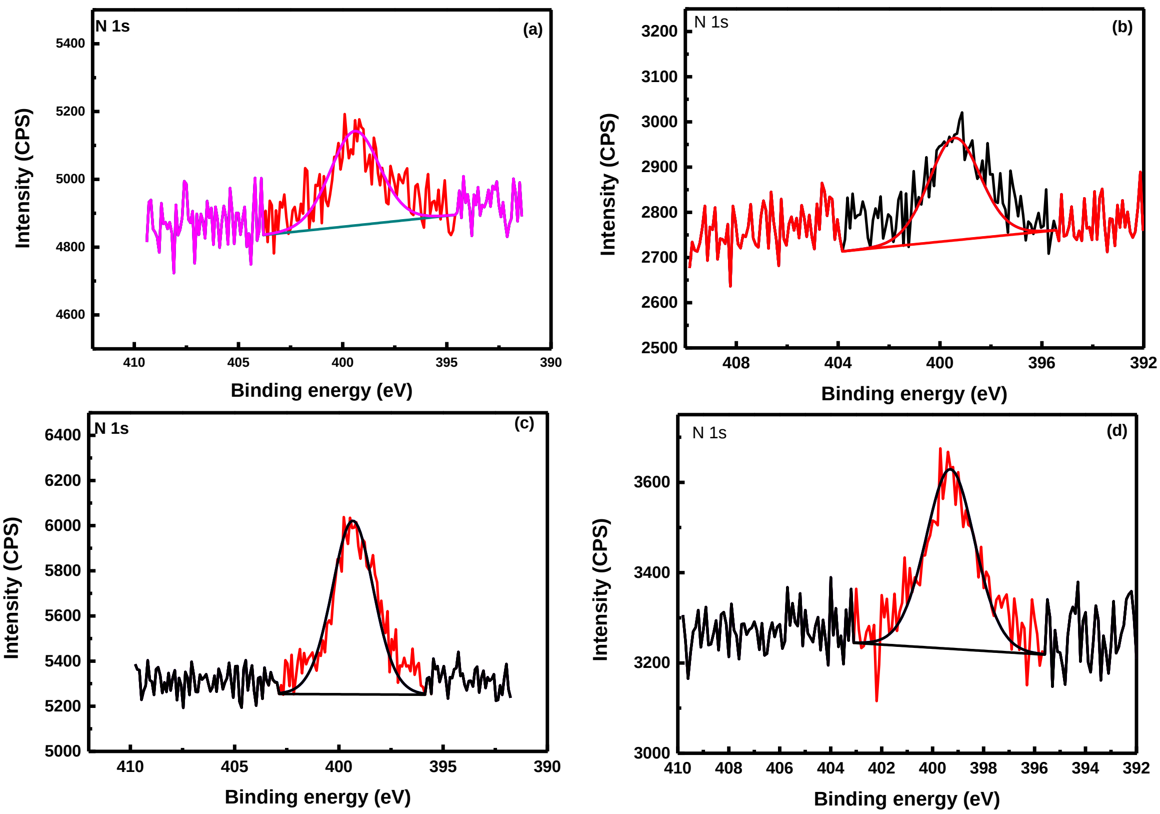

Figure. III. 14. N 1s XPS spectra of the CS surfaces covered with 5. 10^{-3} M of HYD-OH (a), HYD-iso (b), HYD-Me (c) and HYD-Cl (d) immersed in 1.0 M HCl solution for 24 h.

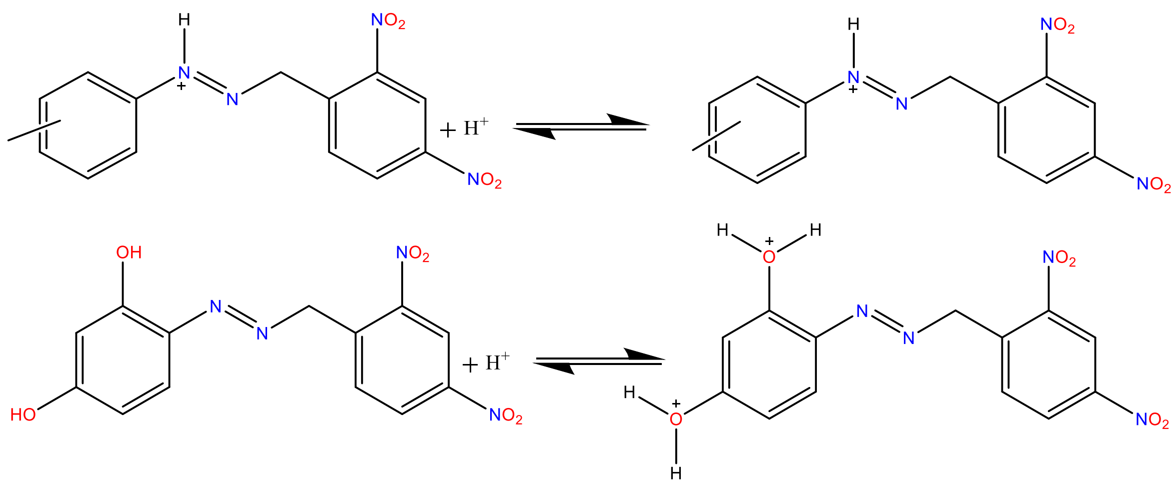

Scheme III. 3. The protonation state of the hydrazone molecule in 1 M HCl

III. 6. 1. Quantum chemical calculation

III. 6. 1. 1. Global reactivity descriptors

To establish a relationship between the inhibitor structure and its corrosion inhibition performance, and to unveil the inhibition mechanism, density functional theory (DFT) approach has been adopted. The optimized molecular structure, HOMOs, LUMOs, and molecular electrostatic potential maps were presented in **Figure III. 15**. It is obvious that the distribution of the HOMO density cover the entire molecular structure of hydrazone derivatives. This could be attributed to the presence of a conjugation effect and a high electron density, which increases the electron-donating ability of the molecule, and thus an enhanced electron transfer interaction between inhibitor's reactive sites and vacant orbitals of the metal **[18]**. On the other hand, the LUMO electron density is well distributed over the 2,4-dinitrophenyl cycle, which an indication of its high ability to receive electrons from the metal surface. Interestingly, the 2,4-dinitrophenyl moiety exhibits both characters, i.e., the ability to receive and donate electrons, and therefore it is expected to play a crucial role in donor-acceptor interactions between inhibitor molecule and iron atoms. Some global reactivity descriptors calculated in the aqueous phase are listed in **Table III. 7**. Organic substances with a higher energy level of HOMO, i.e. a less negative value, easily donate electrons from HOMO to an empty orbital of appropriate acceptors and E_{LUMO} denotes the ability of the molecule to accept electrons **[54, 55]**. Similarly, lower values of the energy gap ΔE are associated with effective inhibition **[56]**. The results indicate that the values of the HOMO energy E_{HOMO} and of the energy gap ΔE support the following ordering of the inhibition effectiveness of hydrazones: HYD-OH > HYD-iso > HYD-Me > HYD-Cl.

The effectiveness of hydrazone derivatives as inhibitor has been further addressed by evaluating the global reactivity parameters. The electronegativity χ, global chemical hardness γ, and the fraction of transferred electron ΔN, are involved in **Table III. 7**. HYD-OH has the lowest and HYD-Cl the highest electronegativity. Similarly, the global hardness value increases from HYD-OH through HYD-iso and HYD-Me to HYD-Cl. The obtained value of Δ*N* is positive and less than 3.6. So, in accordance with the Lukovits et *al.* study **[57]**, the corrosion inhibitive activity of hydrazone derivatives is enhanced by increasing of its ability to donate electrons, which indicates the formation of an adsorbed inhibitive layer at the iron surface and appearance of coordinate bonds between the inhibitive molecules and the iron atoms **[58]**. While it is not possible to discuss these parameters without comparing them with those of a similar compound, it is important to note that energy gap of the present molecules is very low, compared to many reported corrosion inhibitors **[34, 59-61].** Yet again, this observation confirms our findings that the investigated hydrazone derivatives has outstanding corrosion inhibition effects.

III. 6. 1. 2. Molecular electrostatic potential (MEP)

The MEP is an important informative property for identifying the highest and lowest electron density regions in an inhibitor molecule **[62]**. The MEP maps have been extracted after completing geometry optimization (**Figure III. 15**). The red color stand for the negative region (nucleophilic attack), while the blue color stand for the positive region (electrophilic reactivity) **[63]**. In the MEP maps above, it is evident that the most electrostatic potential indicated by deep red color is concentrated around the $-NO_2$ group, indicating its greatest ability to form a covalent bond with *d*-orbital of metal. The other parts of the molecules are mainly associated with nucleophilic reactivity.

Table III. 7. Calculated quantum chemical indices of the studied compounds.

Descriptors	E_{HOMO} (eV)	E_{LUMO} (eV)	ΔE (eV)	I	A	χ	γ	ΔN
HYD-OH	-5.187	-3.700	1.487	5.187	3.700	4.444	0.744	0.253
HYD-iso	-5.355	-3.725	1.630	5.355	3.725	4.540	0.815	0.086
HYD-Me	-5.473	-3.749	1.724	5.473	3.749	4.611	0.862	0.121
HYD-Cl	-5.595	-3.790	1.805	5.595	3.790	4.693	0.903	0.071

Figure. III. 15. The Optimized geometry, HOMO, LUMO and electrostatic potential structure for inhibitors molecule.

Inhibitors	Optimized Structure	HOMO	LUMO	MEP
HYD-OH	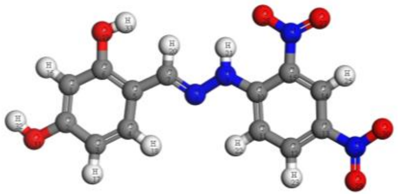	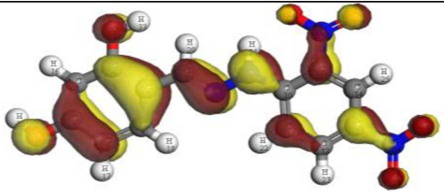	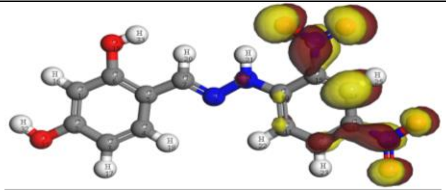	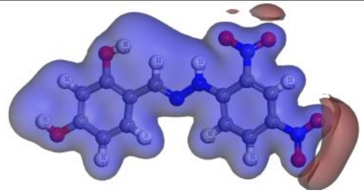
HYD-iso	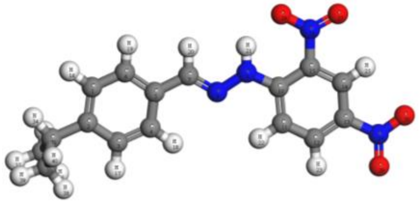	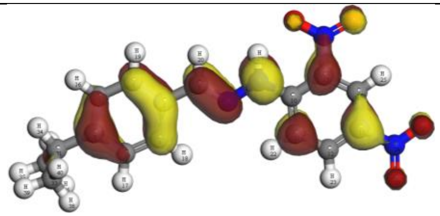	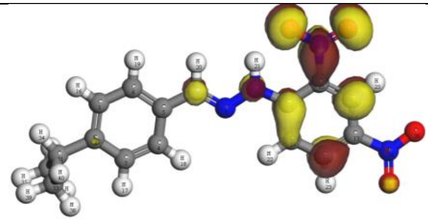	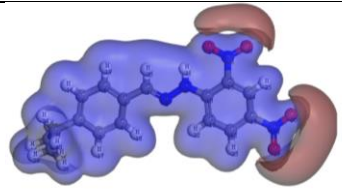
HYD-Me	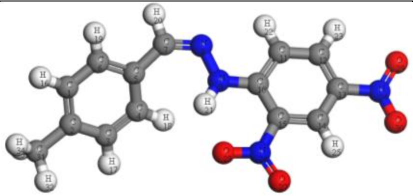	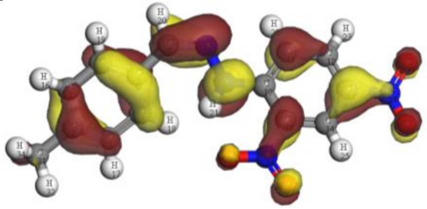	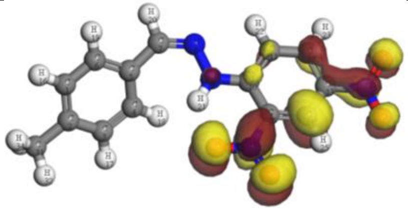	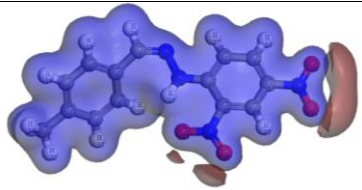
HYD-Cl	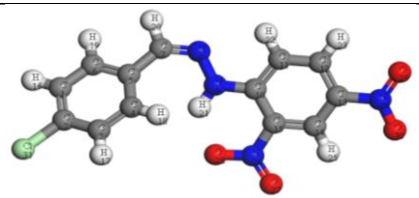	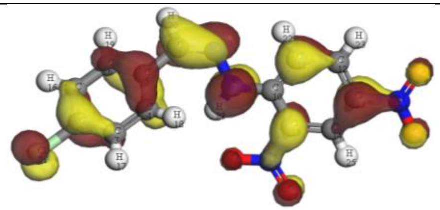	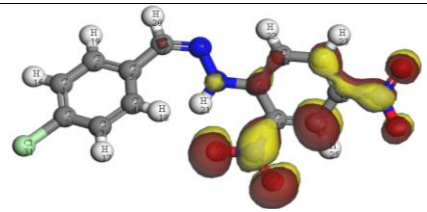	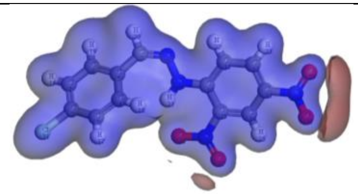

III. 6. 1. 2. Active sites

The active sites responsible for donor-acceptor (D-A) type interactions between inhibitor molecule and iron surface can be determined more precisely from neutral atomic charge distribution and Fukui indices **[64]**. The Mulliken charges and Fukui indices of hydrazone derivatives are displayed in **Figure III. 16**. It is reported that a higher negative charge of heteroatom means a high electronic density, and indicates a high tendency for participation in the D-A types of interaction **[65]**. The analysis of Mulliken results represented in **Figure III. 16** indicates that a high negative Mulliken atomic charge occur on N8, N9, O27, O28, O29, O30 atoms in all tested hydrazone derivatives, and some carbon atoms as well. These atoms are expected to offer electrons to the metal surface and are the most susceptible reactive sites for adsorption [60] . The widespread distribution of reactive sites is mainly the reason for the potent corrosion inhibition performance of the tested molecule.

The Fukui indices are significant for analyzing the local reactive sites responsible for the nucleophilic and electrophilic behavior of an inhibitor. Based on literature, atoms with high values of f_k^+ indicate that these sites have a nucleophilic attack character, whereas those having higher values of f_k^- are the most susceptible sites for the electrophilic attack **[66]** . From the calculated Fukui indices, the most preferable sites for the electrophilic attack are located in the N (8), N (9), O (27), O (28), O (29) and O (30) atoms with the most positive part of f_k^-, whereas the N (24), N (26), O (27), O (28), O (29) and O (30), are the most reactive sites for the nucleophilic attack. Both Fukui indices and Mullikan distribution results are in good agreement with the frontier orbital distribution of inhibitors. From the above analysis, we could conclude that the high inhibitory power of hydrazone derivatives is a result of its widespread active sites, which play the key role in D-A interactions with the metal surface.

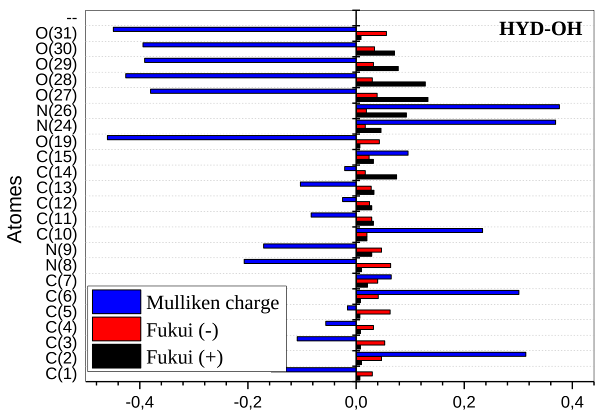

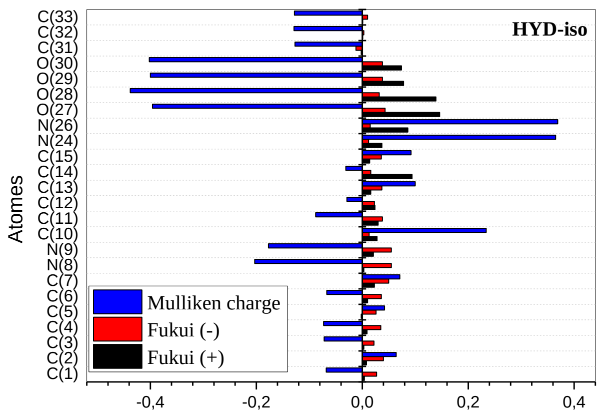

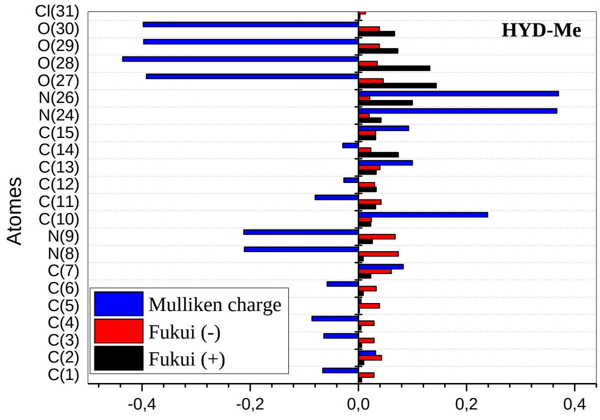

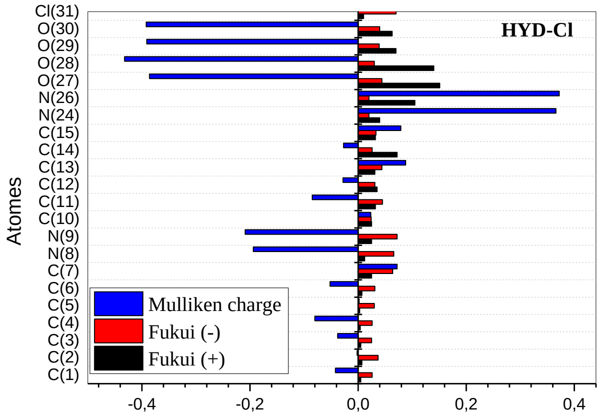

Figure. III. 16. Mulliken atomic charges and condensed Fukui functions for hydrazone derivatives.

III. 6. 1. 3. Molecular dynamics simulation

One of the advantages that provide the molecular dynamics simulation over other methods is the possibility to simulate a wide range of complex systems that include hundreds or thousands of atoms. Herein, given the chemical state of steel surface under corrosive medium, the Fe (110) surface is chosen to simulate the adsorption of hydrazones on steel surface. **Figure III. 17** shows the final adsorption configurations of investigated molecules over Fe (110). A close examination of the figure revealed that the adsorption of the studied inhibitor on the iron surface is almost parallel, indicating a maximum coverage, which in turn leads to a high interaction with the iron surface. Results in **Figure III. 17** shows that all hydrazones molecules assume a nearly flat orientation with respect to the iron surface, suggesting the possibility for a strong interaction with iron surface. It has been shown in the DFT section that inhibitor molecules tend to have strong interaction with the iron surface. Keeping this in mind, we assume that there is a chance for formation of more bonds between reactive atoms, especially nitrogen atoms and carbon atoms attached to bonding orbitals.

The obtained interaction energy $E_{interaction}$ values reported in **Table III. 8** are all negative, indicating the strong adsorption of molecules over the iron surface. Unsurprisingly, large negative value is found for HYD-OH, followed by HYD-iso, HYD-Me and HYD-Cl, confirming once again the excellent adsorption properties of HYD-OH.

Compounds	Side view	Top view
HYD-OH	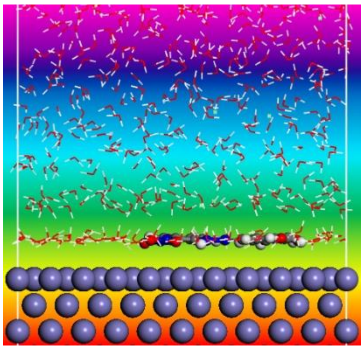	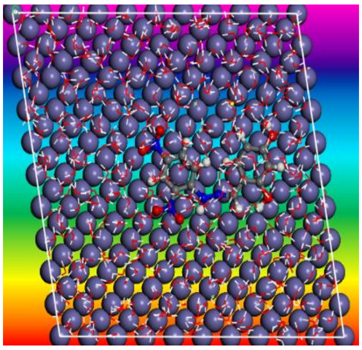
HYD-iso	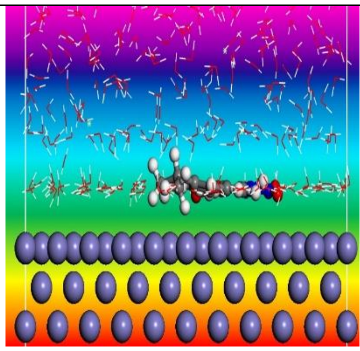	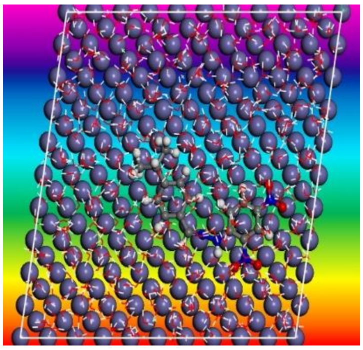
HYD-Me	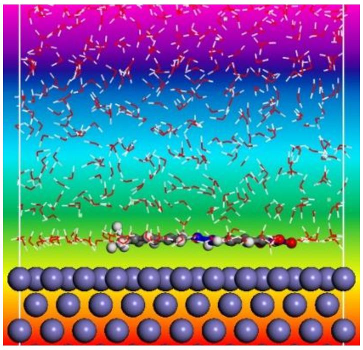	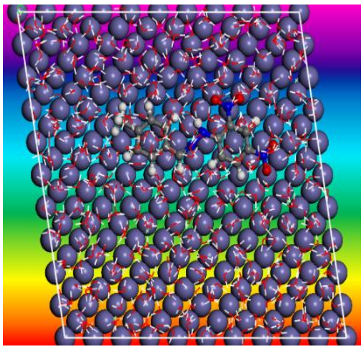
HYD-Cl	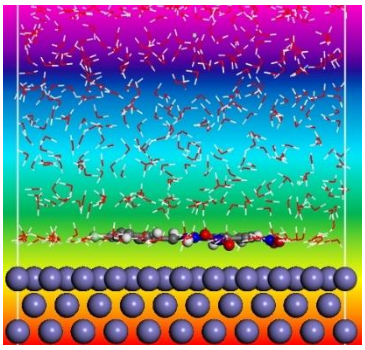	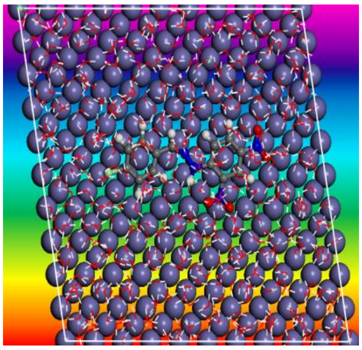

Figure. III. 17. Equilibrium adsorption configuration of the hydrazones on the Fe (110) obtained from MD simulations. Top and side view.

Table III. 8. Interaction energies of hydrazone molecules with Fe (110) estimated from MD simulations.

Simulation system	Interaction energy
Fe (110)-HYD-OH	-2841.35
Fe (110)-HYD-iso	-2402.94
Fe (110)-HYD-Me	-2205.65
Fe (110)-HYD-Cl	-2045.84

III. 6. 1. 4. Radial distribution function (RDF)

Radial distribution function (RDF), g(r), is a commonly used approach to estimate the linking length between the inhibitors molecules and metal surface. In general, the peak between 1 and 3.5 Å characterizes chemisorption, while physisorption is associated with peaks located at more than 3.5 Å **[8]**. In present RDF results (*via* **Figure III. 18**), the first prominent peak is located at 2.98, 3.01, 3.21 and 3.29 A° for HYD-OH, HYD-iso, HYD-Me and HYD-Cl, respectively, which suggests a chemical bonds formation between the hydrazone derivatives molecule and iron atoms. Moreover, several other peaks located outside 3.5 Å may be atributted to physical interactions. Together, these results further support those from experimental and quantum chemical investigations.

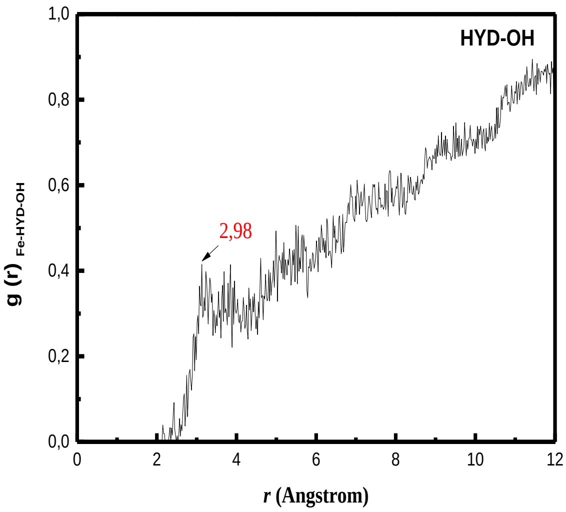

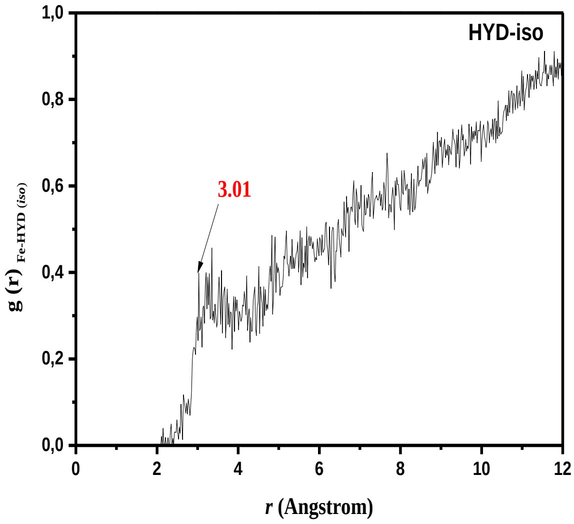

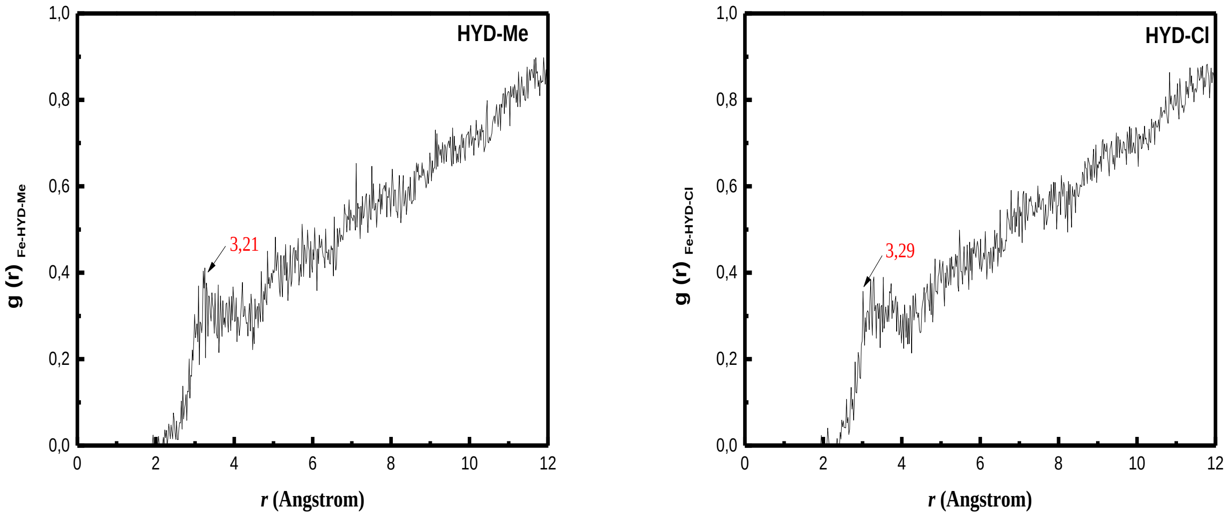

Figure. III. 18. RDF curve for the hydrazone derivatives on Fe (110) surface.

III. 7. Protection mechanism

Generally, the mechanism of action of corrosion inhibitor on metal surface in acid medium is supposed to be influenced by the chemical structure of the inhibitor molecules, the nature and charge of the metal. Through the above results, the adsorption of hydrazone derivatives on CS surface can be explained as follows:

- Corrosion inhibition experiments were carried out in HCl medium, which leads to a positive charge of the metal surface. Also, the tested inhibitors are expected to be protonated. In this form, the positive charge of the metal will favor the adsorption of chlorides (Cl^-) on its surface, creating a bridge between protonated inhibitor molecules and the charged metallic surface, and thus results in increases the attractive forces between inhibitor's molecules and the metal surface. This suggestion is supported by XPS results, which indicated the presence of a charged nitrogen atom. At this stage, corrosion protection is driven primarily by physisorption, therefore, blocking reaction sites of the carbon steel.
- As demonstrated in the results described above, the corrosion process could be also blocked by chemisorption. The presence of electron-rich aromatic rings and heteroatoms is expected to increase the transfer of loosely bound electrons from molecules to electron-deficient iron orbitals. Within this mechanism, the presence of two aromatic rings enables the inhibitor's molecule to donate π-electrons to unfilled iron orbitals.
- Along with these interactions, it should also be emphasized that the high molecular weight and the large size of the hydrazone derivative can also be considered as another

factor that may influence its adsorption on the metal surface. **Scheme III. 4** represents all possible interactions between the hydrazone derivatives and the iron surface.

- In several recent papers, one can find several hydrazone derivatives tested for corrosion inhibition of different metal and alloys. This family of inhibitors has demonstrated good ability to inhibit metal corrosion. A comparison with other hydrazone derivatives in acid media is given in **Table III. 9**, and HYD-OH exhibited better corrosion inhibition behavior.

Table III. 9. Comparison of the inhibition efficiency of hydrazone derivatives tested in this work with that of some hydrazone derivatives previously published at 298 K.

Inhibitors	Metal/medium	Inhibition efficiency (%)	Reference
HZD^2	Mild steel/1M HCl	94	**[66]**
HZD^3	Mild steel/1M HCl	92	**[66]**
HZD^4	Mild steel/1M HCl	86	**[66]**
2-ABNH	Mild steel/1M HCl	95	**[67]**
HZD-1	Mild steel/1M HCl	95	**[68]**
HZD-2	Mild steel/1M HCl	90	**[68]**
HZD-3	Mild steel/1M HCl	84	**[68]**
HYD-1	Mild steel/1M HCl	96	**[69]**
HYD-2	Mild steel/1M HCl	84	**[69]**
TH-1	Mild steel/0.5M HCl	86	**[6]**
TH-2	Mild steel/0.5M HCl	89	**[6]**
TH-3	Mild steel/0.5M HCl	90	**[6]**
CBTH	Mild steel/1M HCl	87	**[70]**
CBFH	Mild steel/1M HCl	85	**[70]**
E-NBPHT	Carbon steel/0.5M H_2SO_4	87	**[71]**
Compound 1	Carbon steel/0.5M H_2SO_4	62	**[72]**
Compound 2	Carbon steel/0.5M H_2SO_4	59	**[72]**
Compound 3	Carbon steel/0.5M H_2SO_4	58	**[72]**
Compound 4	Carbon steel/0.5M H_2SO_4	55	**[72]**
HYD-OH	Carbon steel/1M HCl	97	This work
HYD-iso	Carbon steel/1M HCl	95	This work
HYD-Me	Carbon steel/1M HCl	94	This work
HYD-Cl	Carbon steel/1M HCl	91	This work

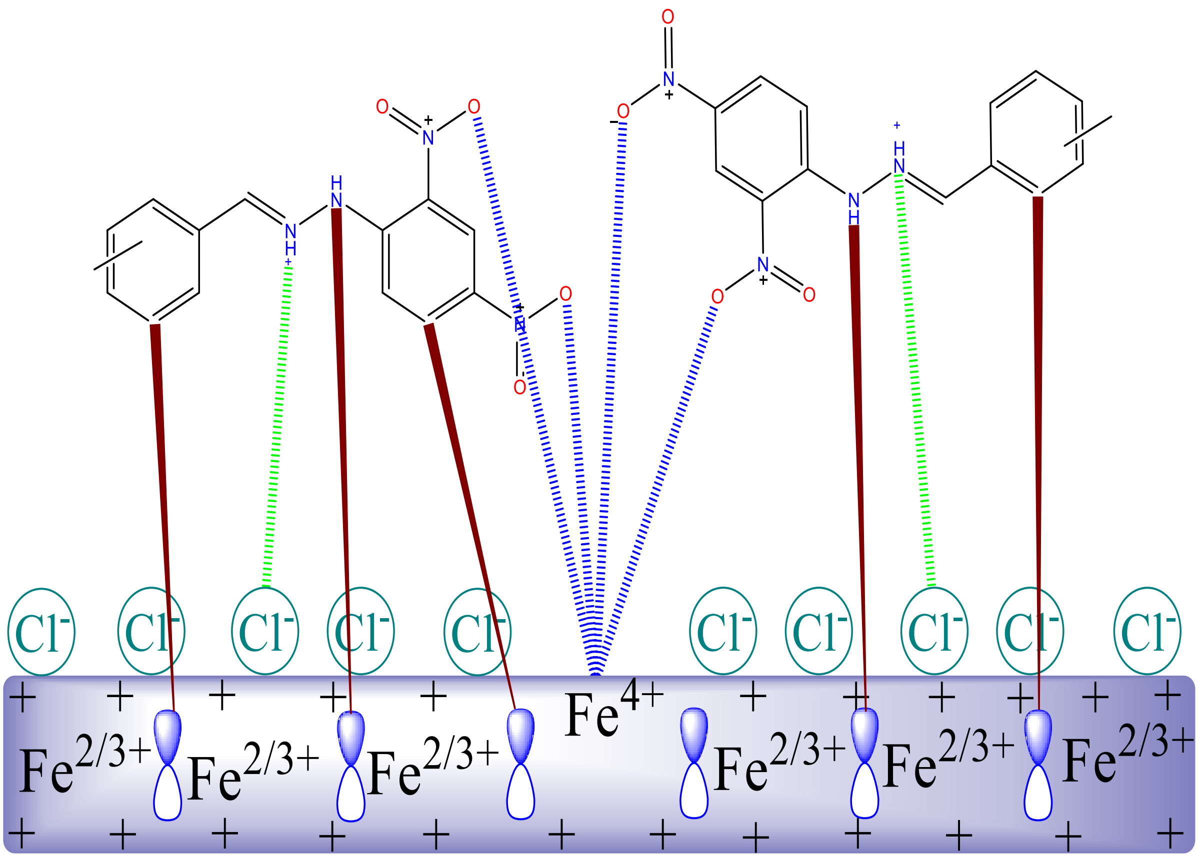

Scheme III. 4. Possible interactions between inhibitor molecule and carbon steel surface.

III. 8. References

[1] F. Bergamini, M. Ribeiro, M. Lancellotti, D. Machado, P. Miranda, A. Cuin, A. Formiga, P. Corbi, Synthesis, spectroscopic characterizations, crystal structures and DFT studies of nalidixic acid carbonyl hydrazones derivatives, Journal of Molecular Structure 1120 (2016) 115-124.

[2] K. Pyta, A. Janas, M. Szukowska, P. Pecyna, M. Jaworska, M. Gajecka, F. Bartl, P. Przybylski, Synthesis, docking and antibacterial studies of more potent amine and hydrazone rifamycin congeners than rifampicin, European journal of medicinal chemistry 167 (2019) 96-104.

[3] T. Nasr, S. Bondock, H.M. Rashed, W. Fayad, M. Youns, T.M. Sakr, Novel hydrazide-hydrazone and amide substituted coumarin derivatives: Synthesis, cytotoxicity screening, microarray, radiolabeling and in vivo pharmacokinetic studies, European journal of medicinal chemistry 151 (2018) 723-739.

[4] M. Moussa, A. El-Far, A. El-Shafei, The use of water-soluble hydrazones as inhibitors for the corrosion of C-steel in acidic medium, Materials chemistry and physics 105(1) (2007) 105-113.

[5] E.-S.M. Sherif, A.H. Ahmed, Synthesizing new hydrazone derivatives and studying their effects on the inhibition of copper corrosion in sodium chloride solutions, Synthesis and Reactivity in Inorganic, Metal-Organic, and Nano-Metal Chemistry 40(6) (2010) 365-372.

[6] T.K. Chaitra, K.N. Mohana, D.M. Gurudatt, H.C. Tandon, Inhibition activity of new thiazole hydrazones towards mild steel corrosion in acid media by thermodynamic, electrochemical and quantum chemical methods, Journal of the Taiwan Institute of Chemical Engineers 67 (2016) 521-531.

[7] Y. SICAK, Investigation of Antioxidant, Anticholinesterase Inhibitory, Tyrosinase Inhibitory and Urease Inhibitory Activities of Some Hydrazone Derivatives, Türk Yaşam Bilimleri Dergisi 2(2) 165-170.

[8] H. Lgaz, I.-M. Chung, R. Salghi, I.H. Ali, A. Chaouiki, Y. El Aoufir, M.I. Khan, On the understanding of the adsorption of Fenugreek gum on mild steel in an acidic medium: Insights from experimental and computational studies, Applied Surface Science 463 (2019) 647-658.

[9] M. Chafiq, A. Chaouiki, H. Lgaz, R. Salghi, K.V. Bhaskar, R. Marzouki, K.S. Bhat, I.H. Ali, M.I. Khan, I.-M. Chung, Inhibition performances of spirocyclopropane derivatives for mild steel protection in HCl, Materials Chemistry and Physics 243 (2020) 122582.

[10] B. Chugh, A.K. Singh, A. Chaouiki, R. Salghi, S. Thakur, B. Pani, A comprehensive study about anti-corrosion behaviour of pyrazine carbohydrazide: Gravimetric, electrochemical, surface and theoretical study, Journal of Molecular Liquids 299 (2020) 112160.

[11] Y. Tang, F. Zhang, S. Hu, Z. Cao, Z. Wu, W. Jing, Novel benzimidazole derivatives as corrosion inhibitors of mild steel in the acidic media. Part I: gravimetric, electrochemical, SEM and XPS studies, Corrosion science 74 (2013) 271-282.

[12] M. Benahmed, I. Selatnia, N. Djeddi, S. Akkal, H. Laouer, Adsorption and Corrosion Inhibition Properties of Butanolic Extract of Elaeoselinum thapsioides and Its Synergistic Effect with Reutera lutea (Desf.) Maires (Apiaceae) on A283 carbon Steel in Hydrochloric Acid Solution, Chemistry Africa 3(1) (2020) 251-261.

[13] F. Benhiba, H. Serrar, R. Hsissou, A. Guenbour, A. Bellaouchou, M. Tabyaoui, S. Boukhris, H. Oudda, I. Warad, A. Zarrouk, Tetrahydropyrimido-Triazepine derivatives as anti-corrosion additives for acid corrosion: Chemical, electrochemical, surface and theoretical studies, Chemical Physics Letters 743 (2020) 137181.

[14] K. Hanini, B. Merzoug, S. Boudiba, I. Selatnia, H. Laouer, S. Akkal, Influence of different polyphenol extracts of Taxus baccata on the corrosion process and their effect as additives in electrodeposition, Sustainable Chemistry and Pharmacy 14 (2019) 100189.

[15] L.O. Olasunkanmi, A.O. Idris, A.H. Adewole, O.O. Wahab, E.E. Ebenso, Adsorption and Corrosion Inhibition Potentials of Salicylaldehyde-based Schiff Bases of Semicarbazide and p-Toluidine on Mild Steel in Acidic Medium: Experimental and Computational Studies, Surfaces and Interfaces (2020) 100782.

[16] C. Verma, M. Quraishi, E.E. Ebenso, I. Bahadur, A green and sustainable approach for mild steel acidic corrosion inhibition using leaves extract: experimental and DFT studies, Journal of Bio-and Tribo-Corrosion 4(3) (2018) 33.

[17] R. Solmaz, Investigation of adsorption and corrosion inhibition of mild steel in hydrochloric acid solution by 5-(4-Dimethylaminobenzylidene) rhodanine, Corrosion Science 79 (2014) 169-176.

[18] I. Selatnia, A. Sid, M. Benahmed, T. Ozturk, N. Gherraf, Synthesis and Characterization of a Bis-Pyrazoline Derivative as Corrosion Inhibitor for A283 Carbon Steel in 1M HCl: Electrochemical, Surface, DFT and MD Simulation Studies, Protection of Metals and Physical Chemistry of Surfaces 54(6) (2018) 1182-1193.

[19] S. Martinez, I. Stern, Thermodynamic characterization of metal dissolution and inhibitor adsorption processes in the low carbon steel/mimosa tannin/sulfuric acid system, Applied surface science 199(1-4) (2002) 83-89.

[20] O.M.A. Khamaysa, I. Selatnia, H. Zeghache, H. Lgaz, A. Sid, I.-M. Chung, M. Benahmed, N. Gherraf, P. Mosset, Enhanced corrosion inhibition of carbon steel in HCl solution by a newly synthesized hydrazone derivative: Mechanism exploration from electrochemical, XPS, and computational studies, Journal of Molecular Liquids 315 (2020) 113805.

[21] A. El Bribri, M. Tabyaoui, B. Tabyaoui, H. El Attari, F. Bentiss, The use of Euphorbia falcata extract as eco-friendly corrosion inhibitor of carbon steel in hydrochloric acid solution, Materials Chemistry and Physics 141(1) (2013) 240-247.

[22] S. Boudiba, K. Hanini, I. Selatnia, I. Saouane, S. Hioun, M. Benahmed, Experimental, theoretical and mathematical studies of Echium italicum L. extract as a corrosion inhibitor for carbon steel in acidic medium, Materials Research Express (2019).

[23] H. Lgaz, R. Salghi, K.S. Bhat, A. Chaouiki, S. Jodeh, Correlated experimental and theoretical study on inhibition behavior of novel quinoline derivatives for the corrosion of mild steel in hydrochloric acid solution, Journal of Molecular Liquids 244 (2017) 154-168.

[24] C. Verma, E. Ebenso, I. Bahadur, I. Obot, M. Quraishi, 5-(Phenylthio)-3H-pyrrole-4-carbonitriles as effective corrosion inhibitors for mild steel in 1 M HCl: Experimental and theoretical investigation, Journal of Molecular Liquids 212 (2015) 209-218.

[25] S. Nwanonenyi, H. Obasi, I. Eze, Hydroxypropyl Cellulose as an Efficient Corrosion Inhibitor for Aluminium in Acidic Environments: Experimental and Theoretical Approach, Chemistry Africa (2019) 1-12.

[26] K. Ansari, M. Quraishi, A. Singh, Corrosion inhibition of mild steel in hydrochloric acid by some pyridine derivatives: an experimental and quantum chemical study, Journal of Industrial and Engineering Chemistry 25 (2015) 89-98.

[27] H. Lgaz, K.S. Bhat, R. Salghi, S. Jodeh, M. Algarra, B. Hammouti, I.H. Ali, A. Essamri, Insights into corrosion inhibition behavior of three chalcone derivatives for mild steel in hydrochloric acid solution, Journal of Molecular Liquids 238 (2017) 71-83.

[28] M.M. Solomon, S.A. Umoren, M.A. Quraishi, D.B. Tripathy, E.J. Abai, Effect of akyl chain length, flow, and temperature on the corrosion inhibition of carbon steel in a simulated acidizing environment by an imidazoline-based inhibitor, Journal of Petroleum Science and Engineering 187 (2020) 106801.

[29] T. Han, J. Guo, Q. Zhao, Y. Wu, Y. Zhang, Enhanced corrosion inhibition of carbon steel by pyridyl gemini surfactants with different alkyl chains, Materials Chemistry and Physics 240 (2020) 122156.

[30] M. Corrales-Luna, T. Le Manh, M. Romero-Romo, M. Palomar-Pardavé, E.M. Arce-Estrada, 1-Ethyl 3-methylimidazolium thiocyanate ionic liquid as corrosion inhibitor of API 5L X52 steel in H2SO4 and HCl media, Corrosion Science 153 (2019) 85-99.

[31] T.K. Sarkar, V. Saraswat, R.K. Mitra, I. Obot, M. Yadav, Mitigation of corrosion in petroleum oil well/tubing steel using pyrimidines as efficient corrosion inhibitor: Experimental and theoretical investigation, Materials Today Communications (2020) 101862.

[32] M. Hegazy, M. Abdallah, M. Awad, M. Rezk, Three novel di-quaternary ammonium salts as corrosion inhibitors for API X65 steel pipeline in acidic solution. Part I: experimental results, Corrosion Science 81 (2014) 54-64.

[33] M. Chafiq, A. Chaouiki, M.R. Al-Hadeethi, R. Salghi, I.-M. Chung, A Joint Experimental and Theoretical Investigation of the Corrosion Inhibition Behavior and Mechanism of Hydrazone Derivatives for Mild Steel in HCl Solution, Colloids and Surfaces A: Physicochemical and Engineering Aspects (2020) 125744.

[34] H. Lgaz, R. Salghi, S. Masroor, S.-H. Kim, C. Kwon, S.Y. Kim, Y.-J. Yang, I.-M. Chung, Assessing corrosion inhibition characteristics of hydrazone derivatives on mild steel in HCl: Insights from electronic-scale DFT and atomic-scale molecular dynamics, Journal of Molecular Liquids (2020) 112998.

[35] A. Chaouiki, H. Lgaz, R. Salghi, M. Chafiq, H. Oudda, K. Bhat, I. Cretescu, I. Ali, R. Marzouki, I. Chung, Assessing the impact of electron-donating-substituted chalcones on inhibition of mild steel corrosion in HCl solution: Experimental results and molecular-level insights, Colloids and Surfaces A: Physicochemical and Engineering Aspects 588 (2020) 124366.

[36] A. El-Faham, S.M. Osman, H.A. Al-Lohedan, G.A. El-Mahdy, Hydrazino-methoxy-1, 3, 5-triazine derivatives' excellent corrosion organic inhibitors of steel in acidic chloride solution, Molecules 21(6) (2016) 714.

[37] D.I. Njoku, P.C. Okafor, H. Lgaz, K.J. Uwakwe, E.E. Oguzie, Y. Li, Outstanding anticorrosion and adsorption properties of 2-amino-6-methoxybenzothiazole on Q235 and X70 carbon steels: Effect of time, XPS, electrochemical and theoretical considerations, Journal of Molecular Liquids (2020) 114663.

[38] D. Chebabe, Z. Ait Chikh, N. Hajjaji, A. Srhiri, F. Zucchi, Corrosion inhibition of Armco iron in 1 M HCl solution by alkyltriazoles, Corrosion Science 45(2) (2003) 309-320.

[39] A. Sedik, D. Lerari, A. Salci, S. Athmani, K. Bachari, İ. Gecibesler, R. Solmaz, Dardagan Fruit extract as eco-friendly corrosion inhibitor for mild steel in 1 M HCl: Electrochemical and

surface morphological studies, Journal of the Taiwan Institute of Chemical Engineers 107 (2020) 189-200.

[40] B. Tan, S. Zhang, J. He, W. Li, Y. Qiang, Q. Wang, C. Xu, S. Chen, Insight into anti-corrosion mechanism of tetrazole derivatives for X80 steel in 0.5 M H2SO4 medium: Combined experimental and theoretical researches, Journal of Molecular Liquids (2020) 114464.

[41] A. Dehghani, A.H. Mostafatabar, G. Bahlakeh, B. Ramezanzadeh, M. Ramezanzadeh, Detailed-level computer modeling explorations complemented with comprehensive experimental studies of Quercetin as a highly effective inhibitor for acid-induced steel corrosion, Journal of Molecular Liquids (2020) 113035.

[42] D. Wang, Y. Li, B. Chen, L. Zhang, Novel surfactants as green corrosion inhibitors for mild steel in 15% HCl: Experimental and theoretical studies, Chemical Engineering Journal 402 (2020) 126219.

[43] B. Xu, Y. Ji, X. Zhang, X. Jin, W. Yang, Y. Chen, Experimental and theoretical studies on the corrosion inhibition performance of 4-amino-N, N-di-(2-pyridylmethyl)-aniline on mild steel in hydrochloric acid, RSC Advances 5(69) (2015) 56049-56059.

[44] N. El Hamdani, R. Fdil, M. Tourabi, C. Jama, F. Bentiss, Alkaloids extract of Retama monosperma (L.) Boiss. seeds used as novel eco-friendly inhibitor for carbon steel corrosion in 1 M HCl solution: Electrochemical and surface studies, Applied Surface Science 357 (2015) 1294-1305.

[45] A. Zarrouk, B. Hammouti, T. Lakhlifi, M. Traisnel, H. Vezin, F. Bentiss, New 1H-pyrrole-2, 5-dione derivatives as efficient organic inhibitors of carbon steel corrosion in hydrochloric acid medium: electrochemical, XPS and DFT studies, Corrosion Science 90 (2015) 572-584.

[46] M. Yadav, T. Sarkar, I. Obot, Carbohydrate compounds as green corrosion inhibitors: electrochemical, XPS, DFT and molecular dynamics simulation studies, RSC advances 6(111) (2016) 110053-110069.

[47] H. Zarrok, A. Zarrouk, B. Hammouti, R. Salghi, C. Jama, F. Bentiss, Corrosion control of carbon steel in phosphoric acid by purpald–weight loss, electrochemical and XPS studies, Corrosion Science 64 (2012) 243-252.

[48] C. Ruttanapun, Effects of Pd substitution on the thermoelectric and electronic properties of delafossite Cu1− xPdxFeO2 (x= 0.01, 0.03 and 0.05), Journal of Solid State Chemistry 215 (2014) 43-49.

[49] H. Kanatani, H. Kume, T. Matsui, Magnetic properties of Sr Ti O 3-buffered Ba (Fe 0.2 Zr 0.8) O 3− δ films on Si (001) substrates, Journal of Applied Physics 105(7) (2009) 07D907.

[50] H. Li, S. Zhang, B. Tan, Y. Qiang, W. Li, S. Chen, L. Guo, Investigation of Losartan Potassium as an eco-friendly corrosion inhibitor for copper in 0.5 M H2SO4, Journal of Molecular Liquids (2020) 112789.

[51] H. Li, S. Zhang, Y. Qiang, Corrosion retardation effect of a green cauliflower extract on copper in H2SO4 solution: Electrochemical and theoretical explorations, Journal of Molecular Liquids (2020) 114450.

[52] P. Shaw, I. Obot, M. Yadav, Functionalized 2-hydrazinobenzothiazole with carbohydrates as a corrosion inhibitor: electrochemical, XPS, DFT and Monte Carlo simulation studies, Materials Chemistry Frontiers 3(5) (2019) 931-940.

[53] A. Singh, K. Ansari, D.S. Chauhan, M. Quraishi, S. Kaya, Anti-corrosion investigation of pyrimidine derivatives as green and sustainable corrosion inhibitor for N80 steel in highly corrosive environment: Experimental and AFM/XPS study, Sustainable Chemistry and Pharmacy 16 (2020) 100257.

[54] A. Lesar, I. Milošev, Density functional study of the corrosion inhibition properties of 1, 2, 4-triazole and its amino derivatives, Chemical physics letters 483(4-6) (2009) 198-203.

[55] I. Obot, D. Macdonald, Z. Gasem, Density functional theory (DFT) as a powerful tool for designing new organic corrosion inhibitors. Part 1: an overview, Corrosion Science 99 (2015) 1-30.

[56] B. Ogunyemi, D. Latona, I. Adejoro, Molecular Modelling and Quantitative Structure-property Relationships (QSPRs) of Purine derivatives as Corrosion Inhibitor in Acid Medium, Scientific African (2020) e00336.

[57] I. Lukovits, K. Palfi, I. Bako, E. Kalman, LKP model of the inhibition mechanism of thiourea compounds, Corrosion 53(12) (1997) 915-919.

[58] Y. Boughoues, M. Benamira, L. Messaadia, N. Ribouh, Adsorption and corrosion inhibition performance of some environmental friendly organic inhibitors for mild steel in HCl solution via experimental and theoretical study, Colloids and Surfaces A: Physicochemical and Engineering Aspects 593 (2020) 124610.

[59] Y. El Aoufir, R. Aslam, F. Lazrak, R. Marzouki, S. Kaya, S. Skal, A. Ghanimi, I. Ali, A. Guenbour, H. Lgaz, The effect of the alkyl chain length on corrosion inhibition performances of 1, 2, 4-triazole-based compounds for mild steel in 1.0 M HCl: Insights from experimental and theoretical studies, Journal of Molecular Liquids 303 (2020) 112631.

[60] H. Lgaz, S.K. Saha, A. Chaouiki, K.S. Bhat, R. Salghi, P. Banerjee, I.H. Ali, M.I. Khan, I.-M. Chung, Exploring the potential role of pyrazoline derivatives in corrosion inhibition of

mild steel in hydrochloric acid solution: Insights from experimental and computational studies, Construction and Building Materials 233 (2020) 117320.

[61] A. Singh, K. Ansari, J. Haque, P. Dohare, H. Lgaz, R. Salghi, M. Quraishi, Effect of electron donating functional groups on corrosion inhibition of mild steel in hydrochloric acid: Experimental and quantum chemical study, Journal of the Taiwan Institute of Chemical Engineers 82 (2018) 233-251.

[62] R. Rahmani, N. Boukabcha, A. Chouaih, F. Hamzaoui, S. Goumri-Said, On the molecular structure, vibrational spectra, HOMO-LUMO, molecular electrostatic potential, UV–Vis, first order hyperpolarizability, and thermodynamic investigations of 3-(4-chlorophenyl)-1-(1yridine-3-yl) prop-2-en-1-one by quantum chemistry calculations, Journal of Molecular Structure 1155 (2018) 484-495.

[63] K. Abderrahim, I. Selatnia, A. Sid, P. Mosset, 1, 2-bis (4-chlorobenzylidene) Azine as new and effective corrosion inhibitor for copper in 0.1 N HCl: A combined experimental and theoretical approach, Chemical Physics Letters 707 (2018) 117-128.

[64] H. Mi, G. Xiao, X. Chen, Theoretical evaluation of corrosion inhibition performance of three antipyrine compounds, Computational and Theoretical Chemistry 1072 (2015) 7-14.

[65] S.K. Saha, M. Murmu, N.C. Murmu, I. Obot, P. Banerjee, Molecular level insights for the corrosion inhibition effectiveness of three amine derivatives on the carbon steel surface in the adverse medium: A combined density functional theory and molecular dynamics simulation study, Surfaces and interfaces 10 (2018) 65-73.

[66] H. Lgaz, A. Chaouiki, M.R. Albayati, R. Salghi, Y. El Aoufir, I.H. Ali, M.I. Khan, S.K. Mohamed, I.-M. Chung, Synthesis and evaluation of some new hydrazones as corrosion inhibitors for mild steel in acidic media, Research on Chemical Intermediates 45(4) (2019) 2269-2286.

[67] D.K. Singh, S. Kumar, G. Udayabhanu, R.P. John, 4 (N, N-dimethylamino) benzaldehyde nicotinic hydrazone as corrosion inhibitor for mild steel in 1 M HCl solution: An experimental and theoretical study, Journal of molecular liquids 216 (2016) 738-746.

[68] H. Lgaz, I.-M. Chung, M.R. Albayati, A. Chaouiki, R. Salghi, S.K. Mohamed, Improved corrosion resistance of mild steel in acidic solution by hydrazone derivatives: an experimental and computational study, Arabian Journal of Chemistry 13(1) (2020) 2934-2954.

[69] A. Chaouiki, M. Chafiq, H. Lgaz, M.R. Al-Hadeethi, I.H. Ali, S. Masroor, I.-M. Chung, Green corrosion inhibition of mild steel by hydrazone derivatives in 1.0 M HCl, Coatings 10(7) (2020) 640.

[70] T.K. Chaitra, K.N. Mohana, H.C. Tandon, Evaluation of newly synthesized hydrazones as mild steel corrosion inhibitors by adsorption, electrochemical, quantum chemical and morphological studies, Arab Journal of Basic and Applied Sciences 25(2) (2018) 45-55.
[71] N. Chafai, S. Chafaa, K. Benbouguerra, A. Hellal, M. Mehri, Synthesis, spectral analysis, anti-corrosive activity and theoretical study of an aromatic hydrazone derivative, Journal of Molecular Structure 1181 (2019) 83-92.
[72] A. Fouda, S. EL-Sayyad, M. Abdallah, N-3-hydroxyl-2-naphthoyl hydrazone derivatives as inhibitors for corrosion of carbon steel in H2SO4 acid solution, Anti-Corrosion Methods and Materials (2011).

Conclusion

"Chemistry is all about getting lucky".
Robert Curl

Conclusion

In this work, four hydrazone derivatives bearing nitro groups were synthesized and evaluated as corrosion inhibitors for carbon steel in 1.0 M HCl solution. A comprehensive characterization of inhibitor's performance was achieved using weight-loss, electrochemical, XPS, contact angle and SEM studies. Besides, theoretical studies using DFT and MD simulation were performed to explore the most reactive sites of the hydrazone's molecules and their interactions with iron's surface, respectively. The following insightful conclusions were made;

1. Four hydrazone derivatives were synthesized, and their structures were confirmed on the basis of UV-Vis, FT-IR, ^{1}H and ^{13}C NMR spectroscopy.
2. The synthesized hydrazones act as effective mixed inhibitors for CS in an acidic solution and their effectiveness increases with their concentration and reached more than 90% at 5.10^{-3} M, and followed the order: HYD-OH>HYD-iso>HYD-Me>HYD-Cl.
3. The slight decrease of inhibition efficiency with increasing temperature confirms that the tested compounds act as efficient inhibitors at higher temperatures.
4. Based on electrochemical measurements, investigated inhibitors blocked both anodic and cathodic corrosion reactions and their additions to HCl result in a sharp increase in the resistance of polarization.
5. The adsorption of the studied compounds obeys Langmuir's model and involves both physical and chemical process.
6. SEM and contact angle analysis confirmed the adsorption of hydrazones on the CS surface and showed that a protective film is formed, and blocked the active sites.
7. DFT and MD simulation investigations reveal that the presence of electron-rich aromatic rings and heteroatoms is expected to increase the transfer of loosely bound electrons from molecules to electron-deficient iron orbitals. Within this mechanism, the presence of two aromatic rings enables the inhibitor's molecule to donate π-electrons to unfilled iron orbitals.
8. The large negative value of interaction energy in MD indicates the strong interaction between metal and inhibitor's molecules.

9. This work showed that this class of compounds can be promising corrosion inhibitors and highlighted the need for the development of more derivatives.

Future work

Other areas of this project to be considered for further investigation (future work), which are beyond the scope of this PhD research have been suggested below:

- Synthesized more organic compounds such as amino acids derivatives, pyrazolines and hydrazone derivatives.
- Investigate them as corrosion inhibitors for different types of material and in different media.
- Investigate the synergistic inhibition performance with other inhibitors or halids.
- Investigate the adsorbed film formed at the CS surface/HCl solution interface to determine the composition of the film as well its thickness during the adsorption-desorption process using other techniques.

Abstract

Corrosion protection of carbon steel is an important challenge in the industry field. The search for an effective protection approach is an issue of considerable concern and still a topic of ongoing research. In the present work, four hydrazone derivatives, namely (*E*) -1- (2,4-dinitrophenyl) -2- (2,4-dihydroxy benzylidene) hydrazine (HYD-OH), (*E*) -1- (2,4-dinitrophenyl) -2- (4-isopropyl benzylidene) hydrazine (HYD-iso), (*E*) -1- (2,4-dinitrophenyl) -2- (4-methyl benzylidene) hydrazine (HYD-Me), and (*E*) -1- (2,4-dinitrophenyl) -2- (4-chloro benzylidene) hydrazine (HYD-Cl) were used in 1.0 M HCl solution for API grade carbon steel corrosion mitigation. Their corrosion inhibition performance was evaluated by electrochemical tests while steel surface was analyzed by X-ray photoelectron spectroscopy (XPS), contact angle and scanning electron microscope (SEM). Electrochemical tests showed about 98%, 96%, 94% and 91% efficiencies for carbon steel exposed to 1.0 M HCl solution containing 5×10^{-3} mol/L of HYD-OH, HYD-iso, HYD-Me, and HYD-Cl, respectively. All compounds were classified as mixed type inhibitors, inhibiting both cathodic and anodic reactions. XPS and isotherm model results revealed that tested compounds adsorbed on steel surface through a combined physical and chemical mechanism following Langmuir model. DFT and MD simulations were used to investigate the most reactive sites of the hydrazone molecule and its adsorption mechanism, respectively.

Keywords: Corrosion inhibition; Hydrazone; Carbon steel; DFT; XPS; Molecular Dynamics.

Résumé

La protection contre la corrosion de l'acier au carbone est un défi important dans le domaine industriel. La recherche d'une approche de protection efficace est un sujet de préoccupation considérable et toujours un sujet de recherche en cours. Dans le présent travail, quatre dérivés d'hydrazone, à savoir (*E*) -1- (2,4-dinitrophényl) -2- (2,4-dihydroxy benzylidène) hydrazine (HYD-OH), (*E*) -1- (2,4 -dinitrophényl) -2- (4-isopropylbenzylidène) hydrazine (HYD-iso), (*E*) -1- (2,4-dinitrophényl) -2- (4-méthylbenzylidène) hydrazine (HYD-Me), et (*E*) -1- (2,4-dinitrophényl) -2- (4-chloro benzylidène) hydrazine (HYD-Cl) ont été utilisés dans une solution de HCl 1,0 M pour l'atténuation de la corrosion de l'acier au carbone de qualité API. Leur performance d'inhibition de la corrosion a été évaluée par des tests électrochimiques tandis que la surface de l'acier a été analysée par spectroscopie photoélectronique aux rayons X (XPS), angle de contact et microscope électronique à balayage (SEM). Les tests électrochimiques ont montré des rendements d'environ 98%, 96%, 94% et 91% pour l'acier au carbone exposé à une solution de HCl 1,0 M contenant 5×10^{-3} mol / L de HYD-OH, HYD-iso, HYD-Me et HYD-Cl, respectivement. Tous les composés ont été classés comme inhibiteurs de type mixte, inhibant à la fois les réactions cathodiques et anodiques. Les résultats du modèle XPS et isotherme ont révélé que les composés testés adsorbés sur la surface de l'acier par un mécanisme combiné physique et chimique suivant le modèle de Langmuir. Des simulations DFT et MD ont été utilisées pour étudier les sites les plus réactifs de la molécule d'hydrazone et son mécanisme d'adsorption, respectivement.

Mots clés: inhibition de la corrosion; Hydrazone; Acier Carbone; DFT; XPS; Dynamique moléculaire.

الملخص

ان حماية الفولاذ الكربوني من التآكل تعد تحديًا مهمًا في مجال الصناعة ، حيث يتحقق ذلك باستعمال طرق حماية فعالة والتي تزال موضوع بحث مستمر. في هذا العمل ، قمنا باستخدام أربعة مشتقات للهيدرازون في محلول 1.0 مولار من حمض الهيدروكلوريك للتخفيف من تآكل الفولاذ الكربوني. تم تقييم أداء تثبيط التآكل عن طريق الاختبارات الكهروكيميائية بينما تم تحليل سطح الفولاذ عن طريق التحليل الطيفي للإلكترون الضوئي بالأشعة السينية وزاوية التلامس والميكروسكوب الإلكتروني وأظهرت الاختبارات الكهروكيميائية كفاءة 91-98٪ للفولاذ الكربوني المعرض لـ 1.0 مولار من محلول حمض الهيدروكلوريك يحتوي على 5×10^{-3} مول / لتر من مشتقات الهيدرازون . تم المختبرة على تصنيف جميع المركبات ،مما يثبط التفاعلات الكاثودية والأنودية. كشفت نتائج الامتزاز أنها مثبطات من النوع المختلط الهيدروزينات على سطح الفولاذ انه يتم من خلال آلية فيزيائية وكيميائية مدمجة وفقًا لنموذج لانجموير. تم استخدام حسابات نظرية و المحاكاة الديناميكية للتحقيق على التوالي ، في المواقع الأكثر تفاعلًا لجزيء الهيدرازون وآلية امتصاصه.

الكلمات المفتاحية: تثبيط التاكل, هيدرازون, الفولاذ الكربوني, التحليل الطيفي للإلكترون الضوئي بالأشعة السينية، المحاكاة الديناميكية و النظرية.

APPENDIX

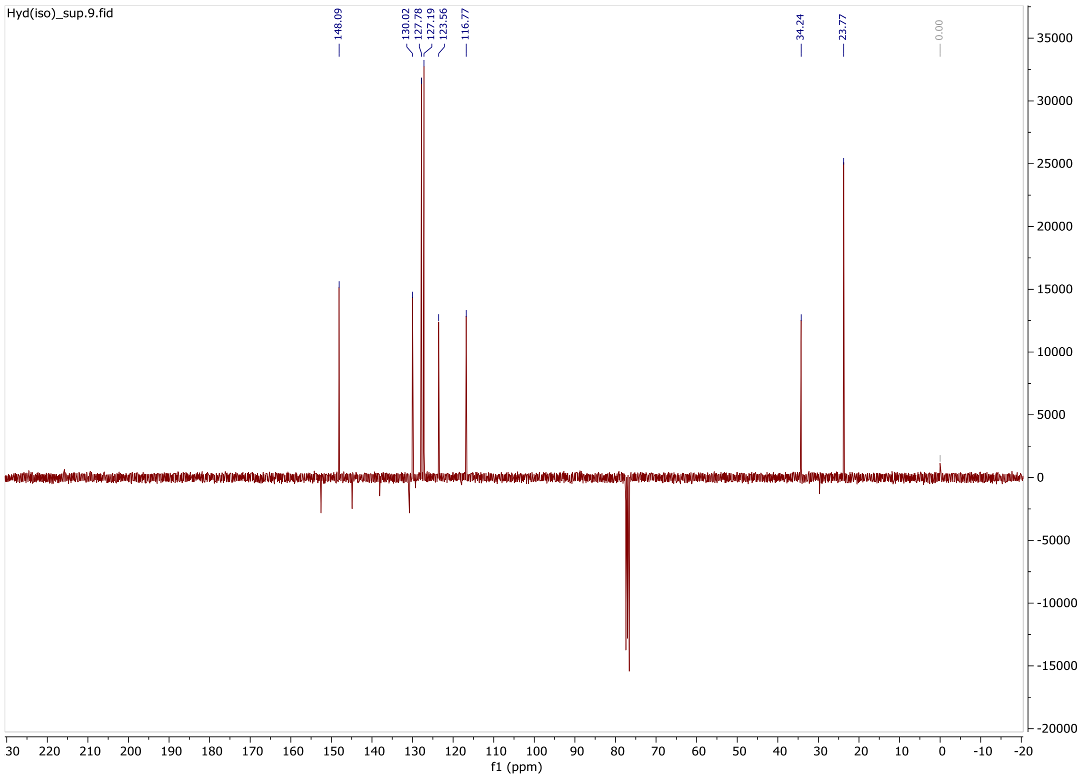
Hyd(iso)_sup.9.fid
148.09
130.02
127.78
127.19
123.56
116.77
34.24
23.77
0.00
f1 (ppm)

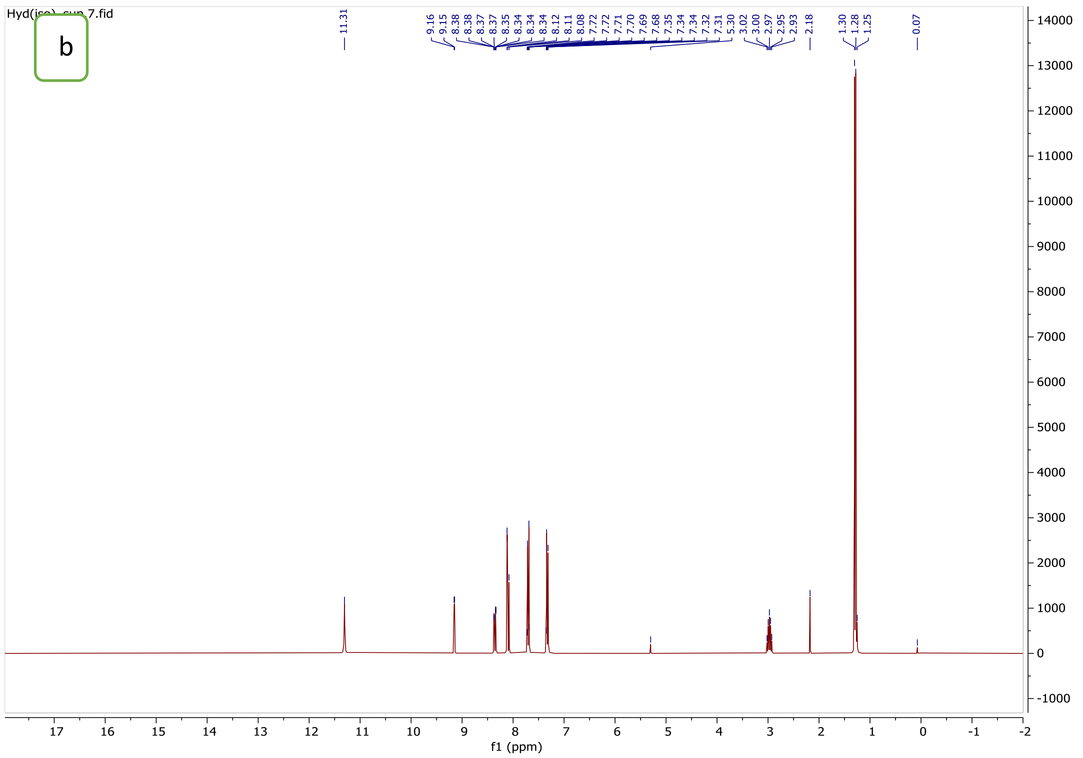
b
11.31
9.16
9.15
2.18
1.30
1.28
1.25
0.07
f1 (ppm)

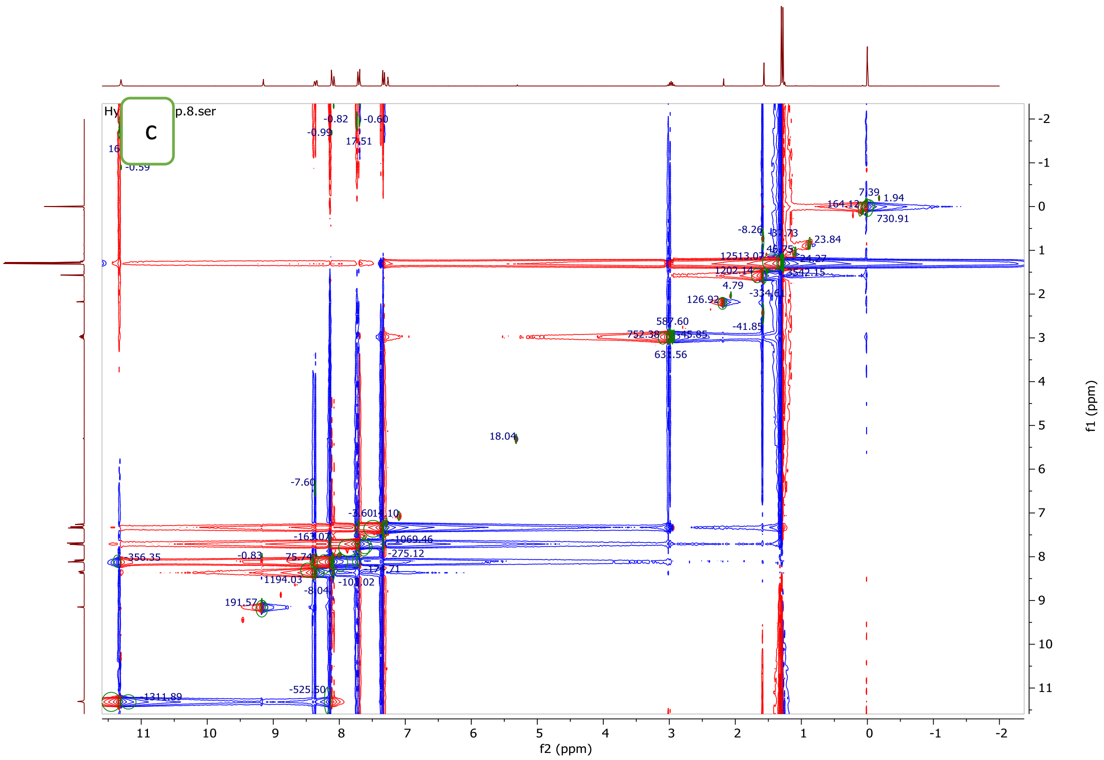

Figure AP. 1.^{13}C NMR (a), ^{1}H NMR (b) and COSY spectra of HYD-iso

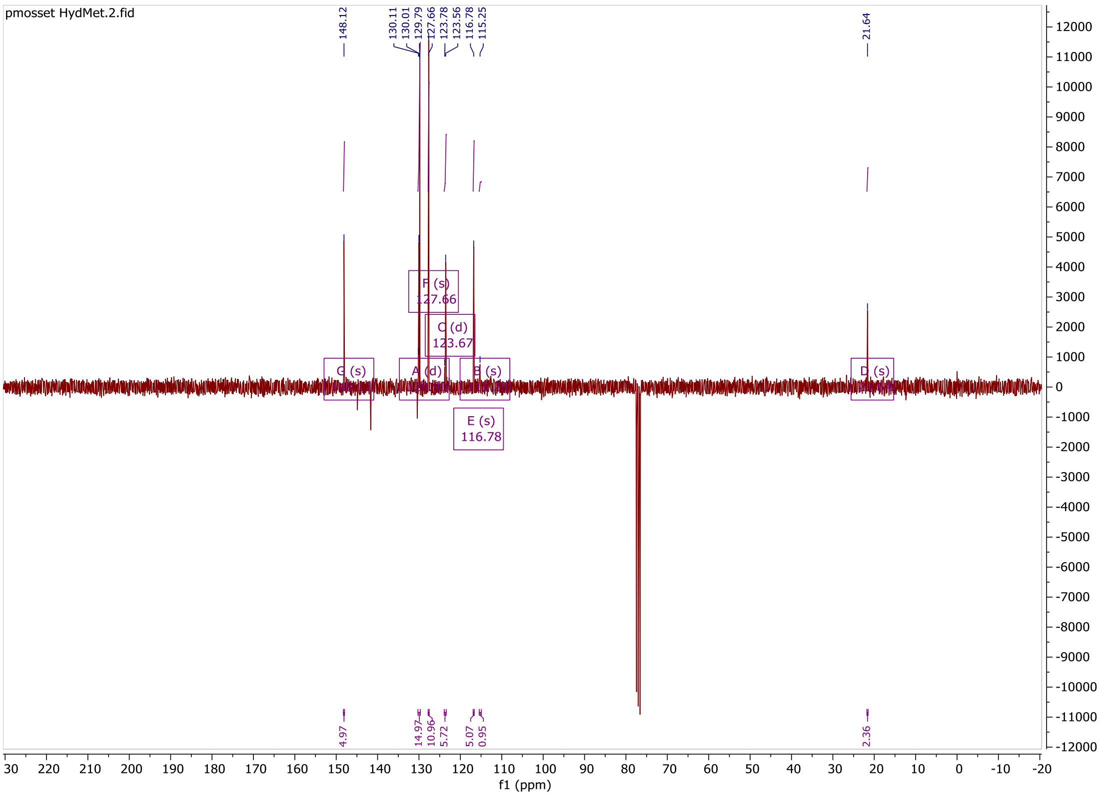

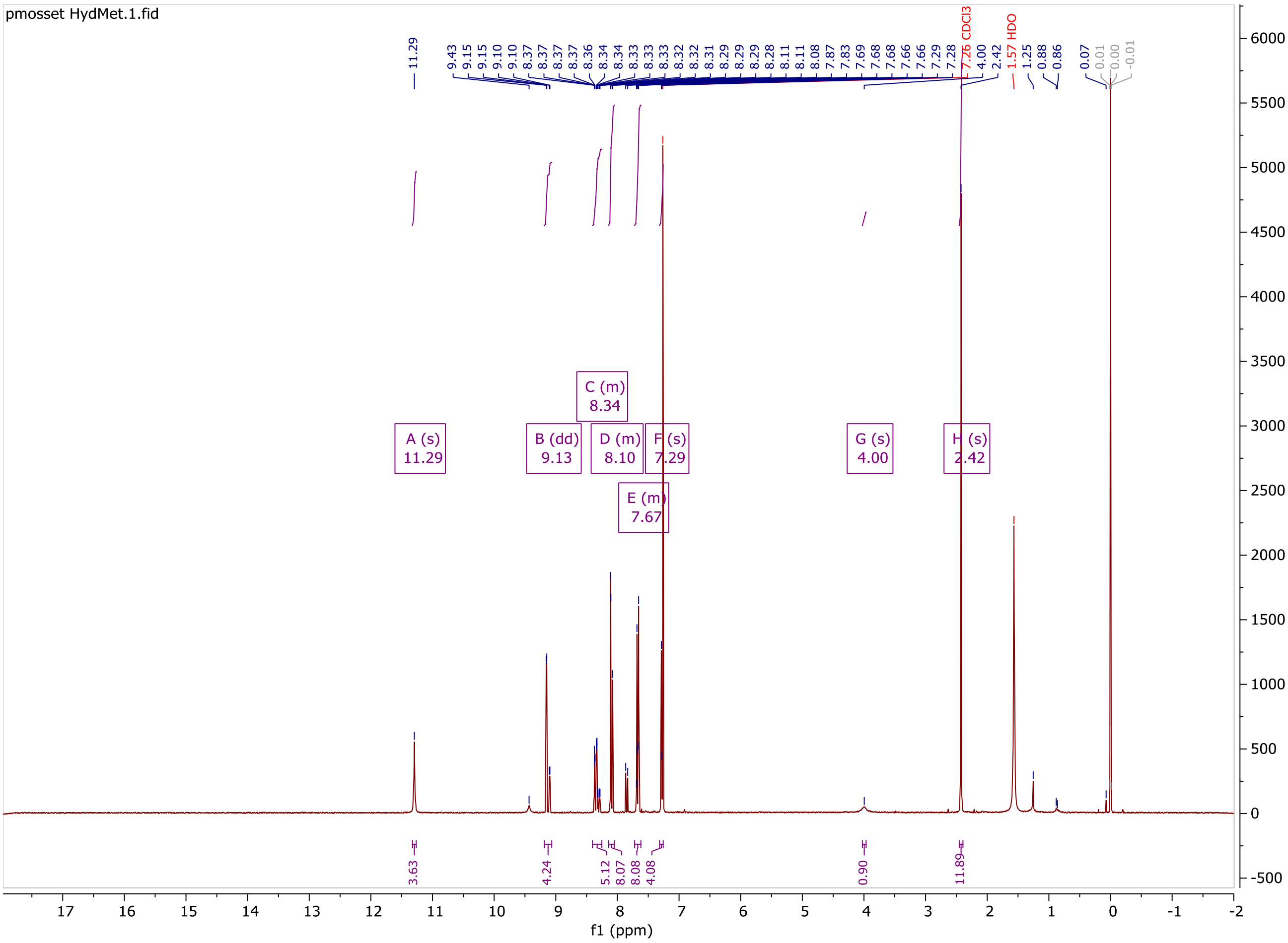

Figure AP. 2. ^{13}C NMR (a) and ^{1}H NMR (b) spectra of HYD-Me

Graphical abstract